THERMODYNAMIC STUDIES ON THE EQUILIBRIUM DISTRIBUTION OF SOLUTE ELEMENTS BETWEEN SOLID AND LIQUID PHASES IN IRON ALLOYS

（鉄合金における溶質元素の固液間平衡分配に関する熱力学的研究）

1984

TOSHIHIRO TANAKA

Contents

Chapter 1

General Introduction.

1.1 Importance of Equilibrium Distribution Coefficient in Metallurgical Processes.

The micro-segregation of solute elements in engineering steels is known to affect considerably the physico-chemical and mechanical properties of the materials, and so far a number of studies have been made to investigate the mechanisms of the segregation of the solutes and to improve the quality of steels. The micro-segregation of the solutes in steels is essentially caused by various factors and its formation mechanism is very complicated. However, the most dominant factor is regarded to be the redistribution of the solutes during solidification, which is caused by the difference between solidus and liquidus in the phase diagram of the alloys. So, the ratio of the concentration of the solute X distributed between solid and liquid phases at the equilibrium state, that is to say, the ratio of the concentration of the solute on solidus and that on liquidus as shown in Fig.1-1 is considered to be very important factor for the micro-segregation. Generally this ratio is given in Eq.(1-1) as k_0^X and called equilibrium distribution coefficient, and also $(1-k_0^X)$ is termed the segregation coefficient.

$$k_0^X = N_X^s / N_X^l \qquad (1\text{-}1)$$

where N_X^s and N_X^l are the concentration of X in solid and liquid phases, respectively.

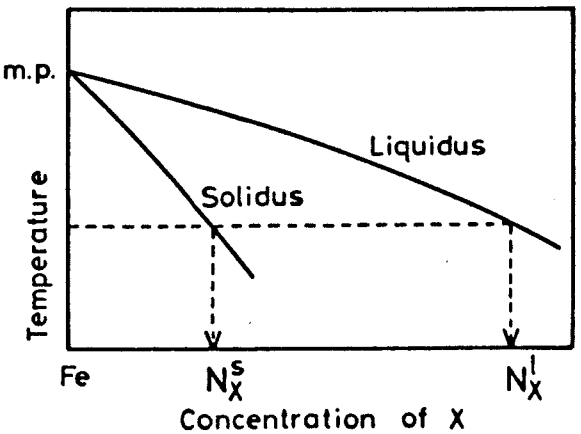

Fig.1-1 Solidus and liquidus near the melting point of iron.

Although k_0 shows the equilibrium distribution of the solute between solid and liquid phases, some equations have been reported to indicate the redistribution of the solute also for the non-equilibrium state, in which the solidification proceeds at a finite rate. For example, the solute distribution along the initial portion of the rod specimen to solidify is given as below by Burton et al.[1] or Smith et al.[2] and so on.

For complete or partial mixing of liquid and no diffusion in solid,

$$\frac{N^S}{N^\circ} \fallingdotseq \frac{k_0}{k_0 + (1 - k_0)\exp(-Rd/D)} \qquad \text{(Burton's equation)} \quad (1\text{-}2)$$

For mixing in liquid by diffusion and no diffusion in solid,

$$\frac{N^S}{N^\circ} \fallingdotseq \frac{1}{2}\left[1 + \mathrm{erf}\sqrt{(R/2D)x} + (2k_0-1)\exp\left\{-k_0(1-k_0)\frac{R}{D}X\right\}\mathrm{erfc}\left\{\frac{(2k_0-1)\sqrt{(R/D)X}}{2}\right\}\right]$$

(Smith's equation) (1-3)

In all of the equations described above, the terms of k_0 of the solute element are surely involved. Hence, it is of considerable importance to know the values of k_0 of various elements in iron alloys whenever the problems, which are ascribed to the redistribution of the solute during solidification, are discussed. The values of k_0 described above are mainly for binary alloys.

There are many kinds of iron and steels including various alloying elements at a wide variety of compositions. Thus, the values of k_0 at various compositions in iron base multi-component alloys should also be required to examine the micro-segregation in such alloys because k_0 of the solute in multi-component iron alloys, i.e. Fe−C base alloy which is one of the most fundamental alloys, are considered to be different from that in binary alloys due to the effects of their solute-interactions. However, the comprehensive studies about k_0 not only in Fe−C base alloys but also in multi-component iron alloys have been done neither experimentally nor theoretically.

With the above background, therefore, the experimental and theoretical

studies on k_0 in iron base multi-component systems are very useful in order to make clear the physico-chemical properties of iron alloys and also to obtain the fundamental information to explain the various phenomena of solidification concerning to the micro-segregation in steels.

1.2 Surveys of Previous Studies.

Values of the equilibrium distribution coefficients of various elements, k_0 in iron alloys previously published by other investigators[3~15] are listed in Table 1-1. It is obvious from this table that there exist noticeable discrepancies among these values of k_0 in each system. The methods obtaining k_0 can almost be divided into the following three kinds, namely,

1) From liquidus and solidus of phase diagram.

2) From thermodynamical calculation.

3) From direct determination of k_0 by experiments, for example, the measurement of concentrations in quenched specimens including solid and liquid coexisted phases or using Burton's equation[1] or Smith's equation[2], and so on.

As is seen from Table 1-1, most of the values of k_0 were determined by means of the above methods 1) and 2).

In the method 1), the accuracy of k_0 obtained from phase diagrams is dependent upon that of phase diagram. In general, it is said that the accuracy of solidus might be less than that of liquidus. This is why the liquidus can be determined by a thermal analysis but it is very difficult to obtain the solidus by such a method. Hence, the accuracy of solidus influences that of k_0 but the phase diagrams whose solidus has been established are very few. Also, the curvature of solidus or liquidus makes the determination of k_0 more difficult. Thus, the method 1), that is to say, to determine k_0 from phase diagrams is considered unreliable.

In the method 2), Hays et al.[8] obtained k_0 for a dilute solution thermodynamically by using the following equation.

$$k_0 = 1 - m\Delta H_m / R T_m^2 \qquad (1\text{-}4)$$

where R is gas constant, T_m and ΔH_m are melting point and heat of fusion of solvent metal respectively, and also m is the slope of liquidus at infinite dilution of the solute.

When k_0 is obtained by using Eq.(1-4), the value m is required but it must be determined by means of the phase diagram. Also, the calculation is very sensitive to the choice of liquidus slope, and an additional difficulty is that there is noticeable curvature on the liquidus curves.

Wada et al.[9] also determined k_0 thermodynamically. They calculated the free energy change accompanied by transfer of alloying elements from one phase to another using solidus, liquidus and phase boundary curves of $\alpha-\gamma$ phase transformation in phase diagrams to obtain k_0.

Consequently, values of k_0 having been decided thermodynamically in the past are dependent upon the accuracy of phase diagram.

So, it is considered more appropriate to determine k_0 experimentally as described in 3). Then, some of the experimental procedure to obtain k_0 are arranged as follows.

① Davis,[16] Fischer et al.[7] and so on determined k_0 from the relation between the concentration distribution of the solute and the distance in the rod specimen solidified uni-directionally. For instance, provided that the mixing in liquid is caused by only diffusion and there is no diffusion in solid, the solute distribution along the initial portion of the rod specimen to solidify is given by Smith et al.[2] in Eq.(1-5).

$$\frac{N^S}{N^\circ} \fallingdotseq \frac{1}{2}\left[1+\mathrm{erf}\sqrt{(R/2D)X}+(2k_0-1)\exp\left\{-k_0(1-k_0)\frac{R}{D}X\right\}\mathrm{erfc}\left\{\frac{(2k_0-1)\sqrt{(R/D)X}}{2}\right\}\right] \quad \cdots\cdots (1\text{-}5)$$

where X is the distance from the start point of solidification, R the solidification velocity and D the diffusion constant of the solute in liquid. A set of concentration-distance curves are calculated for various values of k_0, and by comparison of the curves with an experimental one the correct k_0 can be selected. However, when the above equation is used, the condition, the mixing in the liquid by only diffusion and no diffusion in the solid, must be satisfied. Since the convection in the liquid should further be excluded, the experiment at elevated temperature becomes much more difficult. Also, the data of diffusion

constant of various elements in liquid metals are needed but so far the reliable data have scarcely been obtained.

In this experimental method, a precise measurement for the concentration at a solid-liquid interface can be done at a plane interface than an irregular one. To achieve a plane solid-liquid interface, high G/R values are needed where G is a temperature gradient ahead of interface. However, as the morphology of the interface depends on not only G/R but also the contents of alloying elements, this method is used only for the alloys which contain small amounts of solutes. For example, Davis[16] obtained k_0 of Ag, Sb, Pb and so on in Sn alloys by using Eq.(1-5), but the contents of those solute elements were smaller than 0.05 wt%.

In the case of engineering alloys whose solute contents are comparatively large, higher G/R value is required. So, virtually a plain interface can not be obtained during solidification and the precise measurement of the concentration distribution is very difficult.

② There is another experimental procedure by using the rod specimen. The specimen is set in the furnace with temperature gradient. Solid and liquid phases coexist at the interface. The specimen is quenched when the plain interface is obtained and also the equilibrium is achieved. Then, the concentrations of the solute in both solid and liquid phases at the interface are measured to obtain k_0. Umeda et al.[17,18] used this method to determine values of k_0 of various solute elements in some kind of engineering steels. In this case, the true equilibrium between solid and liquid phases can not be achieved because the two phase region of solid and liquid coexisted is not taken into account in this method. Hence, this experimental procedure can be applied to only the alloys of which the two phase region is very narrow. In other words, it is considerably difficult to determine k_0 of solute elements in Fe−C and Fe−P base alloys, which have wide two phase regions, by this method. Also, as the specimen is large and it is quenched together with the cell, the cooling rate is so small that the equilibrium between solid and liquid phases at elevated tempera-

ture may not be well preserved.

③ Then, other method is described below. The solid and liquid phases are equilibrated at a fixed temperature. After quenching the specimen, the concentrations of the solute elements are measured to determine k_0. This experimental method has been used by Kirkwood et al.;[19,20] Okamoto et al.;[21,22] Takahashi et al.[23] and Schürmann et al.[24~26] to obtain k_0 in iron alloys.

However, in this method some problems are pointed out. For instance, the disturbance of the concentration at the interface and that of the structures in liquid phase occur during quenching. And such problems have not been investigated enough. For example, Kirkwood et al.[19] reported the wrong values of k_0 because of the insufficient metallographical observation of the quenched specimens and then they corrected those values.[20] However, this experimental method seems to be most faithful to the definition of k_0. Thus, if the experimental procedure are carefully checked, this method is considered most suitable to determine k_0.

In Table 1-1, described above, the valus of k_0 are mainly in iron base binary alloys. The equilibrium distribution coefficient k_0 of a solute element in multi-component systems such as engineering alloys is considered to be different from k_0 in iron base binary alloys because of the solute-interactions. In particular, since the interactions between carbon and the alloying element is fairly large in Fe−C base alloys, k_0 of the alloying element is thought to change with the concentration of carbon. For example, the micro-segregation ratio of P[27,28] and Cr[29] were reported to change with carbon content in Fe−C base steels. Okamoto et al.[21,22] showed that k_0 of Si and Cr change with the concentration of C in Fe−C alloys. However, even in these fundamental alloys, enough information of the influences of C on k_0 or the micro-segregation ratios of the alloying elements have hardly been obtained.

Recently, Kirkwood et al.;[19,20] Okamoto et al.[21,22] and Umeda et al.[17,18] measured k_0 of various elements in multi-component iron alloys. However they

reported only the values of k_0 at some compositions in a few kinds of iron alloys. Thus, the comprehensive study concerning the relation between k_0 in multi-component systems and the solute-interactions has not yet been established both experimentally and theoretically.

If the value of k_0 can strictly be calculated thermodynamically, the effects of the solute-interactions on k_0 may be clarified. Kirkwood et al.[20] and Okamoto et al.[21,22,30] calculated k_0 by using the thermodynamical data, but they only compared their experimental results with the calculated ones and did not investigate the relations between k_0 and the solute-interactions enough. Therefore, it is expected that if the thermodynamical and statistical knowledge of the activity or the interaction parameter can be applied to solve the above unknown relations, the useful results would be surely obtained.

Furthermore, if the factor controlling k_0 of the solute element in iron base binary alloys are made clear theoretically, it is very interesting from the view point of physical chemistry and also the prediction of the value of k_0 in the case of no measured values for the equilibrium distribution coefficients. Hume-Rothery et al.[31,32] studied the change of the solidus and liquidus in the phase diagrams of various alloys, and they described that the difference between the partial excess free energy of the solute element in liquid and that in solid, which is obtained from the slope of liquidus and solidus in the various phase diagrams, changes periodically with the atomic number of the element. However, the factors, upon which those differences of the excess free energy and thier periodicity depend, have not been investigated enough.

As described above, there are a lot of problems, which have to be investigated experimentally and also theoretically, about the equilibrium distribution coefficient, k_0 , of various elements and the influences of the solute-interactions on k_0 in iron alloys.

Table 1-1 Equilibrium distribution coefficient in iron alloys.

Element		Composition (Wt. %)	k_0^x	Method	Ref.
Al	(δ)		0.6	E	(3)
			0.60	E	(4)
			0.92	A	(5)
B	(δ)		0.03	E	(4)
			0.05	A	(5)
			0.11	A	(6)
	(γ)		0.04	A	(5)
			0.05	A	(6)
C	(δ)	0.009 - 0.023	0.11 ± 0.025	C	(7)
			0.13	A	(8)
			0.141	E	(7)
			0.17	A	(9)
		0.44	0.18	E	(10)
			0.20	E	(4)
			0.20	A	(6)
			0.25	E	(3)
		0.08	0.25	E	(10)
		0.23 - 0.25	0.29	B	(11)
	(γ)		0.30	A	(6)
			0.34	A	(9)
			0.35	E	(4)
		0.64 - 3.79	0.35 - 0.46	D	(12)
		0.51 - 4.32	0.35 - 0.50	E	(10)
			0.36	A	(5)
Cr	(δ)	0.022 - 0.15	0.89	A	(9)
			0.94	C	(7)
			0.95	A	(5)
			0.97	E	(4)
			1.0	E	(7)
	(γ)		0.85	A	(5)
			0.87	A	(9)

Method:

A : From thermodynamics.

B : From zone melting.

C : From application of Burton's or Smith's equations.

D : From measurement of concentrations in quenched specimens including solid and liquid phases.

E : From phase diagram.

Table 1-1 Continued.

Element		Composition (Wt. %)	k_0^X	Method	Ref.
Co	[δ]		0.90	A	(5)
			0.94	A	(6)
	[γ]		0.95	A	(5)
Cu	[δ]	0.028 - 0.055	0.56	A	(8)
			0.592	E	(7)
			0.70	C	(7)
			0.90	A	(6)
	[γ]		0.70	A	(6)
			0.88	A	(5)
H	[δ]		0.27	E	(4)
			0.27	A	(6)
			0.32	A	(5)
	[γ]		0.45	A	(5)
Mn	[δ]	0.025 - 0.22	0.123	E	(7)
			0.15	E	(3)
		0.3 - 1.0	0.6 - 0.7	E	(13)
			0.68	E	(14)
			0.73 ±0.04	C	(7)
			0.73	D	(12)
			0.76	A	(9)
			0.80 - 0.90	E	(4)
			0.84	A	(8)
			0.90	A	(6)
	[γ]		0.75	A	(6)
			0.78	A	(9)
			0.95	A	(5)
Mo	[δ]		0.7	E	(3)
			0.70	E	(5)
			0.74	A	(9)
			0.80	A	(5)
			0.86	A	(6)
	[γ]		0.57	A	(9)
			0.6	A	(5)
N	[δ]		0.25	A	(6)
			0.28	A	(5)
			0.32	A	(9)
			0.38	E	(4)
	[γ]		0.48	A	(6)
			0.50	A	(9)
			0.54	A	(5)

Table 1-1 Continued.

Element		Composition (Wt.%)	k_0^x	Method	Ref.
Ni	(δ)	0.030 - 0.035	0.549	E	(7)
			0.75	C	(7)
			0.76	A	(9)
			0.80	A	(5)
			0.83	A	(6)
	(γ)		0.85	A	(9)
			0.95	A	(5)
O	(δ)	0.012 - 0.096	0.02	E	(4)
			0.02	A	(5)
			0.022	B	(11)
			0.1	B	(3)
			0.10	A	(8)
	(γ)		0.02	A	(5)
			0.03	A	(6)
P	(δ)		0.13	A	(8)
			0.14	A	(9)
			0.15 - 0.18	E	(4)
		0.015 - 0.092	0.16 ±0.04	C	(7)
		0.204 - 0.211	0.17	B	(11)
			0.2	E	(3)
			0.2 - 0.5	B	(15)
		0.07 - 0.28	0.23	D	(12)
			0.27	E	(15)
			0.28	E	(7)
	(γ)		0.06	A	(5)
			0.08	A	(9)
S	(δ)		0.002	E	(3)
			0.02	A	(5)
		0.20 - 0.45	0.025	D	(12)
			0.04 - 0.05	E	(4)
		0.047 - 0.25	0.04 - 0.06	B	(11)
			0.05	A	(8)
		0.002 - 0.009	0.052 ± 0.01	C	(7)
			0.114	E	(7)
	(γ)		0.02	A	(5)
			0.05	A	(6)
Si	(δ)		0.6	E	(14)
			0.62	A	(9)
			0.66	A	(8)
			0.7	E	(3)
			0.77 ± 0.04	C	(7)
			0.83	A	(6)
		0.4 - 1.0	0.84	D	(12)
			0.84	E	(4)
			0.912	E	(7)

Table 1-1 Continued.

Element		Composition (Wt.%)	k_0^x	Method	Ref.
Si	(γ)		0.5	A	(5)
			0.54	A	(9)
Ti	(δ)		0.14	A	(5)
			0.40	A	(6)
			0.6	E	(3)
			0.60	E	(4)
	(γ)		0.07	A	(5)
			0.3	A	(6)
W	(δ)		0.95	A	(5)
	(γ)		0.5	A	(5)
V	(δ)		0.90	A	(5)
			0.96	A	(6)
Zr	(δ)		0.5	E	(3)
			0.50	E	(4)

1.3 Purpose and Arrangement of the Thesis.

Equilibrium distributions of the solute elements between solid and liquid phases in iron alloys have not been studied enough as described in this chapter 1.2. The purpose of this work is to discuss the equilibrium distribution of the solute in iron base multi-component alloys experimentally and theoretically, and to obtain fundamental knowledge to explain various phenomena during solidification concerning to micro-segregation in iron alloys. In this thesis, these results are described in the following eight chapters.

Chapter 1 of general introduction will be followed by chapter 2 which describes the equilibrum distribution of carbon between solid and liquid phases in iron-carbon binary alloys.

Subsequently, the factors controlling the equilibrium distribution coefficient in iron alloys and also the equilibrium distribution of the third elements in Fe−C base ternary alloys will be discussed experimentally and theoretically in chapter 3.

In chapter 4, the effects of solute-interactions on the equilibrium distribution of solute elements between solid and liquid phases in iron base ternary alloys will be examined and the new thermodynamical coefficient to represent such effects will be derived. The next chapter will describe the derivation of the parameter indicating effects of solute-interactions on the equilibrium distribution of solute elements between solid and liquid phases in iron base multi-component alloys and also the experimental results on the influences of Si, V and Co on the variation of k_0 of Sn and Cu with carbon in Fe−C base quarternary alloys. The experimental results are compared with the calculated ones by using the parameter derived in this chapter.

Then, the equilibrium distribution of P in Fe−P and Fe−P−C alloys will be examined in chapter 6. Also, in this chapter, thermodynamical relation between equilibrium distribution coefficient of various elements for α phase and that for γ phase in iron alloys will be discussed.

Furthermore, the equilibrium distribution of gaseous elements between solid

and liquid phases in Fe, Co, Ni and Cu base alloys will be examined in chapter 7.

Finally, concluding summary will be given in chapter 8.

1.4 References.

1) J.A.Burton, R.C.Primm and W.P.Slichter: J. Chem. Phys., 21 (1953), 1987

2) V.G.Smith, W.A.Tiller and J.W.Rutter: Can. J.Phys., 33 (1955), 723

3) W.A.Tiller: JISI, 192 (1959),338

4) F.Oeters, K.Ruttiger, A.Diener and G.Zahs: Arch. Eisenhüttenw., 40 (1969) ,601

5) J.Chipman: Physical Chemistry of Steelmaking Committee, Iron and Steel Division, AIME, Basic Open Hearth Steelmaking, The American Institute of Mining and Metallurgical Engineering, (1951),632

6) C.E.Sims: Electric Furnace Steelmaking, Vol. 2, John Wiley & Sons, (1962), 99

7) W.A.Fischer and H.Frye: Arch. Eisenhüttenw., 41 (1970), 293

8) A.Hays and J.Chipman: Trans. AIME, 135 (1938), 85

9) T.Wada and H.Wada: The Abstract for the 61st Lecture Meeting of Japan Institute of Metals, JIM, Sendai , (1967), 174

10) J.Tanaka: Tetsu-to-Hagane, 53, (1967), 1586

11) W.A.Fischer, H.Spilzer and M.Hishinuma: Arch. Eisenhuttenw., 31 (1960), 365

12) T.Takahashi, M.Kudo, K.Ichikawa and J.Tanaka: Solidification of Iron and Steel, A Data Book on the Solidification Phenomena of Iron and Steel, ed. by Solidification Comm., Joint Soc. Iron Steel Basic Research of ISIJ ISIJ, Tokyo, (1977). (Appendix).

13) W.A.Hume-Rothery and R.A.Buckley: JISI, 202 (1964), 534

14) E.T.Turkdogan: Trans. Met. Soc. AIME, 233 (1965), 2100

15) R.L.Smith and J.L.Rutherford: J.Metals, 9 (1957), 478

16) K.G.Davis: Met. Trans., 2 (1971), 3315

17) S.Suzuki, T.Umeda and Y.Kimura: The 19th Comm. (Solidification), Japan Soc. Promotion Sci. (JSPS), Rep. No.19-10254, (May, 1980)

18) S.Suzuki, G.Asano, T.Umeda and Y.Kimura: Tetsu-to-Hagane, 66 (1980), S748

19) B.A.Rickinson and D.H.Kirkwood: Metal Sci., 12 (1978), 138

20) A.J.W.Ogilvy, A.Ostrowskii and D.H.Kirkwood: Metal Sci., 15 (1981), 168

21) A.Kagawa and T.Okamoto: Metal Sci., 14 (1980), 519

22) A.Kagawa, S.Moriyama and T.Okamoto: J. Met. Sci., 17 (1982), 135

23) T.Takahashi, M.Kudo, K.Ichikawa and T.Tanaka: Solidification of Iron and Steel, ed. by Solidification Comm., Joint Soc. Iron Steel Basic Research of ISIJ, ISIJ, Tokyo, (1977), 104

24) E.Schürmann and U. Hensgeu: Arch. Eisenhüttenwes., 51 (1980), 1

25) E.Schürmann, H.P.Kaiser and U.Hensgeu: Arch. Eisenhüttenwes., 52 (1980), 5

26) E.Schürmann, H.P. Kaiser and U.Hensgeu: Arch. Eisenhüttenwes., 52 (1980), 127

27) H.Misumi and K.Kitamura: Tetsu-to-Hagane, 69 (1983), S964

28) T.Matsumiya, H.Kajioka, S.Mizoguchi, Y.Ueshima and H.Esaka: Tetsu-to-Hagane, 69 (1983), A217

29) T.Okamoto: Solidification of Iron and Steel, ed. by Solidification Comm., Joint Soc. Iron Steel Basic Research of ISIJ, ISIJ, Tokyo, (1977)

30) A.Kagawa, K.Iwata and T.Okamoto: The Abstract for the 88th Lecture Meeting of Japan Institute of Metals, JIM, Sendai, (1981) 274

31) R.A.Buckley and W.Hume-Rothery: JISI, 201 (1963),227

32) A.K.Sinha, R.A.Buckley and W.Hume-Rothery: JISI, 207 (1969), 36

Chapter 2

Equilibrium Distribution of Carbon between Solid and Liquid Phases in Iron-Carbon Binary System.

2.1 Introduction.

Since the experimental method, in which the liquid and solid phases coexist at equilibrium state and concentrations of the solutes in quenched specimens are measured by EPMA, has been suggested to be most promising procedure to determine k_0 in the previous chapter 1.2, this procedure was used in this work. First of all, the fundamental investigation must be required for this experimental method, for example, the disturbance of the concentration at interface between solid and liquid phases during quenching mainly caused by the diffusion of the solute, which is one of the most important problems in this procedure.

So, in this work, this procedure was applied to Fe−C alloys because the diffusivity of carbon in this system has been known to be large, and the validity of the application of the experimental method to this alloy was also discussed. On the other hand, there seems to exist some discrepancies, particularly, about solidus in this alloy and no detail discussion on this point in the previous studies. Then, solidus and liquidus obtained experimentally were compared with the curves given in other works and also with the calculated results using thermodynamical data.

2.2 Experimental.

2.2.1 Apparatus for Quenched Specimens.

The apparatus for preparing quenched specimens is shown in Fig.2-1. A sample weighing 7 g was placed into an alumina crucible in purified argon atmosphere. After melting down of the sample, it was cooled to a fixed temperature between 1423K and 1673K, at which austenite and liquid phases coexist,

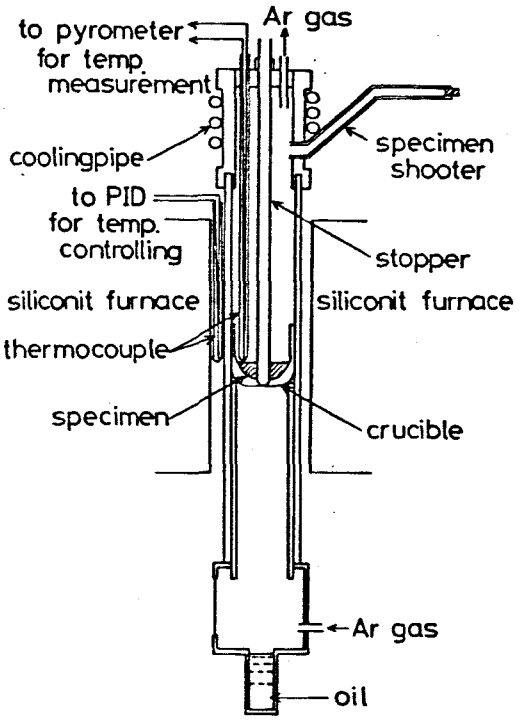

Fig.2-1 Apparatus for quenching specimens.

and held at that temperature for a given time. When equilibrium was achieved, by withdrawing the stopper, the sample fell through the hole at the bottom of the crucible and was quenched into oil, to make specimen including two phases having been liquid and solid before quenching.

As the vertical tube furnace used had a hot zone of 50 mm length and the height of the sample was within 10 mm, it is reasonable to expect that the solid distribution in the sample was uniform.

2.2.2 Sample and Holding Temperature.

Compositions of samples used and their equilibrium holding temperatures are listed in Table 2-1. These samples were prepared in the high frequency induction furnace from electrolytic iron and pure graphite.

The equilibrium holding temperature was fixed to make the ratio of solid in the specimens from 5 to 10 %.

Table 2-1 Chemical compositions(wt%) and equilibration temperatures (K) for Fe－C specimens.

No.	Temp. (K)	C	Si	Mn	P	S	Al
1	1446	3.81	0.153	0.005	0.003	0.005	0.111
2	1521	3.30	0.164	0.005	0.003	0.003	0.164
3	1596	2.57	0.104	0.005	0.003	0.004	0.080
4	1632	2.41	0.109	0.010	0.003	0.004	0.064
5	1672	1.79	0.065	0.005	0.003	0.005	0.025

2.2.3 Equilibration Time.

To determine the time required to establish complete equilibrium between the two phases, a series of experiments were carried out on Fe-3.8 wt% C alloys, in which specimens were quenched after different holding times at 1446 K. The results of the analysis of carbon from the central regions of the the solid phases are given in Fig.2-2. This figure shows clearly that the equilibrium was achieved after holding the specimens for about 30 min. Consequently, the holding time was determined to be 1 hr.

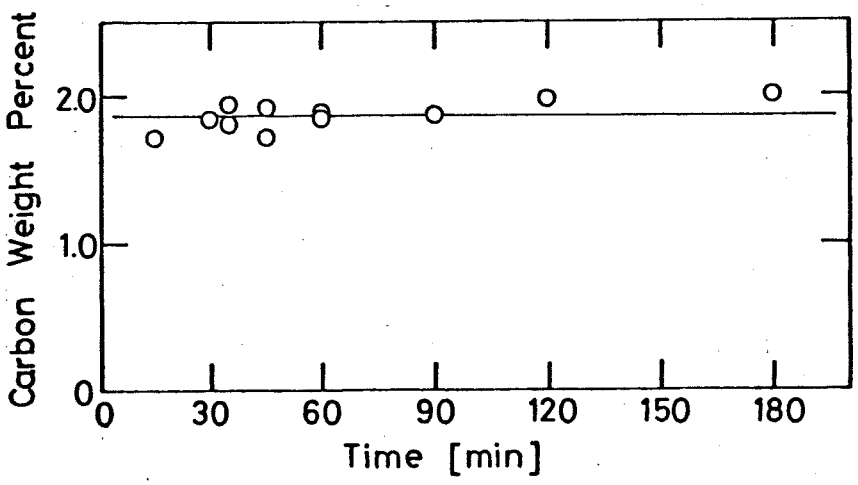

Fig.2-2 Carbon concentration in austenite of the Fe－C alloy held at 1446K with equilibration time.

2.2.4 Metallographic Structure of Quenched Specimens and Measurement of Concentration Distribution by EPMA.

All the specimens were spherical, and the solid phases were distributed uniformly in each specimen. Photograph 2-1 shows the metallographic structures of the quenched specimens, where circulars are solid phases and the other part is liquid one which had existed before quenching. In these photographs, Nos. 1 and 5 are the specimens held at the lowest and highest temperature, respectively. It is obvious from these photographs that the quantities of dendrites which crystallized in liquid phase during quenching increase as the holding temperature becomes higher and higher. Since the carbon content of No. 1 specimen is approximately equal to the eutectic one, the quantities of crystallized austenite are quite small during solidification as obvious from Photo.2-2 (A). On the other hand, although the carbon content of No. 5 specimen is less than the maximum carbon solubility in austenite, its structure consists of austenite grains surrounded by cementite divorced from ledeburite as shown in Photo.2-2(B). As exhibited in Photo.2-1, the average diameter of the solid phase is about 100 ~200 μm in the specimen held at lower temperature but about 300 μm in the specimen held at higher temperature because the rate of coarsening of the solid phase at higher temperature is larger than at lower one.

Electron probe micro analysis was carried out by scanning the focussed beam over a region which included both solid and quenched liquid. Since the structure of the liquid phase in the specimen was not so uniform as that of the solid phase, in the liquid phases a focussed beam was moved over the distance which was 2 or 3 times of the diameter of the solid phase, and the concentrations at the liquid region of each specimen were averaged. In this experiment, using electrolytic iron, 0.69 wt% C steel and 4.24 wt% C cast iron, the relation between X-ray intensity and carbon content was established. The caron concentrations were determined by use of the calibration curve as shown in Fig.2-3.

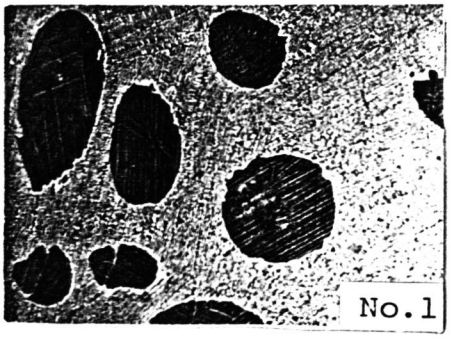

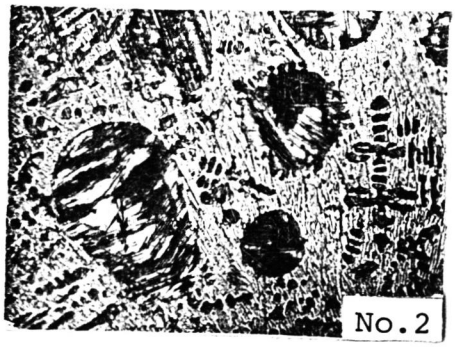

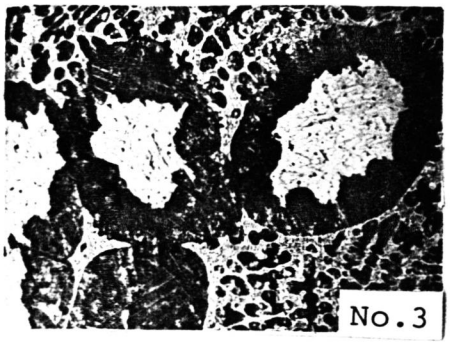

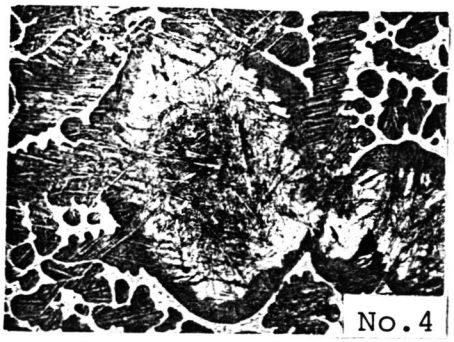

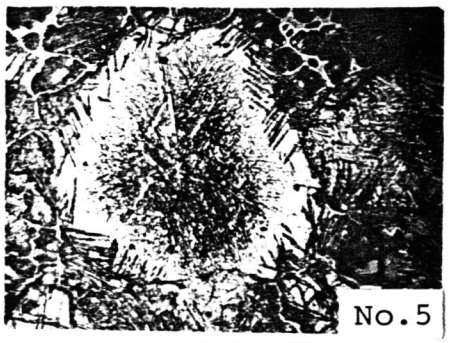

100 μm

No.	Equilibration temperature [K]
1	1446
2	1521
3	1596
4	1632
5	1672

Photo.2-1 Microstructures of quenched specimens.

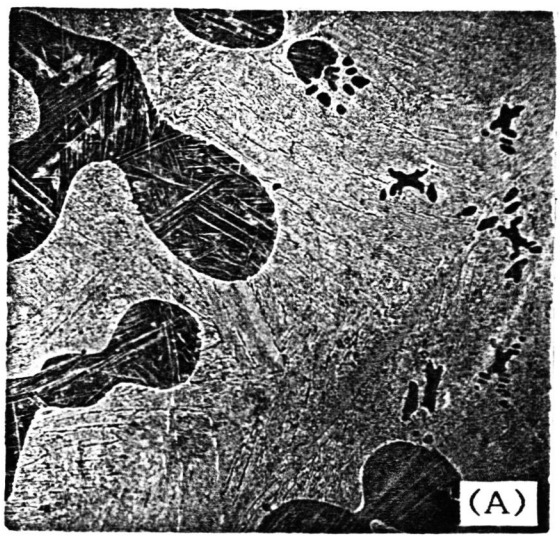

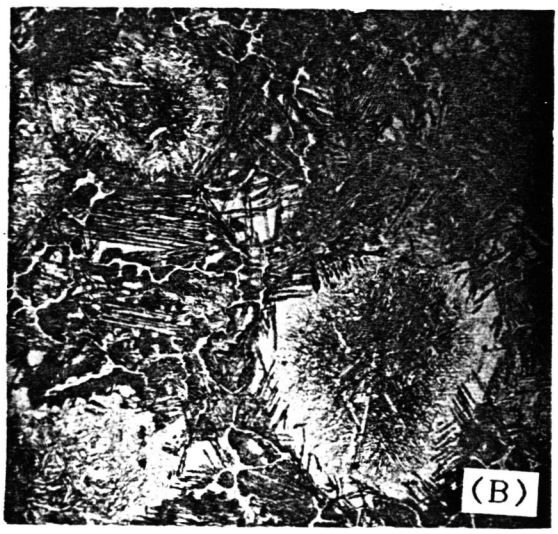

100 μm

Photo.2-2 Microstructures of quenched specimens,(A) No.1 and (B) No.5.

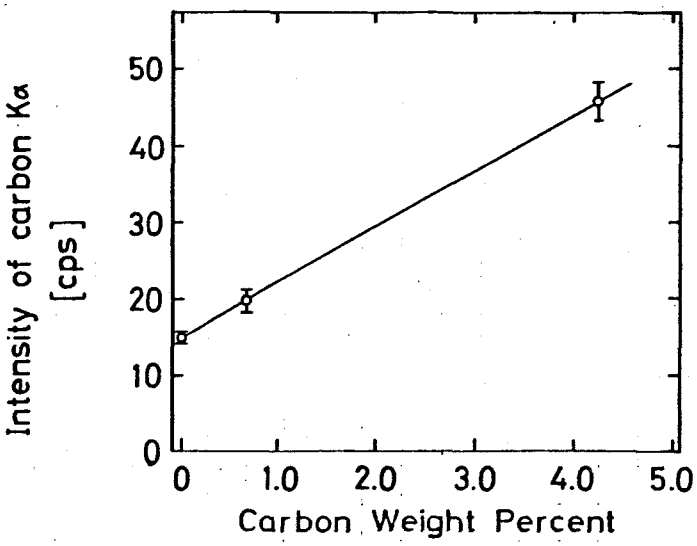

Fig.2-3 The calibration curve for carbon in electron probe micro analysis.

2.2.5 Concentration Distribution.

Some examples of the concentration distribution measured by EPMA are given in Fig.2-4. It is obvious from this figure that in the specimen held at higher temperature, the disturbance of concentration distribution is remarkable because the quantity of dentrite crystallized in the liquid phases is large. In determination of equilibrium carbon concentration in the solid phase, the values at the center of the solid phase in which carbon concentration is uniform as illustrated in Fig.2-4, were used.

2.3 Results and Discussion.

2.3.1 Experimental Results.

Figure 2-5 shows the measured carbon concentration in both solid and liquid phases as a function of temperature in the Fe−C system, and the solidus and liquidus which were obtained by fitting the plots by curves. This figure also indicates the liquidus by Buckley and Hume-Rothery[1], and the solidus by Benz and Elliott,[2] Adcock,[3] and Honda and Endo.[4] So far a number of studies have been carried out on the liquidus except Buckley and Hume-Rothery, but all

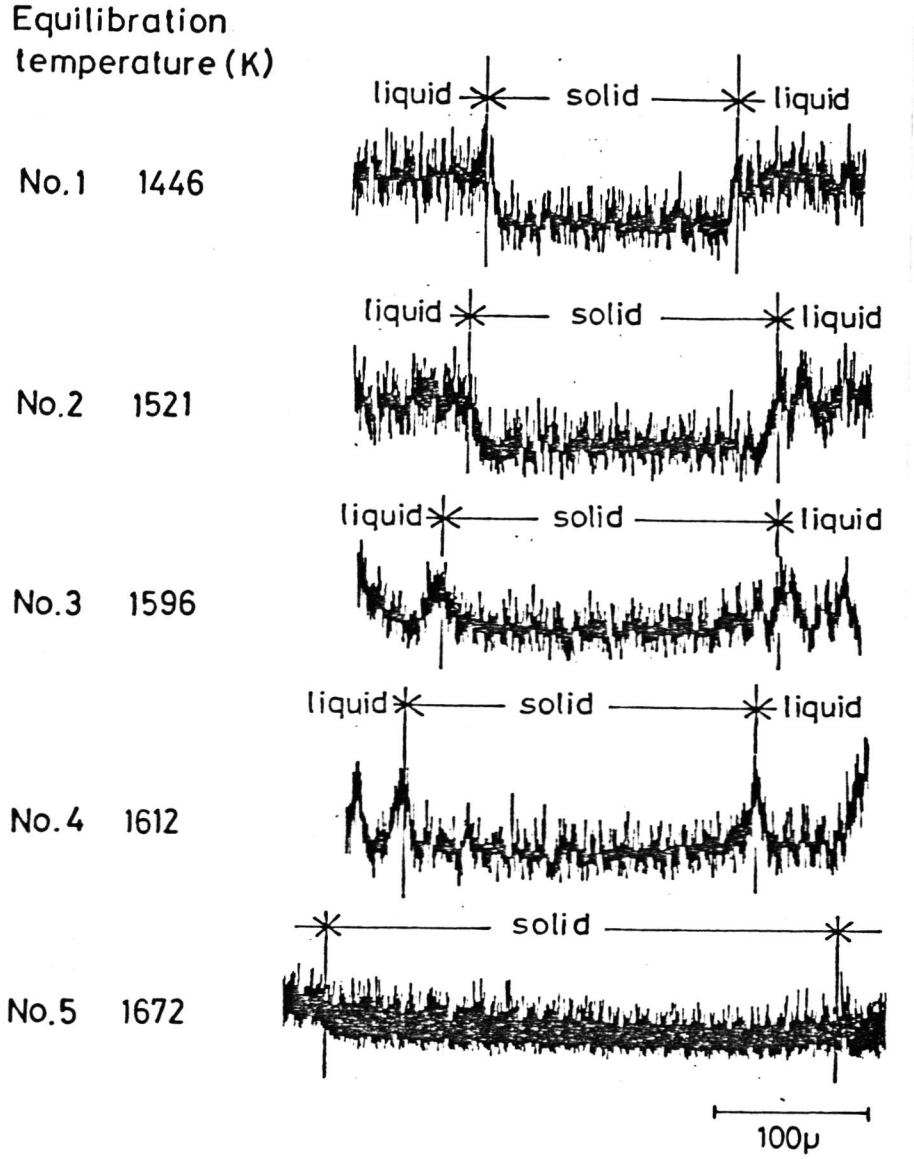

Fig.2-4 Carbon distribution in quenched specimen.

these results coincide very well with that of Buckley and Hume-Rothery. So, those results are not shown in this figure. On the other hand, there are some types of solidus curves, for example, the curve convex downward by Honda and Endo, the one slightly convex upward by Adcock and the straight line by Benz and Elliott. This fact means that the determination of solidus is more difficult than that of the liquidus. The liquidus obtained in this work corresponds to that of Buckley and Hume-Rothery, and extrapolating the liquidus of this work it reaches eutectic point which has already been established as most reliable.

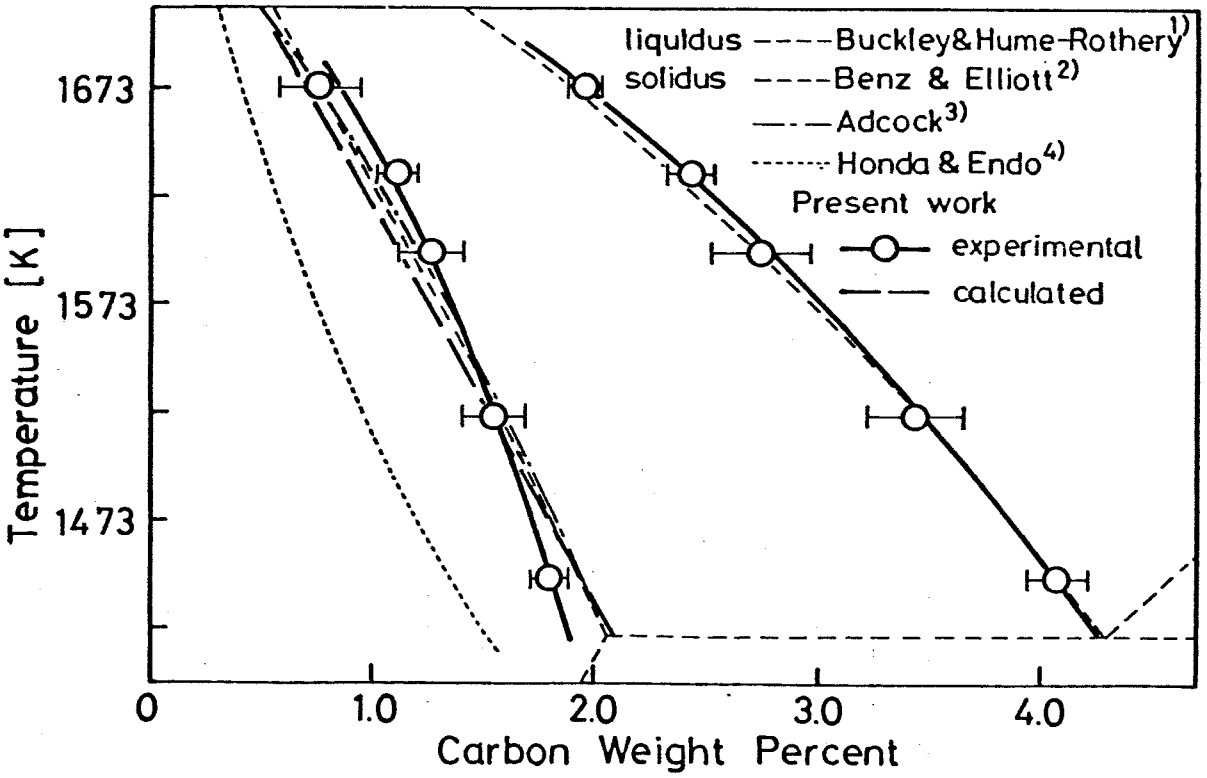

Fig.2-5 Experimental and calculated results corresponding to the solidus and liquidus of austenite-liquid iron in the Fe−C system.

The solidus obtained in the present work coincides comparatively well with that of Benz and Elliott. The solidus calculated using thermodynamic data is also shown in Fig.2-5. The detail of this calculation will be discussed later in the section 2.3.3.

2.3.2 Validity of the Experimental Method and Results.

When this experimental method is applied to Fe−C system in which carbon diffusivity is known to be large, it is considered that carbon diffuses even in the solid phase during quenching, and in some cases the carbon concentration in solid after quenching may differ from the equilibrium one. So first of all, considering the change of carbon concentration at the solid-liquid interface and the change of carbon diffusivity in the solid phase with the temperature during quenching, the diffusion distance of carbon from the liquid-solid interface into the solid phase during quenching was calculated by use of the data of cooling rates obtained in this work.

First, supposing that these phenomena are based on one dimensional diffusion of carbon, Fick's second law in Eq.(2-1) is changed into the difference equation (2-2), and then the explicit method was used for this purpose as shown in Fig.2-6. The diffusivity of carbon in austenite measured at 1173 1673K using the Fe-0.6 wt%C alloy[5] is assumed to be applicable to the carbon content in this work.

$$\frac{\partial C}{\partial t} = D \frac{\partial^2 C}{\partial x^2} \tag{2-1}$$

$$\frac{C_{i,j} - C_{i-1,j}}{\Delta t} = D \frac{C_{i-1,j-1} - 2C_{i-1,j} + C_{i-1,j+1}}{(\Delta x)^2} \tag{2-2}$$

$$D = 1.75 \times 10^{-2} \exp\left(- \frac{27.1 \times 10^3}{RT} \right)$$
$$= 1.75 \times 10^{-2} \exp\left(- \frac{27.1 \times 10^3}{R(T_0 - V\Delta t \cdot i)} \right) \tag{2-3}$$

where, i , j : step number of time on the vertical axis and distance on the abscissa, respectively, in Fig.2-6.

V: cooling rate [K/Sec]

T_0 : equilibration temperature [K]

$T_0 - V\Delta t \cdot i$: temperature at step i after start of quenching.

Also, initial and boundary conditions are shown in Eqs.(2-4) and (2-5), respectively.

$$C_{0,j} = C^o \tag{2-4}$$

$$C_{i,0} = C^o + \frac{V}{m}\Delta t \cdot i \tag{2-5}$$

where, C° : equilibrium concentration in the solid phase [wt%]

m: gradient of the solidus [K/wt%]

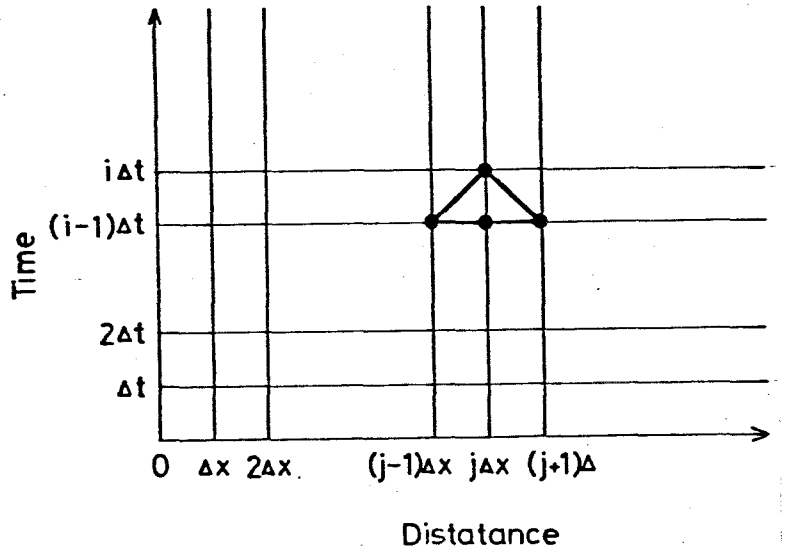

Fig.2-6 Explicit method.

Cooling rate V was calculated by using Eq.(2-6)[6]

$$V = \left[\frac{340 \times (1/\%C - 1/4.3)^{0.35}}{Z}\right]^{100/27} \tag{2-6}$$

where, Z: the secondary dendrite arm spacing [μm], obtained from photographs of microstructure of the quenched specimens in this work.

Figure 2-7 indicates the measured cooling rate. Since dendrite structures could not clearly be observed in liquid phases in Nos. 1 and 5 specimens, the extrapolated values obtained from linear approximation of the relation between the cooling rate and temperature of other specimens were adopted as the cooling rates of these specimens.

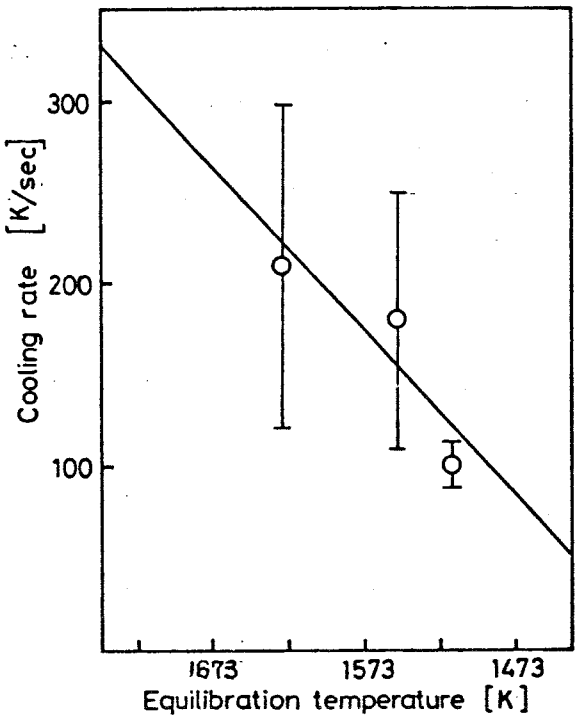

Fig.2-7 Change of cooling rates of the Fe−C alloy with equilibration temperature before cooling.

Thus, the change of concentration distribution in the solid phase due to carbon diffusion during quenching were calculated by using Eq.(2-2). Some examples of the calculated results are given in Fig.2-8, which shows the concentration distributions of carbon in the solid phase at the end of solidification when it is assumed that each specimen solidifies completely at temperature of 100 K under than eutectic one. It is obvious from Fig.2-8 that the diffusion distance of carbon in even the specimen held at higher temperature is less than 100 μm from solid-liquid interface. Comparing these diffusion distances with

the diameters of solid phases as shown in Photo.2-1, that is to say, about 100 ~ 200μm of the specimen held at low temperature and about 300μm held at high one, and also from Fig.2-8, which shows that the calculated diffusion distances of carbon into austenite during quenching are larger than the measured values from the C Kα intensity profiles in Fig.2-4 , it is supposed that present experimental results were in the equilibrium state enough as far as the carbon concentration at the center of the solid phase was used in the quenched specimens obtained in this work.

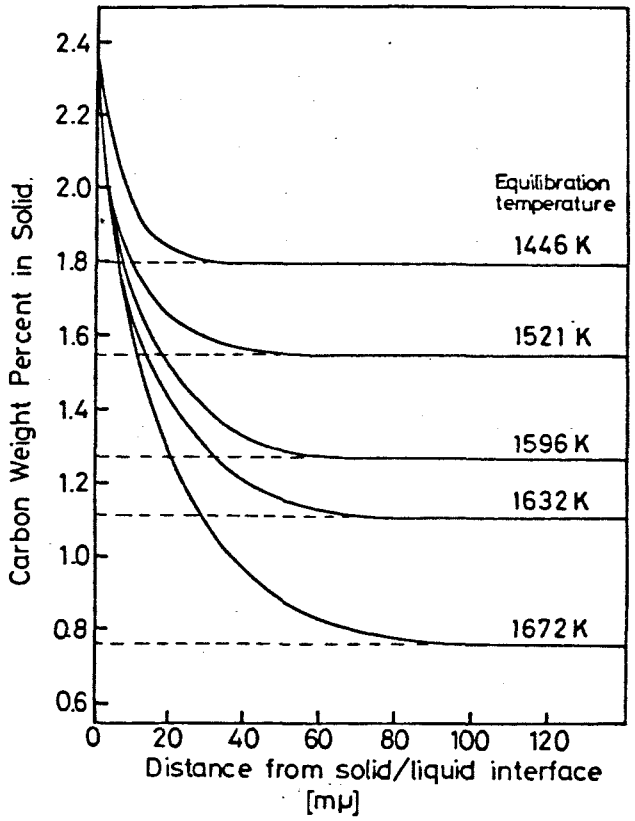

Fig.2-8 Carbon diffusion distances in the solid phase during quenching.

There may exist the depression of temperature during quenching, namely, until the specimen dropped into oil after withdrawing the stopper. In this regard, it was found from the preliminary experiments that it took 0.35 sec during quenching and the depression of temperature was 15 K. Then, assuming that the depression of temperature of the specimen is 15 K during quenching and calculating the carbon diffusion distance in the same way as described above, the results are found to be as same as in Fig.2-8. Thus, the depression of tem-

perature during quenching can be neglected.

2.3.3 Thermodynamical Calculation of the Equilibrium Distribution of Carbon.

In order to discuss thermodynamically the distribution of carbon between solid and liquid phases, the solidus corresponding to the liquidus obtained in this experiment was calculated using the thermodynamic data and compared with the experimental results.

Equilibrium between liquid and solid phases in an Fe−C alloy is represented by Eqs.(2-7) to (2-9)

$$\mu_C^l = \dot{\mu}_C^l + RT \ln \gamma_C^l N_C^l \tag{2-7}$$

$$\mu_C^s = \dot{\mu}_C^s + RT \ln \gamma_C^s N_C^s \tag{2-8}$$

$$\mu_C^l = \mu_C^s \tag{2-9}$$

where, μ_C : chemical potential of carbon

$\dot{\mu}_C$: chemical potential of carbon in standard state

N_C : mole fraction of carbon

γ_C : activity coefficient of carbon

R : gas constant

T : absolute temperature

Superscripts l and s : liquid state and solid state

From the equilibrium condition Eq.(2-9), the equilibrium distribution coefficient of carbon k_0^C , is obtained as follows.

$$k_0^C = N_C^s / N_C^l = (\gamma_C^l / \gamma_C^s) \exp \{ (\dot{\mu}_C^l - \dot{\mu}_C^s) / RT \} \tag{2-10}$$

If the standard state of carbon in both liquid and solid phases is taken to solid graphite, i.e.,

$$\dot{\mu}_C^l = \dot{\mu}_C^s \tag{2-11}$$

Equation (2-10) can be written as

$$k_0^C = \gamma_C^l / \gamma_C^s \tag{2-12}$$

Thus, substituting the values of activity coefficients γ_C, reported by other investigators into the above equation (2-12), and also using the equilibrium distribution coefficient obtained from Eq.(2-12), the solidus corresponding to the liquidus obtained experimentally can be calculated.

When the equilibrium distribution coefficient k_0^C is calculated in Eq.(2-12), the thermodynamic data have to be correct and reasonable. Then, the data[7~13] previously obtained on the activity of carbon in liquid iron and austenite were investigated. Among these data, the values, which are applicable to the temperature range (1423~1673K) in this work, and also are being given as a function of both temperature and concentration, were selected. Furthermore, in determination of the data used in the above calculation, the values, whose degrees of the quotation and the convergency are high, were adopted. Figures 2-9 and 2-10 show some representative data of activity coefficients of carbon in liquid iron and austenite, respectively, at 1473, 1573 and 1673 K as a function of N_C. From Fig.2-9, the agreement between the data of Chipman[8] and that of Ueda et al.[7] is very good. However, since the data of Chipman was calculated from the activity in austenite using the equilibrium condition between solid and liquid phases, it is thought to be unsuitable for this discussion. On the other hand, as the data of Ueda et al. was reported more recently that of Chipman, and was obtained by measuring the rate of effusion of iron vapour, it is considered to be more suitable for this discussion than that of Chipman. Then, the data of Ueda et al. was adopted as

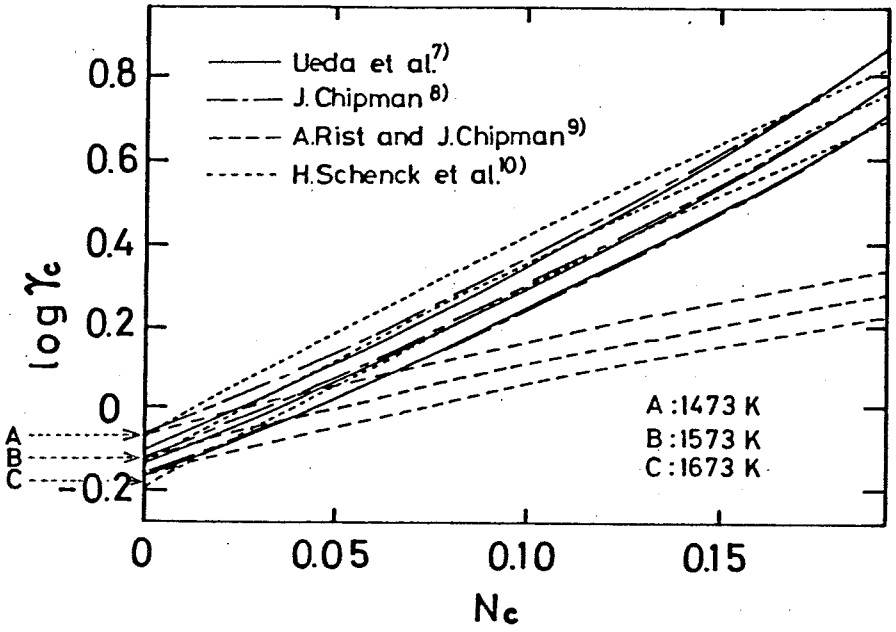

Fig.2-9 Activity coefficient of carbon in liquid iron.

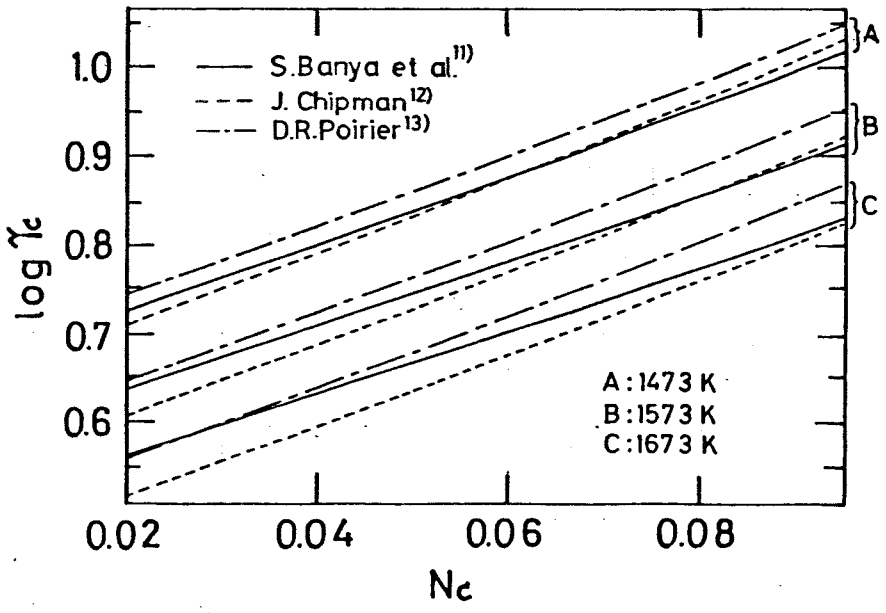

Fig.2-10 Activity coefficient of carbon in austenite.

$$\log \gamma_C^l = \left(\frac{5\,300}{T} + 0.507\right)\frac{\mathcal{N}_C^l}{1-\mathcal{N}_C^l} + \left(\frac{694}{T} - 0.587\right) \tag{2-13}$$

About the data of activity of carbon in austenite in Fig.2-10 the value of Ban-ya et al.[11] approaches that of Chipman[12] at higher temperature range and also that of Poirier[13] at lower temperature range. So, the data of Ban-ya et al. was adopted as

$$\log \gamma_C^s = \left(\frac{3\,770}{T} - 10.5\right) + \left(0.43 + \frac{3\,900}{T}\right)\frac{\mathcal{N}_C^s}{1-\mathcal{N}_C^s} + 2.72 \log T - \log(1-\mathcal{N}_C^s) \tag{2-14}$$

Substituting Eqs.(2-13) and (2-14) into Eq.(2-12) and also using the relation $N_C^s = k_0^C \cdot N_C^l$, the solidus corresponding to the liquidus obtained experimentally can be calculated. The result is shown in Fig.2-5. From this figure, the calculated result is in comparatively good agreement with the experimental one. Thus, present experimental results are thought to be appropriate also in the thermodynamical standpoint.

2.4 Conclusion.

In order to investigate the validity of the experimental procedure for equilibrium distribution coefficient and to obtain carbon distribution between solid and liquid phases in Fe－C binary system, austenite-liquid phases equilibrated in the temperature range from 1423 to 1673K were quenched and the carbon concentrations in each phase were determined by EPMA.

The results obtained are summarized as follows.

① Solidus and liquidus obtained coincided well with the curves given in other works.

② Diffusion distance of C from liquid-solid interface into solid phase during quenching was calculated. From the results of the calculation, it became clear that carbon concentration in the center of solid phase was not influenced

by the carbon diffusion during quenching. Thus, this experimental procedure is considered to be valid for even the Fe−C alloys including carbon whose diffusivity is very large.

③ Equilibrium distribution coefficient of C in Fe−C system was determined thermodynamically. Solidus corresponding to the liquidus obtained experimentally was calculated by using the above coefficient and it was in good agreement with the experimental one.

2.5 References.

1) R.A.Buckley and W.Hume-Rothery: JISI, 196 (1960),403.

2) M.G.Benz and J.F.Elliott: Trans.Met.Soc.AIME, 221 (1961),323.

3) F.Adcock: JISI, 135 (1937),720.

4) K.Honda and H.Endo: Science Reports Tohoku Univ., 16 (1927),235.

5) D.F.Kalinovich, I.I.Kovenskii and M.D.Smolin: Izv. Vyssh. Ucheb. Zaved, Fiz, 9 (1971),116.

6) T.Okamoto and H.Matsumoto: 39th International Foundry Congress, AFS, Philadelphia, May 1972.

7) A.Ueda, K.Fujimura and T.Mori: Tetsu-to-Hagane, 61 (1975), 42.

8) J.Chipman: Met. Trans., 1 (1970),2163.

9) A.Rist and J.Chipman: Rev. Met., 53 (1956),796.

10) H.Schenck, E.Steinmetz and M.Gloz: Arch. Eisenhuttenw., 42 (1971),307.

11) S.Ban-ya, J.F.Elliott and J.Chipman: Met. Trans., 1 (1970), 313.

12) J.Chipman: Trans. Met. Soc. AIME, 239 (1967),2.

13) D.R.Poirier: Trans. Met. Soc. AIME,242 (1968),685.

Chapter 3

Equilibrium Distribution of Solute Elements between Solid and Liquid Phases in Iron-Carbon Base Ternary Alloys.

3.1 Introduction.

As described in chapter 1, the equilibrium distribution coefficients of solute elements in multi-component systems are thought to be different from those in binary systems since some interactions among solutes are expected to exist in multi-component systems, but a comprehensive theory concerning this problem has not yet been developed.

Recently, some investigators[1~4] have measured the equilibrium distribution coefficients of solute elements in various kinds of iron alloys and calculated them by using thermodynamical data. However, in their works, mainly, they studied if the experimental results were valid or not in comparison with the calculated values, and did not discuss the mechanism of the equilibrium distribution of solute and the effect of solute interaction on it.

The purpose of this chapter is to obtain the equilibrium distribution coefficients for C, Ni and V in Fe−C−Ni(up to 4 wt% C and 1 wt% Ni) and Fe−C−V (up to 4 wt% C and 3 wt% V) alloys and to discuss the mechanisms of these solute distributions between solid and liquid phases. In these systems, there are few data for the equilibrium distribution coefficients of the solutes, especially in a wide temperature range. Since the thermodynamic interaction between Ni and C in iron alloy is known to be opposite to that between V and C, it is also interesting from a thermodynamic standpoint to make clear the mechanisms of distributions of Ni and V. Moreover, based on the results on these systems, the factors which control the solute distributions between solid and liquid phases in iron base binary alloys and iron-carbon base ternary ones were discussed thermodynamically.

3.2 Experimental.

3.2.1 Procedure for making Quenched Specimens.

The apparatus for preparing quenched specimens is the same as shown in Fig. 2-1. A sample weighing about 5 g was placed into an alumina crucible in purified argon gas atmosphere. After the sample melted down, it was cooled to a fixed temperature between 1453 K and 1693 K, at which austenite and liquid phases coexisted,and held at that temperature for a given time. When the equilibrium was achieved, by withdrawing the stopper, the sample fell through the hole at the bottom of crucible and was quenched in oil or 10 % KOH aqua, to make the specimen including two phases of liquid and solid before quenching.

As the vertical tube furnace had a hot zone of 30 mm over which the temperature was constant within ±2K and the height of the sample was shorter than 10 mm, it is reasonable to expect that the temperature distribution in the sample was uniform. The sample was often stirred when it was held at a given temperature so that the solids could distribute uniformly in the sample.

3.2.2 Sample and Holding Temperature.

The compositions of the samples used and their equilibrium holding temperatures are listed in Table 3-1. These samples were prepared in a high frequency induction furnace from electrolytic iron, pure graphite, nickel and vanadium.

The equilibrium temperature was fixed at ahout 20 K lower than the liquidus temperature to make the ratio of solid to liquid in the specimen as small as possible.

3.2.3 Equilibration Time.

To determine the time required for the establishment of the complete equilibrium between the two phases, a series of experiments were carried out on the Fe−C−V alloys, in which the specimens were quenched after different holding times at the same temperature. The results of the analysis of V from

Table 3-1 Chemical composition and equilibration temperature for Fe−C−Ni and Fe−C−V alloys.

wt% C	wt% V	wt% Ni	Holding Temperature[K]		
2.57	1.03		1543	1548	
3.50	1.06		1468	1476	
2.30	0.44		1628	1643	1653
3.34	0.44		1536	1546	
2.45	2.96		1622	1632	
3.37	2.80		1543		
1.62		0.39	1673	1683	
2.77		0.48	1573	1593	
3.28		0.59	1526	1556	
2.71		1.03	1605	1608	1613
3.84		0.93	1473	1483	1490

the central regions of the solid phases are given in Fig. 3-1. This figure shows clearly that the equilibrium has been achieved after 3 hr. Consequently, the holding time was determined to be 3 to 4 hr.

3.2.4 Metallographic Structure of Quenched Specimens and the Measurement of Concentration Distribution by EPMA.

All the specimens were spherical, and the solid phases were distributed uniformly in each specimen. Photograph 3-1 shows the microstructures of the quenched specimens, where circulars and the rest are the solid and liquid phases, respectively, which had coexisted before quenching.

All the specimens quenched were prepared for metallographic examinations by polishing and etching in 10 % Nital. Then, the parts of solid and liquid to be microanalysed were marked out with microhardness impressions, and then repolished to remove the etching.

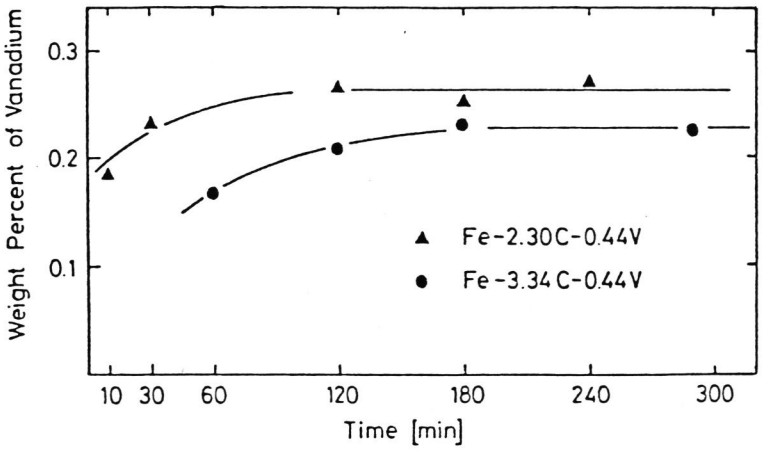

Fig.3-1 Vanadium concentration in austenite of Fe−C−V alloys with equilibration time.

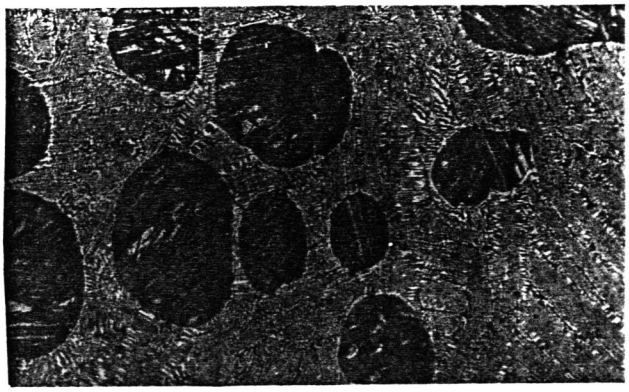

Fe-3.84C-0.93Ni

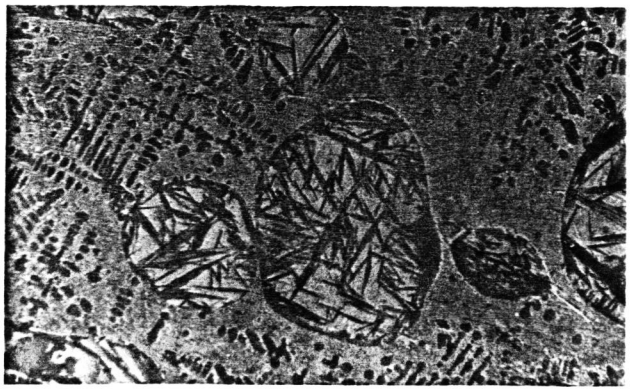

Fe-3.28C-0.59Ni

Photo.3-1 Microstructures of quenched specimens.

Electron probe microanalysis was carried out at an accelerating voltage of 20 KV by scanning the focussed beam at 50 μm/min over the region which included both solid and liquid. Since, particularly, the structure of the part of the liquid phase in the specimen was not so uniform as that of the solid phases, in the part of the liquid phase a focussed beam was moved over the distance corresponding to 2 or 3 times of the diameter of the part of the solid phase, and then the concentrations of the solutes at the liquid region of each specimen were averaged.

The actual composition were obtained from the calibration curve which was previously established with the chemically analysed specimens of Fe−C−V and Fe−C−Ni alloys, shown in Fig.3-2. The chemical composition of these samples used are listed in Table 3-2. Some examples of the concentration distribution measured by EPMA are given in Fig.3-3.

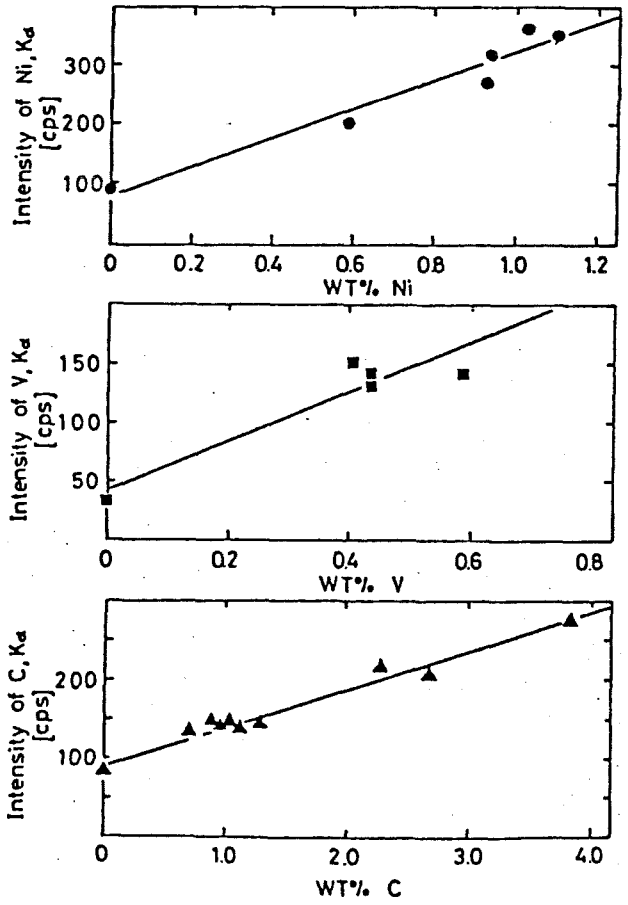

Fig.3-2 Calibration curves for Ni, V and C in electron prove micro analysis.

Table 3-2 Chemical composition for standard specimens.

wt% C	wt% V	wt% Ni	
0.00	0.00	0.00	(pure iron)
0.71	0.44		
0.97	0.59		
1.04	0.41		
2.30	0.44		
3.34	0.44		
0.92		1.10	
1.14		0.59	
1.31		0.94	
2.71		1.03	
3.84		0.93	

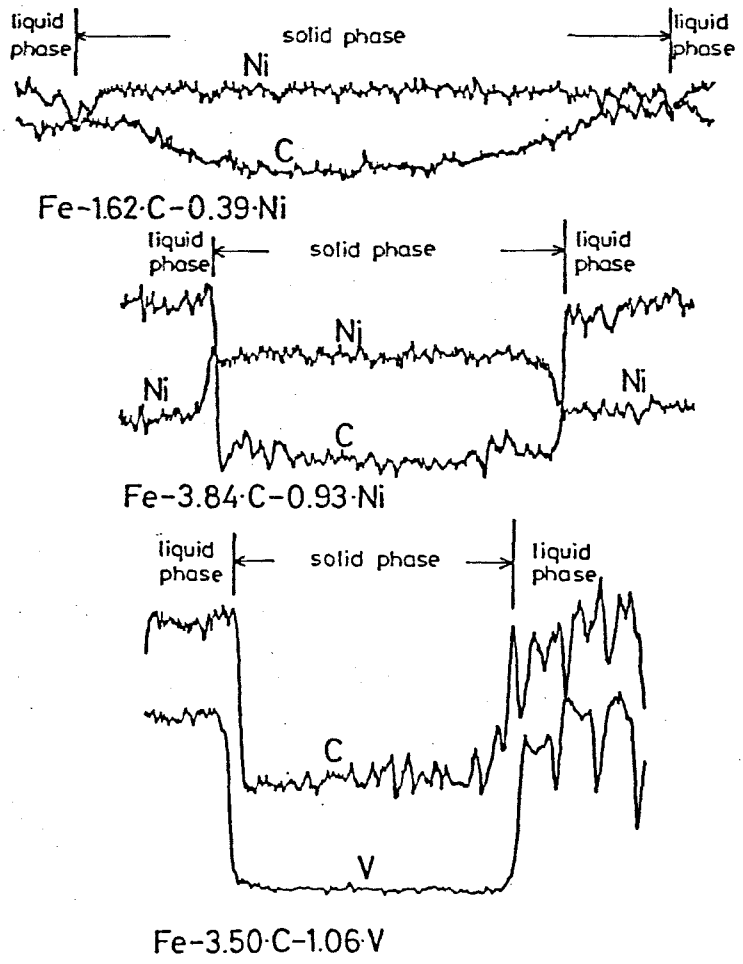

Fig.3-3 Carbon, nickel and vanadium distributions in quenched specimens.

3.3 Experimental Results.

Figure 3-4 shows the experimental results on a plot of the carbon concentration in both the austenite and liquid phases in Fe−C−Ni and Fe−C−V systems together with the liquidus and solidus in Fe−C binary system. It is obvious that the distribution of C between the solid and liquid phases in Fe−C−Ni and Fe−C−V alloys with 1 ~ 3 wt% Ni and V differs little from that in Fe−C binary system.

The variation of the equilibrium distribution coefficient of Ni, k_0^{Ni}, in Fe−C−Ni system and that of V, k_0^V, in Fe−C−V system are given as function of the carbon concentration of liquidus, respectively, in Figs.3-5 and 3-6. In these figures, the calculated values of k_0^{Ni} and k_0^V using thermodynamic data are also shown. This calculation will be discussed in detail at the later section. It can be seen from Figs.3-5 and 3-6 that k_0^{Ni} increases in Fe−C−Ni system and k_0^V decreases in Fe−C−V system with the increasing carbon content. The effects of Ni and V contents on k_0^{Ni} and k_0^V in Figs.3-5 and 3-6 are seemingly negligible. Also the experimental results are thought to be in reasonable agreement with the calculated ones.

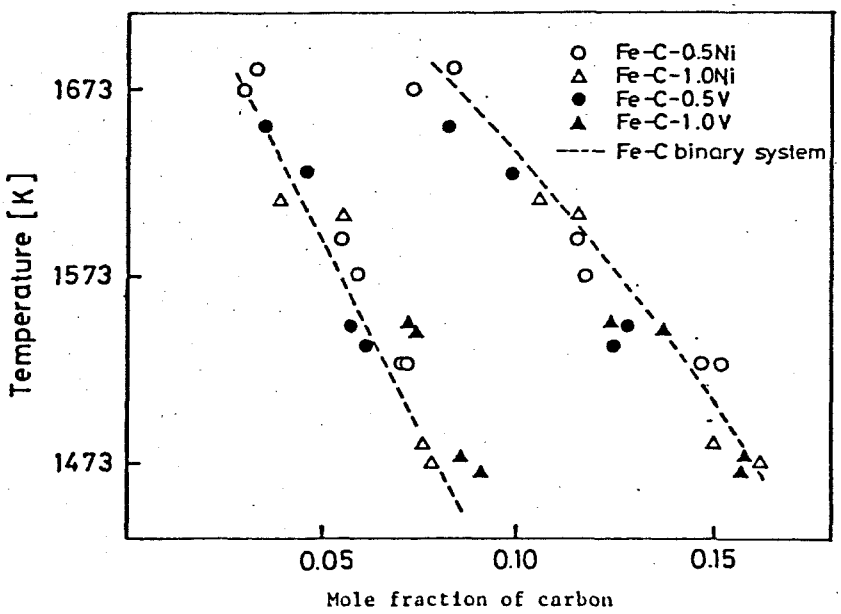

Fig.3-4 Carbon distribution between austenite and liquid phases in Fe−C−Ni and Fe−C−V systems.

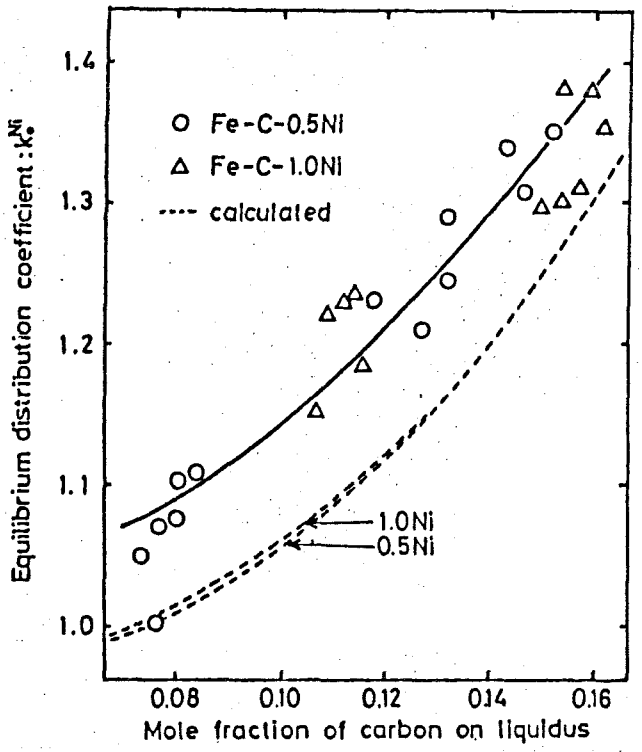

Fig.3-5 Change of k_o^{Ni} of Ni in Fe-C -Ni alloys with carbon concentration on liquidus.

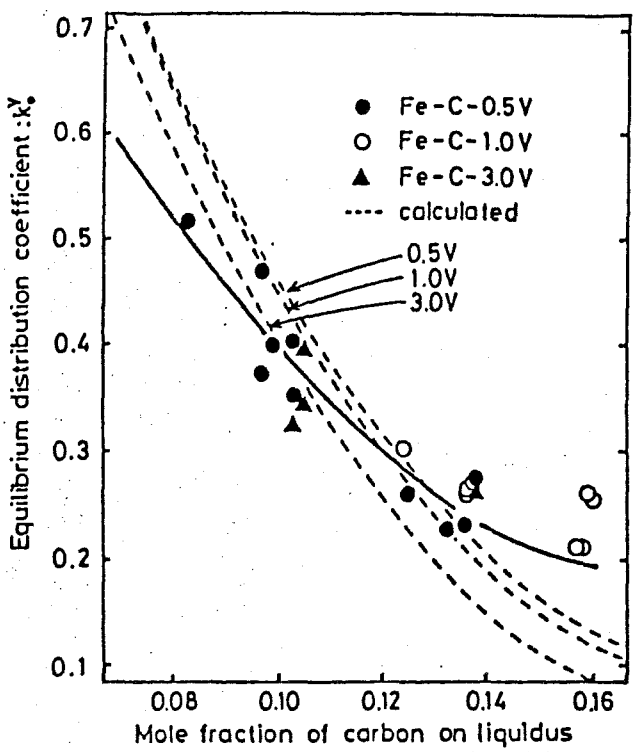

Fig.3-6 Change of k_o^{V} of V in Fe-C -V alloys with carbon concentration on liquidus.

3.4 Discussion.

In this section, the equilibrium distribution coefficient was discussed thermodynamically in order to clarify the controlling factor of solute distribution between solid and liquid phases in iron alloys and the effects of carbon on the equilibrium distribution coefficients of the third elements in Fe−C base alloys.

3.4.1 Thermodynamic Treatment of Equilibrium Distribution Coefficient k_o^X and the Periodicity of k_o^X of Solute X against Atomic Number in Iron Alloys.

Equilibrium between liquid and solid phases in an iron-rich alloy is represented by Eqs.(3-1) to (3-3) as stated in chapter 2.

$$\mu_X^l = \dot{\mu}_X^l + RT\ln(\gamma_X^l N_X^l) \qquad (3\text{-}1)$$

$$\mu_X^S = \dot{\mu}_X^S + RT\ln(\gamma_X^S N_X^S) \qquad (3\text{-}2)$$

$$\mu_X^l = \mu_X^s \qquad (3\text{-}3)$$

where, μ_X : chemical potential of X

μ_X : chemical potential of X in standard state

N_X : mole fraction of X

γ_X : activity coefficient of X

R : gas constant

T : absolute temperature

superscripts l and s: liquid state and solid state.

From Eq. (3-3) of the equilibrium condition, the equilibrium distribution coefficient of X, k_0^X , is derived as follows.

$$k_0^X = N_X^s / N_X^l$$
$$= \exp\{(\mu_X^l - \mu_X^s)/RT\} \exp(\ln\gamma_X^l - \ln\gamma_X^s) \qquad (3\text{-}4)$$

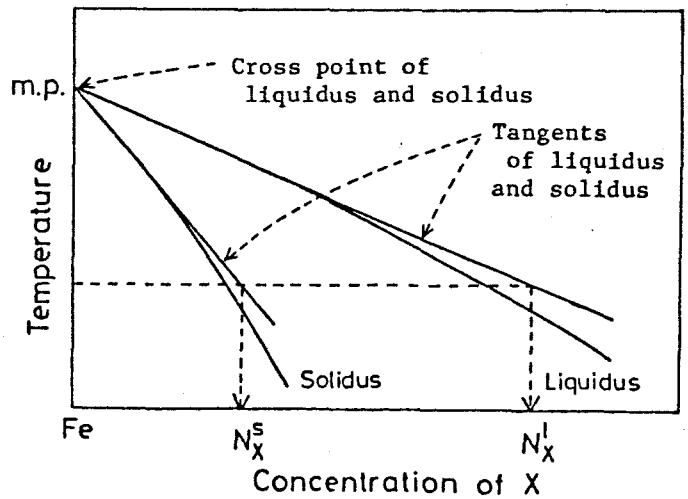

Fig.3-7 Sketch of solidus and liquidus near the melting point of iron.

Generally, when the equilibrium distribution coefficient is read from the phase diagram, the value obtained from the tangents of the solidus and the liquidus at their cross point, that is to say, the point $N_X^{l\,or\,s} \longrightarrow 0$ as sketched in Fig.3-7, is regarded to be valid near the melting point of iron. Then, as

$N_X^{l \text{ or } s} \longrightarrow 0$, Eq. (3-4) can be simplified to

$$(\ln k_0^X)_{Nx\to 0} = (N_X^s / N_X^l)_{Nx\to 0}$$
$$= \exp\{(\dot{\mu}_X^l - \dot{\mu}_X^s)/RT\} \exp(\ln \dot{\gamma}_X^l - \ln \dot{\gamma}_X^s) \quad (3\text{-}5)$$

where, $\dot{\gamma}_X$ is the activity coefficient of element X at the infinite dilution.

In Bragg-Williams approximation, the activity coefficient of element X in a binary system of Fe-substitutional element X is given by

$$\ln \gamma_X = \{W_{Fe\text{-}X}(1 - N_X)\}/RT \quad (3\text{-}6)$$

and in system of Fe-interstitial element X binary one

$$\ln \gamma_X = (W_{Fe\text{-}X} + 2N_X \chi_X)/RT \quad (3\text{-}7)$$

where, W and χ represent the interchange energy between Fe and X, and the binding energy of solute X, respectively.

As $N_X \longrightarrow 0$ in Eqs.(3-6) and (3-7), both these equations are expressed as

$$(\ln \gamma_X)_{Nx\to 0} = \ln \dot{\gamma}_X = W_{Fe\text{-}X}/RT \quad (3\text{-}8)$$

Substituting Eq.(3-8) into Eq.(3-5) gives

$$(\ln k_0^X)_{Nx\to 0} = (N_X^s / N_X^l)_{Nx\to 0}$$
$$= \exp\{(\dot{\mu}_X^l - \dot{\mu}_X^s)/RT\} \exp\{(W_{Fe\text{-}X}^l - W_{Fe\text{-}X}^s)/RT\} \quad (3\text{-}9)$$

It is obvious from Eq. (3-9) that the equilibrium distribution coefficient of solute element X at the infinite dilution consists of the free energy of fusion of element X and the difference between the interchange energies of Fe−X in liquid phase and in solid one. Also these energies are dependent

upon only the properties of element X. Then, in order to examine the above results the change of equilibrium distribution coefficient of element X with its atomic number is considered.

The equilibrium distribution coefficients of element X in iron alloys published by other investigators[7] are plotted against the atomic number of the element X in Fig.3-8. As exhibited in this figure, the equilibrium distribution coefficients of element X are thought to change periodically against atomic number. Then, this periodical change will be discussed through the comparison with the above equation (3-9).

First of all, the calculated free energy of fusion of each element at the melting point of iron is shown in Fig.3-9(A). It is obvious from this figure that the free energy of fusion changes periodically against the atomic number of the element.

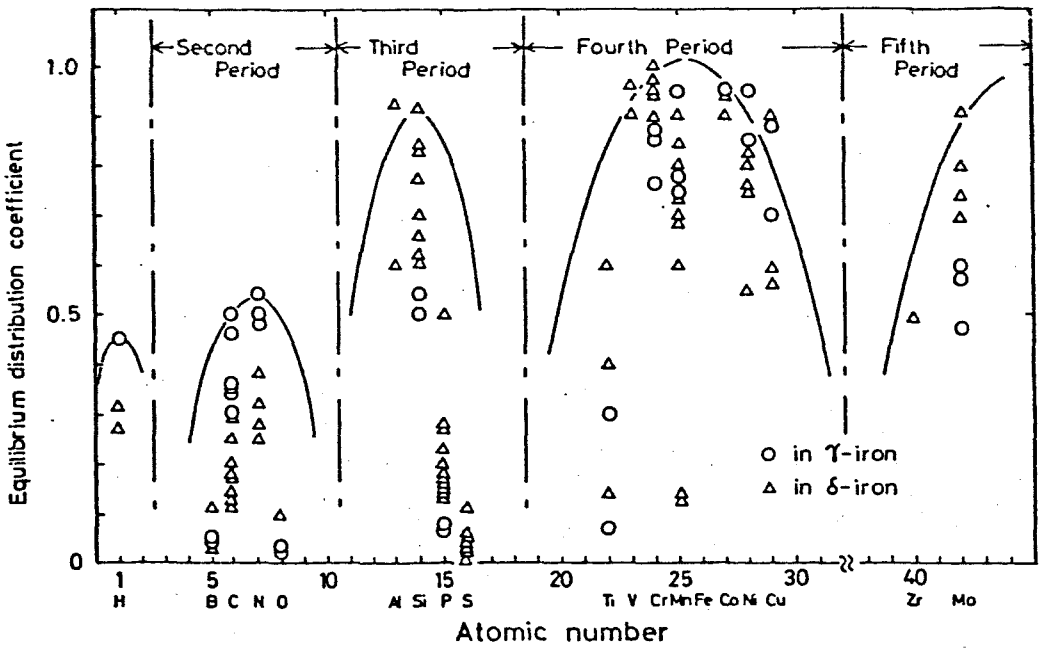

Fig.3-8 Change of equilibrium distribution coefficients in iron alloys with atomic number.

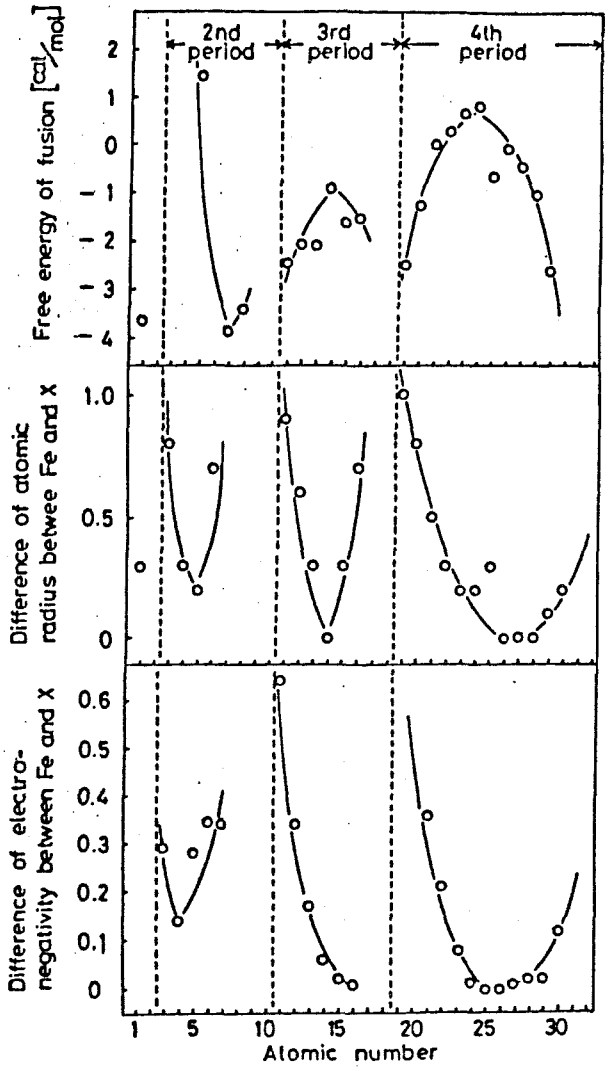

Fig.3-9 Periodicity for free energy of fusion of element X and difference of atomic radius and electronegativity between Fe and X.

Generally, the interchange energy is considered to be dependent upon both the differences in the atomic size (size factor) and the chemical property (chemical factor). For example, Mott[8] proposed the following equation as the interchange energy between A and B elements.

$$W_{A-B} = V_M \cdot (\delta_A - \delta_B)^2 - 23060\ n\ (\chi_A - \chi_B)^2 \qquad (3\text{-}10)$$

where, V_M : atomic volume of the alloy

δ : solubility parameter

χ : electronegativity

n : number of A−B boding.

Therefore, the differences of the atomic radius as the size factor and the electronegativity as the chemical factor between Fe and a solute element are taken into account and plotted against the atomic number of the element, respectively, in Figs.3-9(B) and (C). As exhibited in these figures, both the size factor and the chemical one also change periodically against the atomic number, and this fact suggests the existence of a physical periodicity in interchange energy.

Thus, from the foregoing Eq. (3-9) it is considered reasonable that the equilibrium distribution coefficients of the solute element in iron base alloys change periodically against the atomic number of the element.

Consequently, the free energy of fusion of element X and the difference of interchange energy between Fe and element X are considered to be the fundamental factors controlling the equilibrium distribution of the element X in iron alloys.

3.4.2 Factors controlling Equilibrium Distribution Coefficient of Solute Elements in Iron Base Binary Alloys.

In the foregoing section, the quantity ($W^{l}_{Fe-X} - W^{s}_{Fe-X}$) was obtained as one of the factors controlling k_0 and mainly the effect of it on the periodicity of k_0^X was discussed. In this section, $(W^{l}_{Fe-X} - W^{s}_{Fe-X})$ is discussed furthermore. In infinite dilution of the solute in iron alloy, the equilibrium distribution coefficient of a solute element X, k_0^X is written in the following equation as described before.

$$(k_0^X)_{Nx\to 0} = (N_X^S / N_X^l)_{Nx\to 0}$$
$$= \exp\{(\dot{\mu}_X^l - \dot{\mu}_X^S)/RT\} \exp\{(W^{l}_{Fe-X} - W^{s}_{Fe-X})/RT\} \quad (3\text{-}11)$$

($W^{l}_{Fe-X} - W^{s}_{Fe-X}$) might be derived from the thermodynamical properties of the components. Several studies[8~11] have been reported to derive the excess energies in liquid alloys from the thermodynamical properties of their components deductively. For example, Mott gave the foregoing equation (3-10) and described that the excess energy could be determined by the electronegativity and solubility parameter of the components. Also, Miedema et al.[11] recently showed that the excess energy in liquid solution consists of the work function and the electron density at the boundary of Wigner-Seitz cell.

About the excess energy in solid solution, Simoji et al.[10] and Miedema et al. stated that there is an essential difference between solid and liquid solutions. In solid solution, where atoms of different sizes have to occupy equivalent lattice positions, an additional positive contribution to the excess energy arises, due to the elastic deformations necessary to accommodate the size mismatch. In liquid solution such a size mismatch energy makes a less dominant contribution to the excess energy than in solid solution.

Hence, when the difference of the excess energy between solid and liquid solution is discussed, it is considered that $(W^{l}_{Fe-X} - W^{s}_{Fe-X})$ is nearly equal to the size mismatch energy in solid solution. Namely,

$$(W^{l}_{Fe-X} - W^{s}_{Fe-X})$$

$$\fallingdotseq -(\text{ the size mismatch energy in solid solution }) \qquad (3\text{-}12)$$

in which the size mismatch energy ΔE_{SIZE} can be estimated from the elastic constants and the relative size difference of the two metals, using Eshelby's elastic continuum theory.[12]

$$\Delta E_{SIZE} \propto \overline{B V_m} \times \delta^2 \qquad (3\text{-}13)$$

where $\overline{B V_m}$ is the average value of the product of bulk modulus and molar volume, and δ is the relative size difference defined as

$$\delta = (V^{1/3} - V^{1/3}) / (V^{1/3} + V^{1/3}) \qquad (3\text{-}14)$$

Substitution of Eqs.(3-12) and (3-13) into (3-11) gives

$$RT \ln k_0 - (\mu^{l}_{X} - \mu^{s}_{X}) \propto -\overline{B V_m} \times \delta^2 \qquad (3\text{-}15)$$

Then, the relation in Eq.(3-15) is discussed when the solute elements are the substitutional transition elements in iron alloys. The results are illustrated in Fig.3-10. In this figure, a plot of $\{RT\ln k^{X}_{0} - (\mu^{l}_{X} - \mu^{s}_{X})\}$ with $\overline{B V_m} \times \delta^2$ is shown for various elements. It is obvious from this figure that transition elements are nearly satisfied with the relation in Eq.(3-15). Thus, the size mismatch energy is considered as one of the factors governing the equilibrium distribution coefficient of the solute in iron base binary alloys.

Figure 3-11 indicates the variation of $\{RT\ln k^{X}_{0} - (\mu^{l}_{X} - \mu^{s}_{X})\}$ with $\overline{B V_m} \times \delta^2$ for the semi-metals and the noble metals as solute elements together with the results for transition metals as shown in Fig.3-10. As can be seen from this figure, these metals except transition ones are not satisfied with the

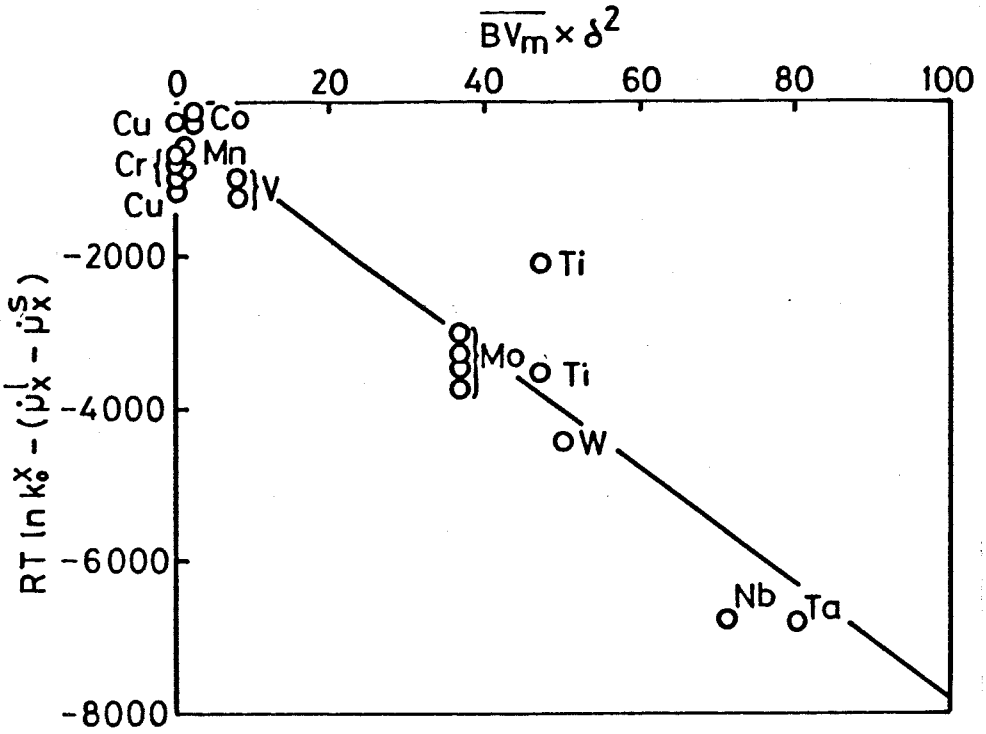

Fig.3-10 Relation between $RT \ln k_0^x - (\mu_x^l - \mu_x^s)$ and $\overline{BVm} \times \delta^2$ for substitutional transition elements as solute in iron base alloys.

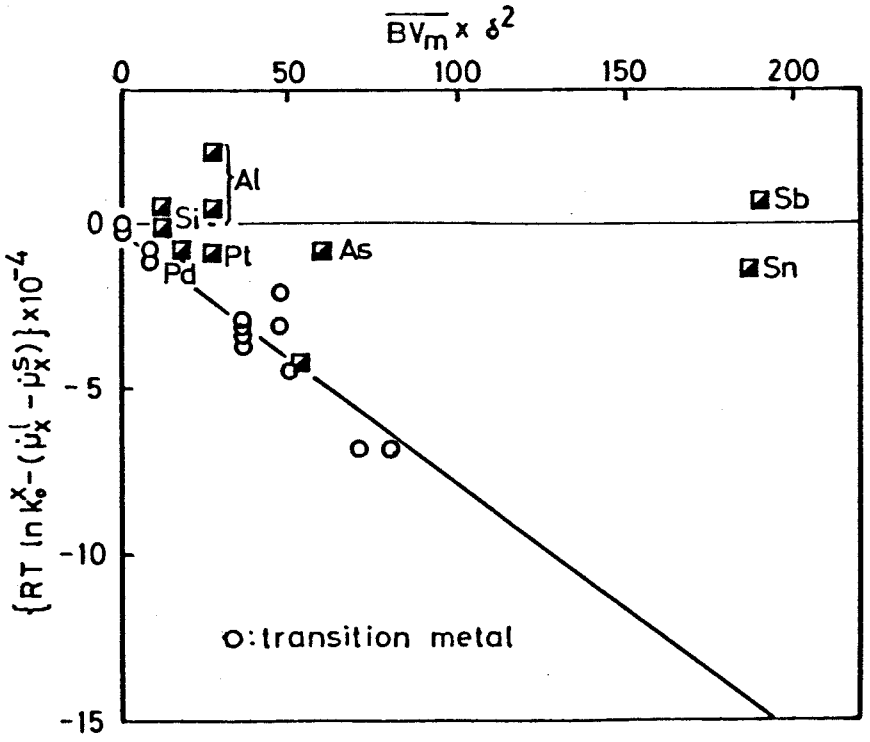

Fig.3-11 Relation between $RT \ln k_0^x - (\mu_x^l - \mu_x^s)$ and $\overline{BVm} \times \delta^2$ for semi-metals and noble metals as solute in iron base alloys.

relation in Eq.(3-15). In other words, it is considered that another excess energy ΔE, which is represented in the following equation (3-16), is influenced on k_0 together with the size mismatch energy for the semi-metals and noble metals.

$$RT\ln k_0^x = (\dot{\mu}^l - \dot{\mu}^s) + (W^l_{Fe-x} - W^s_{Fe-x}) + \Delta E$$
$$\Delta E > 0 \qquad (3\text{-}16)$$

Hereupon, it should be necessary to refer to the excess energy ΔE in Eq.(3-16). According to Miedema et al., an additional energy is required to describe the excess energy between the semi metals or the noble metals and the transition metals. That is to say,

$$W_{A-B} \propto \{-P\ (\Delta\phi)^2 + Q\ (\Delta n)^2 - R\} \qquad (3\text{-}17)$$

where, ϕ and n are the work function and the electron density at the boundary of Wigner-Seitz cell of the components, respectively. P and Q are the constants to be determined empirically. R is required for the alloys which consist of semi metals or noble metals - transition metals but it is negligible for transition metals - transition metals alloys. They also reported

$$R^l < R^s \qquad (3\text{-}18)$$

In this case,

$$\Delta E = (-R^l) - (-R^s) > 0 \qquad (3\text{-}19)$$

which satisfies Eq.(3-16). However, Miedema et al. have not described the physical meanings about the parameter R.

Consequently, the problems of ΔE are obviously related to the structure and thermodynamical properties of alloys in both solid and liquid phases and more detail studies are needed for further discussion in the near future.

The relation in Eq.(3-15) is discussed for the interstitial elements in

iron alloys. However, in this case, Eq.(3-14) must be rewritten for the these elements because these elements dissolute into the interstitial sites and the size mismatch is not due to the difference of the radius between solute and solvent atoms. Then, the difference between half of the interatomic distance of iron r and the radius of the interstitial atom, r_0 is used instead of δ as shown in Fig.3-12.

Figure 3-13 represents a plot of $RT\ln k_0$ with $(r - r_0)$ for B, C and N. From this figure, the size mismatch energy is considered to be the important factor to affect k_0 also for the interstitial elements.

Figures 3-14 and 3-15 show the variation of $RT\ln k_0^X - (\mu_X^l - \mu_X^s)$ with $\overline{BV_m} \times \delta^2$ for transition metals as solute elements in Co and Ni base alloys, respectively. Also in these alloys, the size mismatch energy is thought as the factor governing k_0, as described in iron alloys.

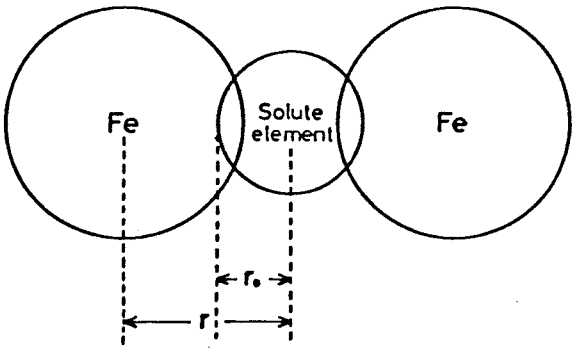

Fig.3-12 Relation between r and r_0.

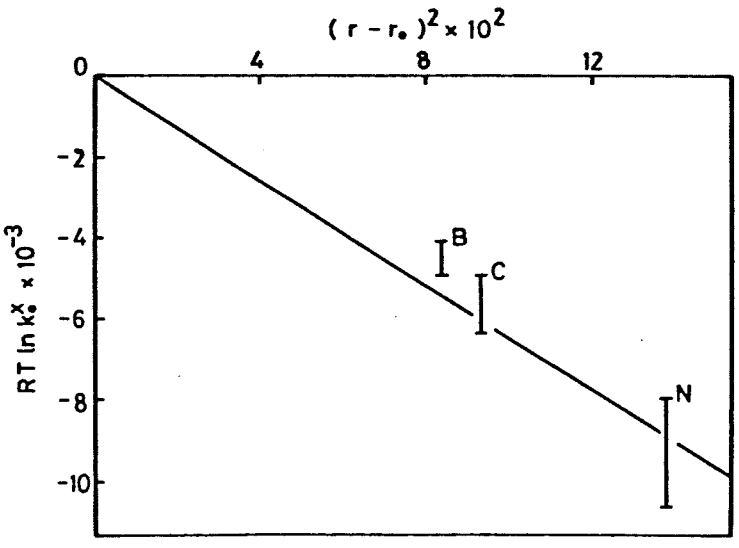

Fig.3-13 Rekation $RT\ln k_0^X$ and $(r - r_0)^2$.

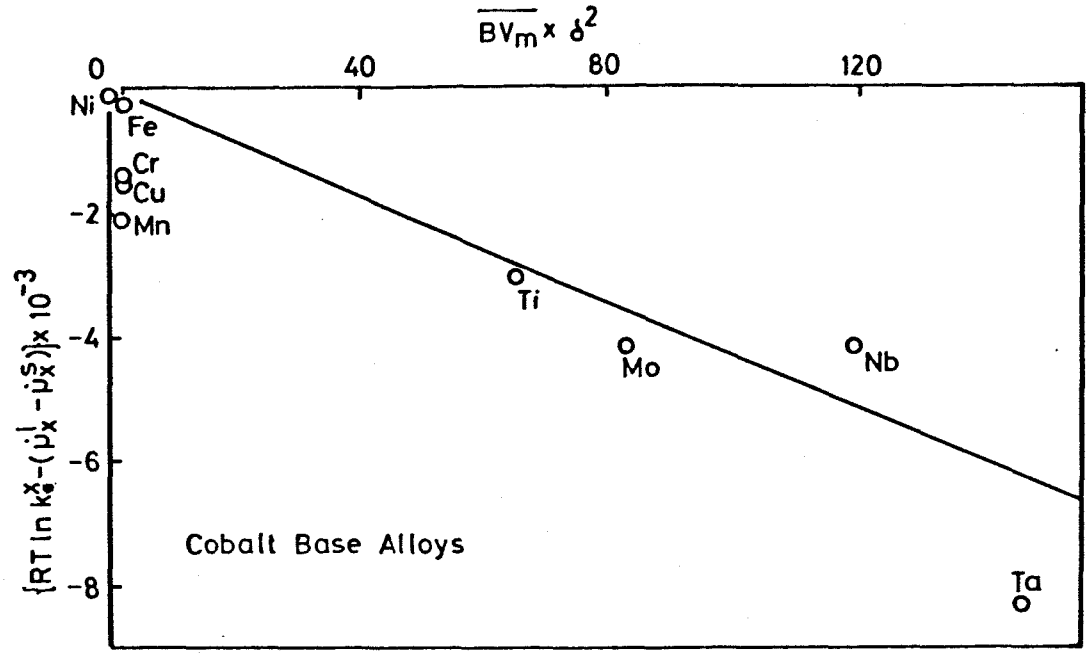

Fig.3-14 Relation between $RT \ln k_0^x - (\mu_x^l - \mu_x^s)$ and $\overline{BVm} \times \delta^2$ for substitutional transition metals as solute in Co base alloys.

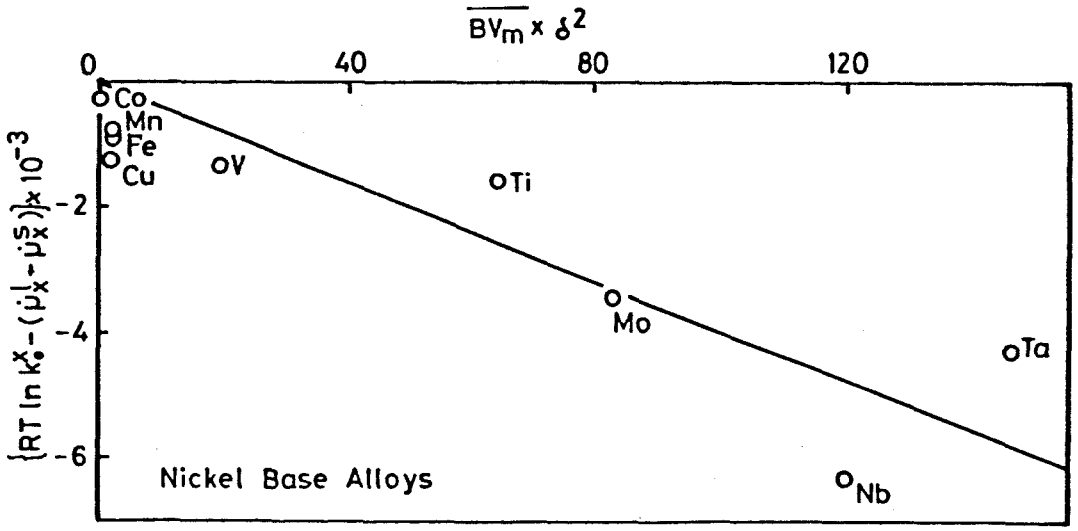

Fig.3-15 Relation between $RT \ln k_0^x - (\mu_x^l - \mu_x^s)$ and $\overline{BVm} \times \delta^2$ for substitutional transition metals as solute in Ni base alloys.

3.4.3. Equilibrium Distribution Coefficient of the Third Element in Fe−C Base Ternary Alloys.

The foregoing experimental results of this work showed that k_0^{Ni} in Fe−C−Ni system increased and k_0^{V} in Fe−C−V system decreased with the increasing carbon content. In this section let us examine these results thermodynamically.

Equation (3-4) can also be applied for the equilibrium distribution coefficient of element X in Fe−C−X ternary system. In this case, the effect of carbon must be included in the activity coefficient γ_X of element X in Eq.(3-4). Then, to consider the effect of C, the activity coefficient of element X can be expressed in terms of the interaction parameter ε as follows:

$$\ln \gamma_X = \ln \dot{\gamma}_X + \varepsilon_X^X N_X + \varepsilon_X^C N_C \qquad (3\text{-}20)$$

where, ε_X^X : self-interaction parameter of element X

ε_X^C : interaction parameter of C on X

By substituting Eq.(3-20) and the relations $N_X^s = k_0^X \cdot N_X^l$ and $N_C^s = k_0 \cdot N_C^l$ into Eq.(3-4), the equilibrium distribution coefficient of element X in Fe−C−X ternary system is represented by

$$\ln k_0^X = (\dot{\mu}_X^l - \dot{\mu}_X^s) + \ln \dot{\gamma}_X^l / \dot{\gamma}_X^s + (\varepsilon_X^{X,l} - \varepsilon_X^{X,s} k_0^X) N_X^l + (\varepsilon_X^{C,l} - \varepsilon_X^{C,s} k_0^C) N_C^l \qquad (3\text{-}21)$$

Here, the first and the second terms show the fundamental factor controlling k_0^X, the third and the fourth terms denote the concentration dependences of X and C, respectively, on k_0^X. Thus k_0^X can be calculated by substituting thermodynamical data into Eq.(3-21). The calculated k_0^{Ni} and k_0^{V} are shown in Figs.3-5 and 3-6 with the experimental ones. The thermodynamical data used in the above calculation are given in Table 3-3.[13~20]

Now, let us call attention to the fourth term in the right-hand side of Eq.(3-21). Mori and Ichise[24] proposed that there exists a linear relation of ε_X^C in solid and liquid phases, $\varepsilon_X^{C,s} = m \cdot \varepsilon_X^{C,l}$, in iron-nitrogen-X systems. The value m, which is not strictly equal to unity, is considered to be related to the difference of the structure between solid and liquid phases. Then, this treatment has been applied for Fe−C−X systems. The relations of some elements X between $\varepsilon_X^{C,l}$ in liquid phase[13] and $\varepsilon_X^{C,s}$ in solid one[13~16,18,23] are shown in Fig.3-16. In this figure, it is obvious that a linear relation holds approximately between $\varepsilon_X^{C,l}$ and $\varepsilon_X^{C,s}$. This relation obtained by the least square method is given as

$$\varepsilon_X^{C,s} = 0.925 \cdot \varepsilon_X^{C,l} \qquad (3\text{-}22)$$

Table 3-3 Thermodynamical data for calculating k_0^{Ni} and k_0^V.

		Austenite	Ref.	Liquid	Ref.
Nickel	$\ln \dot{\gamma}_{Ni}$	-0.386 (1573K), $-\frac{607}{T}$ *2	(14)	-0.416 (1873K), $-\frac{773}{T}$ *2	(13)
	ε_{Ni}^{Ni}	$\frac{1200}{T}$	*1	$\frac{1560}{T}$	*1
	ε_C^{Ni}	$\frac{4640}{T} + 0.65$	(15)	2.85 (1873K), $\frac{5340}{T}$ *2	(13)
	$\dot{\mu}_{Ni}^l - \dot{\mu}_{Ni}^\gamma = 21.6 \cdot T + 0.90\times10^{-3} \cdot T^2 - 3.2 \cdot T \cdot \ln T + 1257$ (Ref.(20))				
Vanadium	$\ln \dot{\gamma}_V$	-3.10 (1273K) α phase), $-\frac{3950}{T}$ *2,*3	(22)	-1.80 (1873K), $-\frac{3360}{T}$ *2	(17)
	ε_V^V	$\frac{7900}{T}$	*1	3.23 (1873K), $\frac{6050}{T}$ *2	(13)
	ε_C^V	-18.4 (1273K), $-\frac{23400}{T}$ *2	(16)	-16.1 (1873K), $-\frac{30100}{T}$ *2	(13)
*3	$\dot{\mu}_V^l - \dot{\mu}_V^\alpha = 48.6 \cdot T + 1.29\times10^{-3} \cdot T^2 - 0.1\times10^5 \cdot T^{-1} - 6.45 \cdot T \cdot \ln T - 3935$ (Ref.(20))				
Carbon	$\ln \dot{\gamma}_C$	$\frac{8680}{T} + 2.72 \ln T - 24.3$	(18)	$\frac{2720}{T} - 2.00$	(19)
	ε_C^C	$\frac{8980}{T} + 3.00$	(18)	$\frac{7830}{T} + 3.66$	(19)

*1 estimated from the equation $\varepsilon_X^X = -2 \ln \dot{\gamma}_X$ *2 Temperature dependence is estimated in this work.

*3 The value of the term $\{ (\dot{\mu}_V^l - \dot{\mu}_V^\gamma) + RT \ln \dot{\gamma}_V^l / \dot{\gamma}_V^\gamma \}$ in liq. − γ phase equilibrium is calculated from the equation:

$\{ (\dot{\mu}_V^l - \dot{\mu}_V^\gamma) + RT \cdot \ln \dot{\gamma}_V^l / \dot{\gamma}_V^\gamma \} = \{ (\dot{\mu}_V^l - \dot{\mu}_V^\alpha) + RT \cdot \ln \dot{\gamma}_V^l / \dot{\gamma}_V^\alpha \} + \{ (\dot{\mu}_V^\alpha - \dot{\mu}_V^\gamma) + RT \cdot \ln \dot{\gamma}_V^\alpha / \dot{\gamma}_V^\gamma \}$

in liq. − γ equilibrium in liq. − α equilibrium in α − γ equilibrium

where the last term is equal to ($RT \ln k_o^V(\alpha-\gamma) = RT \ln N_V^\gamma / N_V^\alpha$ in Fe-V binary system)$_{N_V \to 0} = -0.577 \cdot T$ (Ref.(21)).

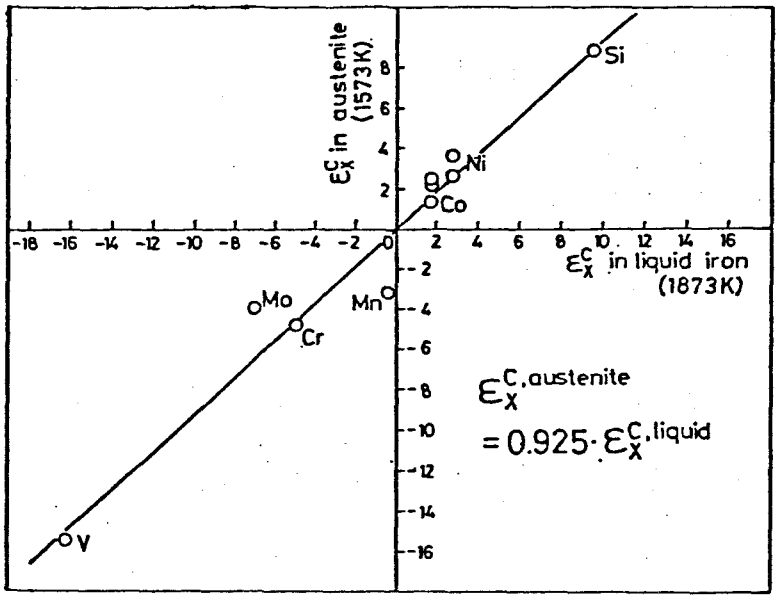

Fig.3-16 Relation between $\varepsilon_X^{C,l}$ in liquid and $\varepsilon_X^{C,s}$ in austenite.

Substituting Eq.(3-22) into the fourth term in the right-hand side of Eq.(3-21) yields

$$(\varepsilon_X^{C,l} - \varepsilon_X^{C,s} k_0^C) N_C^l = (1 - 0.925\ k_0^C) \varepsilon_X^{C,l} N_C^l \qquad (3\text{-}23)$$

As the equilibrium distribution coefficient of C, k_0^C , takes the value smaller than unity,

$$(1 - 0.925\ k_0^C) > 0 \qquad (3\text{-}24)$$

It is obvious from Eqs.(3-21) and (3-23) that since ε_X^C is positive for the element X with the repulsive effect against C, the value of the fourth term in the right-hand side of Eq.(3-21) becomes positive and the k_0^X increases with the increasing C content. On the other hand, since ε_C^X is negative for the element X with the attractive effect against C, the value of the fourth term of Eq.(3-21) becomes negative and the k_0^X decreases with the increasing C

content.

Figure 3-17 shows plots of the present experimental results, k_0^{Ni} and k_0^{V} as a function of the carbon content, together with k_0^{X} for some kinds of elements published by other workers.[1~3,25~30] As illustrated in this figure, in Fe−C−Ni, Fe−C−Si and Fe−C−Co systems, k_0^{Ni}, k_0^{Si} and k_0^{Co} increase with the increasing C content because these elements denote the repulsive effect against C. While V, Mn and Cr indicate the attractive effect in Fe−C base alloy systems, so k_0^{V}, k_0^{Mn} and k_0^{Cr} decrease with the increasing carbon content. Thus, the present experimental results could be understood as described above.

Consequently, the fourth term in the right-hand side of Eq.(3-21) can be expected as an important factor controlling the variation of k_0^{X} as a function of the carbon content in Fe−C−X alloys.

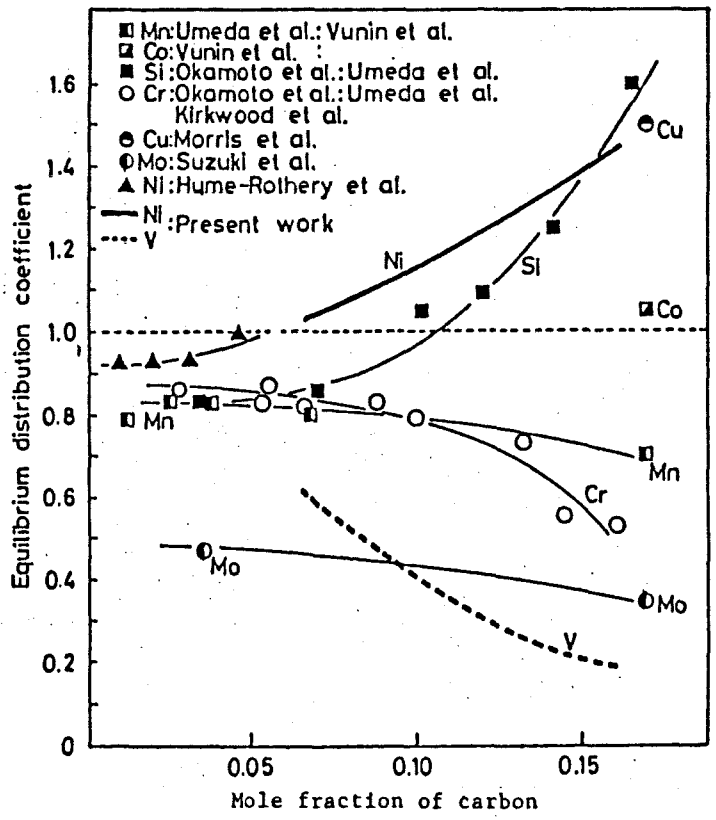

Fig.3-17 Change of equilibrium distribution coefficients of some elements with carbon concentration in iron-carbon base alloys.

Moreover, in order to investigate the fourth term of Eq.(3-21) the influence of C on k_0^X is intended to be estimated quantitatively in terms of free energy. Namely, multiplying each term in Eq.(3-21) by RT where R is the gas constant and T is the absolute temperature, we derive

$$\begin{aligned} RT\ln k_0^X = (\dot{\mu}_X^l - \dot{\mu}_X^s) + RT\ln \dot{\gamma}_X^l / \dot{\gamma}_X^s \\ + RT\,(\varepsilon_X^{X,l} - \varepsilon_X^{X,s} k_0^X)\, N_X^l \\ + RT\,(\varepsilon_X^{C,l} - \varepsilon_X^{C,s} k_0^C)\, N_C^l \end{aligned} \qquad (3\text{-}25)$$

We define the physical meaning of each term in this equation as follows:

The left-hand term: the energy to let X distribute by the ratio k_0^X into liquid and solid phases.

The first and second terms of the right-hand side: the energy controlling distribution of X fundamentally.

The third term: the energy depending on the X content.

The forth term: the energy depending on the interaction of C on X.

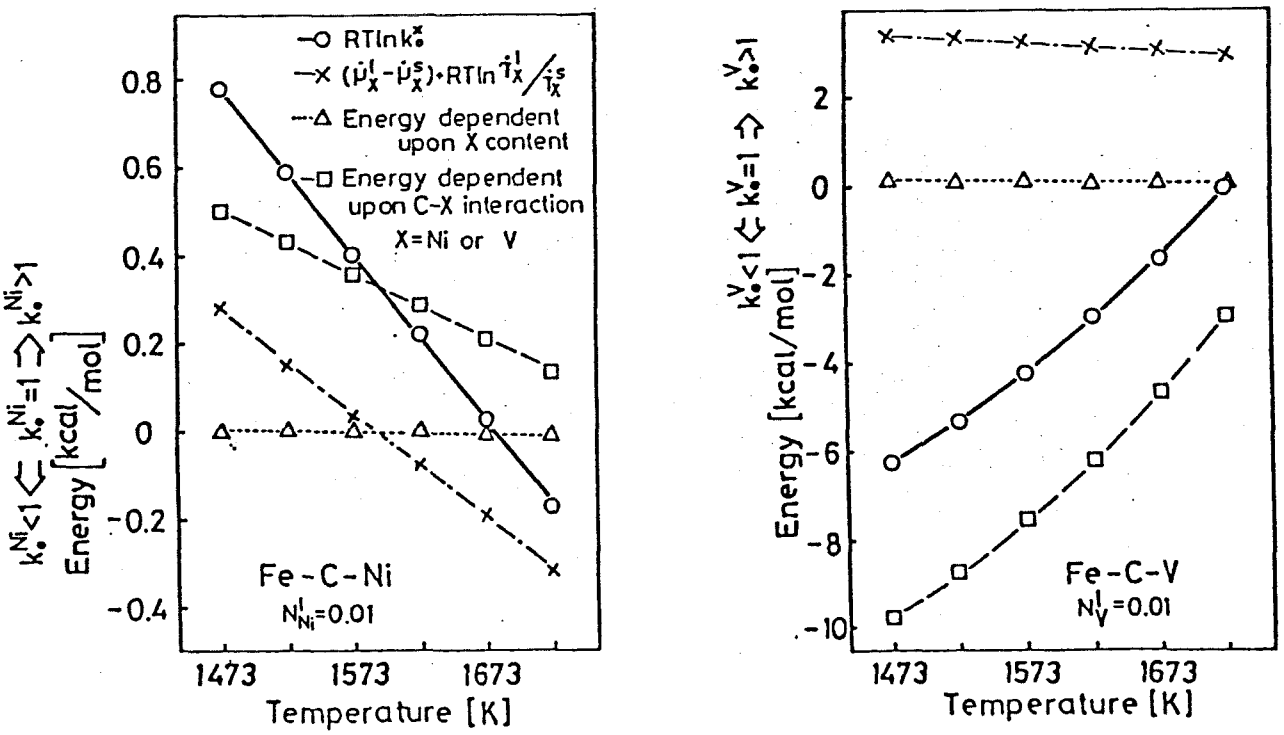

Fig.3-18 Change of energy components concerning the distributions of Ni and V between solid and liquid with temperature.

Figure 3-18 depicts the variation of the calculated energies of each term in Eq.(3-25) as a function of temperature in Fe−C−Ni and Fe−C−V systems, respectively. It is clear from this figure that the energy depending on the interaction of C on Ni and V is the most dominant factor among these energies related to $RT\ln k_0^X$.

3.5 Conclusion.

In order to investigate nickel and vanadium distribution between the solid and liquid phases in Fe−C base ternary systems, austenite-liquid phases equilibrated in the temperature range from 1453 to 1693 K were quenched and the nickel and vanadium and carbon concentrations in each phase were analysed by EPMA to obtain the equilibrium distribution coefficients of these solutes. Moreover, the factors which control the equilibrium distribution between solid and liquid phases in iron alloys were discussed thermodynamically. The results obtained are summarized as follows:

① The fundamental factors controlling the equilibrium distribution of solute element in iron alloys are the free energy of fusion of the solute element and the difference of the interchange energy of iron with the solute element between the solid and liquid phases.

② The difference of the interchange energy of iron with the solute element between solid and liquid phases is dependent upon the size mismatch energy in solid solution for transition metals and interstitial elements as solute element but for semi-metals and noble ones, the difference of another excess energy between solid and liquid phases is required together with the size mismatch energy.

③ In iron base binary alloys the equilibrium distribution coefficient of the solute element changes periodically against the atomic number of the element

④ Particularly, in Fe−C base ternary alloys the most important factor controlling the equilibrium distribution of the 3rd element X is the interaction energy between C and X.

⑤ In Fe−C base ternary alloys, with the increasing carbon content the equilibrium distribution coefficient of the 3rd element X, k_0^X increases for the repulsive interaction between C and X while k_0^X decreases for the attractive one.

3.6 References.

1) S.Suzuki, T.Umeda and Y.Kimura: The 19th Comm. (Solidification), Japan Soc. Promotion Sci. (JSPS), Rep. No. 19-10254, (May,1980).

2) A.Kagawa and T.Okamoto: Metal Sci., 14 (1980), 519.

3) A.J.W.Ogilvy, A.Ostrowskii and D.H.Kirkwood: Metal Sci., 15 (1981), 168.

4) A.Kagawa, K.Iwata and T.Okamoto: The Abstract for the 88th Lecture Meeting of Japan Institute of Metals, JIM, Sendai, (1981), 274.

6) H.Wada and T.Saito: J.Japan Inst. Metals: 25 (1961), 159.

7) T.Takahashi, M.Kudo and K.Ichikawa: Solidification of Iron and Steel, A Data Book on the Solidification Phenomena of Iron and Steel, ed. by Solidification Comm., joint Soc. Iron Steel Basic Research of ISIJ, ISIJ, Tokyo, (1977). (Appendix).

8) B.W.Mott: Phil. Mag., 2 (1957), 259.

9) J.H.O.Varley: Phil. Mag., 45 (1954),887

10) M.Shimoji and K.Niwa: Acta. Met., 5 (1957), 496

11) A.R.Miedema, P.F. de Chatel and F.R. de Boer: Physica 100B (1980),1

12) D.J.Eshelby: Solid State Physics 3, F.Seitz and D.Turnbull, eds. (Academic Press, New York, 1956), 79

13) G.K.Sigworth and J.F.Elliott: Metal Sci., 8 (1974), 298.

14) E.J.Grinsey: J. Chem. Thermo., 9 (1979), 415.

15) T.Wada, H.Wada, J.F.Elliott and J.Chipman: Met. Trans., 2 (1971), 2199.

16) J.Chipman and J.F.Elliott: Trans. Met. Soc. AIME, 242 (1968), 35.

17) T.Furukawa and E.Kato: Tetsu-to-Hagane, 61 (1975), 3050.

18) S.Ban-ya, J.F.Elliott and J.Chipman: Met. Trans., 1 (1970), 1313.

19) J.Chipman: Met. Trans., 3 (1972), 55

20) O.Kubaschewski and C.B.Alcock: Metallurgical Thermochemistry, 5th ed., Pergamon Press, New York, (1979),336.

21) T.Nishizawa and M.Hasebe: Tetsu-to-Hagane, 67 (1981), 2086.

22) R.Hultgren, P.D.Desai, D.T.Hawkins, M.Gleiser and K.K.Kelley: Selected Values of the Thermodynamic Properties of Binary Alloys, ASM, Ohio, (1973).

23) T.Wada, H.Wada, J.F.Elliott and J.Chipman: Met. Trans., 3 (1972), 2865.

24) T.Mori and E.Ichise: J. Japan Inst. Metals, 32 (1968), 949.

25) K.Parameswaran, K.Metz and A.Morris: Met. Trans., 10A (1979), 1929.

26) R.A.Buckley and W.Hume-Rothery: JISI, 197 (1964), 895.

27) B.A.Rickinson and D.H.Kirkwood: Met. Sci., 12 (1978), 138.

28) K.P.Vunin and U.N.Taran: On the Structure of Cast Iron, The New Japan Soc. Casting and Forging, Osaka, (1979)

29) A.Kagawa, S.Moriyama and T.Okamoto: J.Mat.Sci., 17 (1982), 135.

30) K.Suzuki, A.Taniguchi and K.Hirota: Tetsu-to-Hagane, 64 (1978), S606.

Chapter 4

Effects of Solute Interactions on the Equilibrium Distribution of Solute Elements between Solid and Liquid Phases in Iron Base Ternary Alloys.

4.1 Introduction.

The equilibrium distribution coefficients of some elements in ternary systems are considered to be different from those in binary systems because of the possible existence of solute interactions as described in the foregoing chapter, but the mechanisms are so complicated that any detailed information has not yet been obtained. So, it would be very useful if the effect of the addition of an alloying element on the distribution could be known by a simple equation which indicates such effects.

The purpose of this chapter is to derive an equation for the change of the equilibrium distribution coefficients with solute-interaction in iron base ternary system and to discuss the influences of the solute-interaction on the equilibrium distribution of some elements in Fe−C, Fe−N, Fe−H, Fe−P and Fe−S base ternary systems.

4.2 Derivation of an Equation describing the Effect of Solute Interaction on the Equilibrium Distribution Coefficient.

In this section, the equilibrium distribution coefficient is discussed thermodynamically in terms of activity coefficients, interaction parameters as described in the previous chapter. First of all, the equilibrium distribution coefficients of solute i in Fe−i binary and Fe−i−j ternary system, $k_0^{i,2}$ and $k_0^{i,3}$ are given by Eqs.(4-1) and (4-2), respectively.

$$\ln k_0^{i,2} = (\dot{\mu}_i^l - \dot{\mu}_i^s)/RT + \ln \dot{\gamma}_i^l / \dot{\gamma}_i^s + (\varepsilon_i^{i,l} - \varepsilon_i^{i,s} k_0^{i,2}) N_i^l \qquad (4\text{-}1)$$

$$\ln k_0^{i,3} = (\dot{\mu}_i^l - \dot{\mu}_i^s)/RT + \ln \dot{\gamma}_i^l / \dot{\gamma}_i^s + (\varepsilon_i^{i,l} - \varepsilon_i^{i,s} k_0^{i,3}) N_i^l + (\varepsilon_i^{j,l} - \varepsilon_i^{j,s} k_0^{j,3}) N_j^l \qquad (4\text{-}2)$$

where μ_i is the chemical potential of solute i in standard state, γ_i the activity coefficient of solute i at the infinite dilution, ε_i^i the self-interaction parameter of solute i, ε_i^j the interaction parameter of j on i, and superscripts l and s show liquid and solid states, respectively.

The fourth term in the right-hand side of Eq.(4-2) indicates the effect of alloying element j on the equilibrium distribution coefficient of solute i. As the parts from the first term to the third one in the right-hand side of Eq.(4-2) are equal to $k_0^{i,2}$ of Eq.(4-1), the following equations (4-3) and (4-4) are derived.

$$\ln k_0^{i,3} = \ln k_0^{i,2} + (\varepsilon_i^{j,l} - \varepsilon_i^{j,s} k_0^{j,3}) N_j^l \qquad (4\text{-}3)$$

$$\ln k_0^{i,3} / k_0^{i,2} = (\varepsilon_i^{j,l} - \varepsilon_i^{j,s} k_0^{j,3}) N_j^l \qquad (4\text{-}4)$$

The left-hand side of Eq.(4-4) shows the ratio of the equilibrium distribution coefficient of solute i in Fe−i−j ternary system to that in Fe−−i binary system and this ratio is considered as a parameter indicating the effect of the addition of the alloying element j on the equilibrium distribution coefficient of solute i. Then, the right-hand side of Eq.(4-4) is discussed furthermore.

In order to simplify the right-hand side of Eq.(4-4), the correlation between the interaction parameter of j on i in solid phase and that in liquid one was investigated. Figures 4-1 (A),(B) and (C) show the relations between $\varepsilon_i^{j,s}$ in solid phase[1~7] and $\varepsilon_i^{j,l}$ in liquid one[1,6,7] in Fe−C base (where i: C), Fe−H base (where i: H) and Fe−N base (where i: N) ternary systems, respectively. It is obvious from these figures that a linear relation holds approximately between $\varepsilon_i^{j,l}$ and $\varepsilon_i^{j,s}$ in each ternary system.

Mori et al.[6,7] proposed that in Fe−N, Fe−H base ternary systems, the gradients of these linear relations become unity as the temperature of

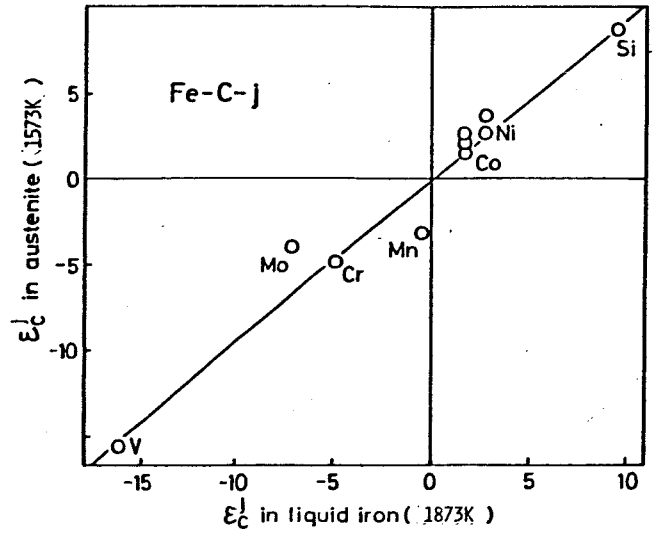

Fig.4-1(A) Relation between interaction parameter in liquid iron and that in austenite in Fe−C−j ternary system.

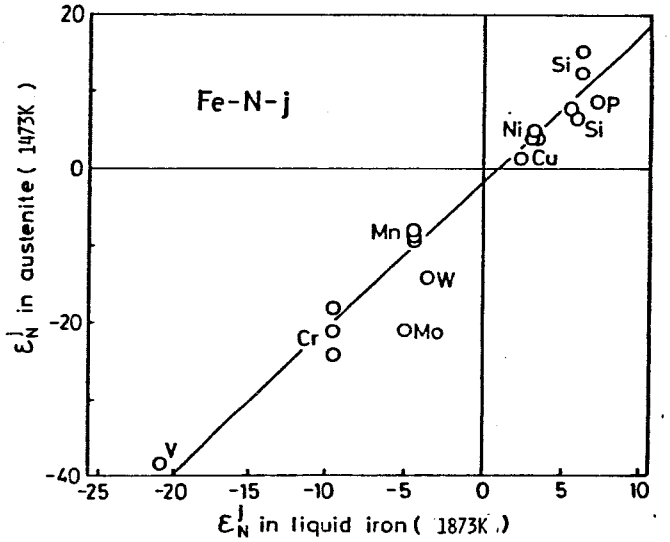

Fig.4-1(B) Relation between interaction parameter in liquid iron and that in austenite in Fe−N−j ternary system.

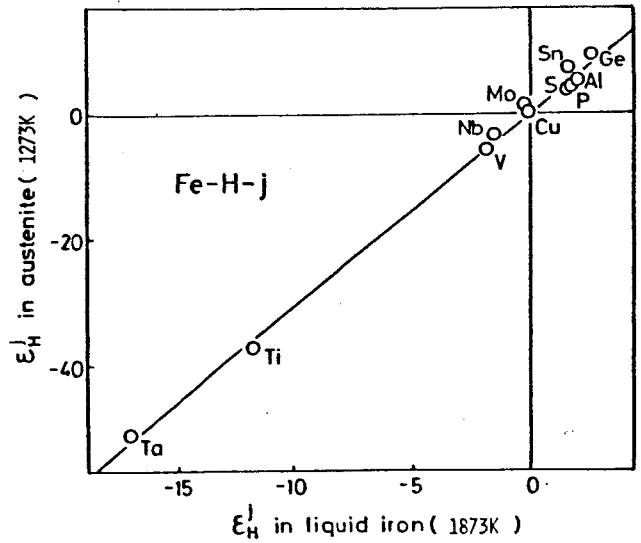

Fig.4-1(C) Relation between interaction parameter in liquid iron and that in austenite in Fe−H−j ternary system.

liquid phase approaches that of solid one. They also suggested that these gradients are not strictly equal to unity because of the difference of the structure in solid and liquid phases. Then, this relations are discussed here thermodynamically.

Based on the zeroth approximation of the quasi-chemical model, the activity coefficient at the infinite dilution and ε_i^j are derived as follows:[8)]

$$\ln \dot{\gamma}_i \ (\text{in Fe}) = W_{Fe-i} / RT \tag{4-5}$$

$$\varepsilon_i^j = (W_{i-j} - W_{Fe-i}) / RT \tag{4-6}$$

where W_{i-j} is the interchange energy. Also, the equilibrium distribution coefficient of solute i at the infinite dilution is represented by

$$(\ln k_0^i)_{Fe-i,Ni\to 0} = (\dot{\mu}_i^l - \dot{\mu}_i^s) / RT + \ln \dot{\gamma}_i^l / \dot{\gamma}_i^s \tag{4-7}$$

Combining these equations (4-5), (4-6) and (4-7), the difference between the interaction parameter in liquid phase and that in solid one, $\Delta\varepsilon$, is given by Eq.(4-8).

$$\begin{aligned} \Delta\varepsilon &= \varepsilon_i^{j,l} - \varepsilon_i^{j,s} \\ &= (\ln k_0^i)_{Fe-i,Ni\to 0} - (\ln k_0^i)_{j-i,Ni\to 0} \end{aligned} \tag{4-8}$$

As is obvious from Eq.(4-8), $\Delta\varepsilon$ can be obtained from the difference between the equilibrium distribution coefficient of solute i in Fe−i binary system and that in j−i binary one. Then, the relation between $\varepsilon_i^{j,l}$ in liquid phase and $\varepsilon_i^{j,s}$ in solid one which is given by using $\Delta\varepsilon$ in Eq.(4-8), i.e. $\varepsilon_i^{j,s} = \varepsilon_i^{j,l} - \Delta\varepsilon$ in iron-carbon base ternary systems is obtained as shown in Fig.4-2. This figure indicates that a linear relation holds approximately between $\varepsilon_i^{j,l}$ and $\varepsilon_i^{j,s}$. Also, the gradient of this line obtained

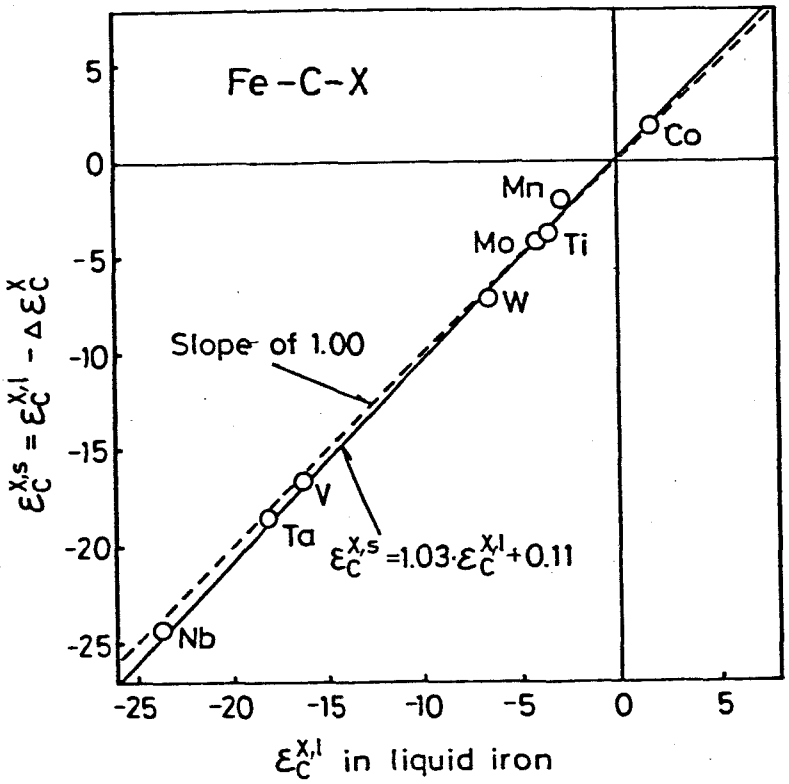

Fig.4-2 Relation between interaction parameter in liquid iron and that in solid iron in Fe−C base ternary system

by the least square method is 1.03 and it is reasonable that the gradient of this line is approximately equal to unity. Thus, the relation of ε_i^j between solid and liquid phases is shown by Eq.(4-9).

$$\varepsilon_i^{j,l} \fallingdotseq \varepsilon_i^{j,s} \tag{4-9}$$

From Eqs.(4-4) and (4-9), the ratio of the equilibrium distribution coefficient of the solute i in Fe−i−j ternary system to that in Fe−i binary system is represented by the following simple equation (4-10).

$$\ln k_i^j \equiv \ln k_0^{i,3} / k_0^{i,2} = (1 - k_0^{j,3})\ \varepsilon_i^{j,l} N_j^l \tag{4-10}$$

In Eq.(4-10), the ratio of $k_0^{i,3}$ to $k_0^{i,2}$, that is to say, the parameter indicating the change of the equilibrium distribution coefficient of solute i with the addition of the alloying element j, is defined as k_i^j,

named Distribution Interaction Coefficient (D I C). Furthermore, the equilibrium distribution coefficient of solute i in Fe−i−j ternary system can be obtained from this coefficient k_i^j when that in Fe−i binary system is known.

4.3 Results and Discussion.

4.3.1 Effect of Carbon on the Equilibrium Distribution of Various Alloying Elements between Solid and Liquid Phases in Fe−C Base Ternary Alloys.

Effects of solute-interaction on the equilibrium distribution coefficients in a few kinds of iron alloys are discussed in this section by using the foregoing coefficient D I C, k_i^j .

First, the change of the coefficient D I C of solute i with carbon concentration is discussed when the concentration of solute i is dilute in Fe−C−i ternary system. Then, the equilibrium distribution coefficient of solute i in Fe−C−i ternary system is calculated from the D I C for the carbon concentration range up to the eutectic point on the equilibrium between austenite and liquid phases and also compared with the experimental results.

The change of the coefficient D I C of solute i with carbon concentration is given by

$$\ln k_i^C = \ln k_0^{i,3} / k_0^{j,2} = (1 - k_0^{C,3})\, \varepsilon_i^{C,1} N_C^1 \qquad (4\text{-}11)$$

Since the concentration of solute i is considered to be dilute in this work, the values of the equilibrium distribution coefficient of carbon in Fe−C binary system can be used as $k_0^{C,3}$ in Eq.(4-11). Besides, the data of $\varepsilon_i^{C,1}$, being valid for the wide concentration range and at any temperature, must be used, but nothing has been reported. Then, such values are obtained in the following way.

Using the interaction parameter ε_C^i at the infinite dilution reported by Sigworth et al.[1] and that at the carbon-saturated state obtained by Neumann

et al.[10] , and also assuming that ε_C^i is proportional to carbon concentration and the reciprocal of the absolute temperature, the value of ε_C^i at arbitraly carbon concentration and temperature can be obtained. In this case, as the interaction parameter reported at the carbon-saturated state is the interaction parameter at constant carbon activity ω_C^i , this parameter has to be converted into the interaction parameter at constant concentration, ε_C^i ,which can be expanded at arbitraly concentration. When the concentration of solute i is dilute in Fe−C base ternary system, the equation for the conversion of the interaction parameter at constant activity to that at constant concentration is shown by Eq.(4-12).[11]

$$(\varepsilon_C^i)_{N_C = N_C^\circ, N_i = 0} = \left(\frac{\partial \ln \gamma_C}{\partial N_i}\right)_{N_C = N_C^\circ, N_i = 0}$$
$$= \left\{1 + \left(\frac{\partial \ln \gamma_C}{\partial N_C}\right)_{N_i = 0, N_C = N_C^\circ} \cdot N_C^\circ\right\} \cdot \left(\frac{\partial \ln \gamma_C}{\partial N_i}\right)_{a_C = a_C^\circ, N_i = 0} \qquad (4\text{-}12)$$

In this equation, the left-hand side is the interaction parameter at constant concentration and the last term in the right-hand side is the interaction parameter at constant activity. The second term in the parentheses of the right hand side corresponds to the self-interaction parameter of carbon and this term can be obtained from the change of the activity of carbon with its concentration in Fe−C binary system reported by Ban-ya et al.[12]

Finally, ε_C^i obtained above has to be converted into ε_i^C . The equation for this conversion is given by Eq.(4-13).[13]

$$(\varepsilon_i^C)_{Ni} = (\varepsilon_C^i)_{Nc} + (\varepsilon_{Fe}^C)_{NFe} \qquad (4\text{-}13)$$

In the infinite dilution, ε_i^C is equal to ε_C^i . However, the last term in the right-hand side of the equation is needed when this conversion is applied at the arbitraly concentration. The last term shows the change of the activity of Fe with carbon concentration and can be obtained from the data by Chipman.[14]

Thus, the interaction parameters ε_i^C at any temperature and carbon concentration can be obtained. Figure 4-3 indicates the change of ε_i^C of various elements with the temperature and carbon concentration corresponding to the liquidus in Fe－C binary system.

Using Eq.(4-11) and ε_i^C obtained above, the change of the coefficient DIC of various elements with the temperature and carbon concentration corresponding to the liquidus in Fe－C binary system can be calculated. The results are shown in Fig.4-4. As illustrated in this figure, the coefficient DIC of Si, Al, Ni and so on having the repulsive effects against carbon increase with increasing carbon concentration. On the other hand, the DIC of Cr, V and so on having the attractive effect against carbon decrease with increasing carbon concentration.

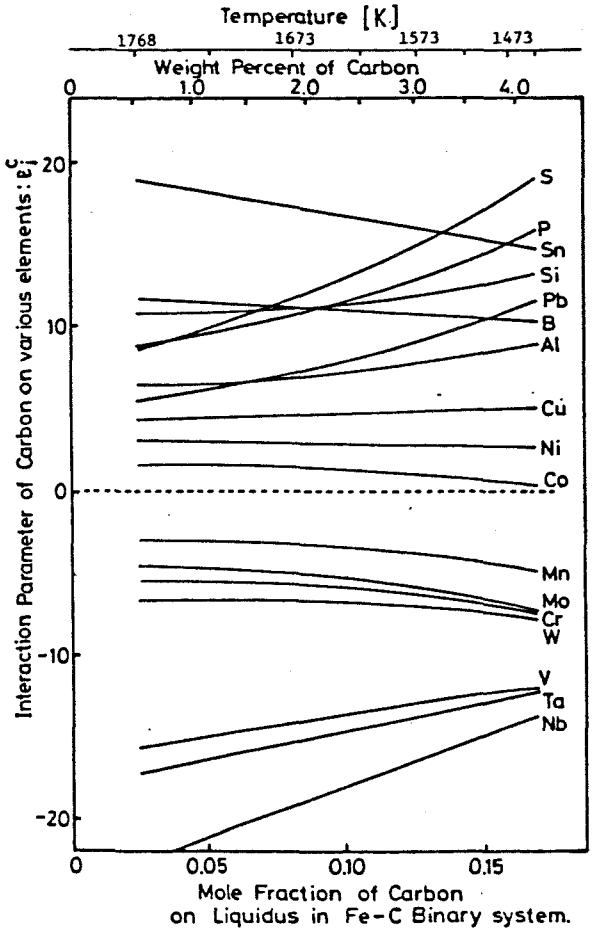

Fig.4-3 Change of interaction parameter of various elements with carbon concentration in Fe－C base ternary system.

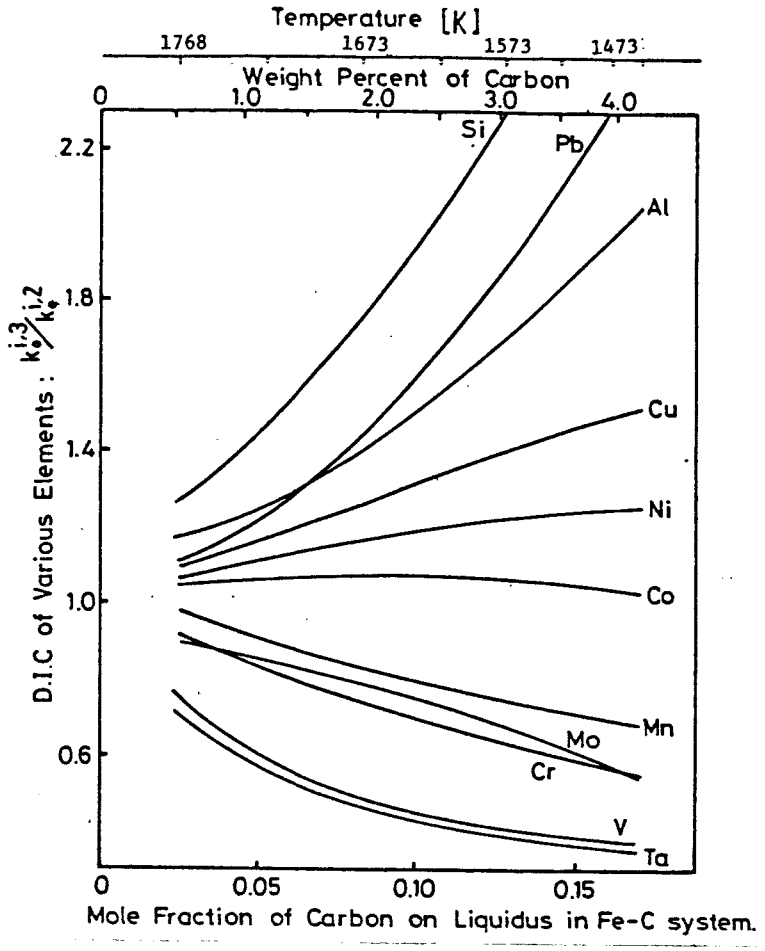

Fig.4-4 Change of D I C of various elements with carbon concentration in F e − C base ternary system.

Moreover, the equilibrium distribution coefficients of various elements in F e − C base ternary system are calculated from the coefficient D I C and the equilibrium distribution coefficient in iron base binary system, and the calculated results are compared with the measured values by various investigators,[15~23] as shown in Fig.4-5. Here, regarding the data of the equilibrium distribution coefficients of various elements in iron base binary system, the values in the report by Takahashi et al.[24] about the equilibrium distribution coefficient are assumed to be approximately equal to the values in binary system and then adopted. In Fig.4-5, the solid and dashed lines denote the calculated and experimental results, respectively. This figure indicates that the calculated results obtained from the coefficient D I C are in good agreement with the experimetal ones in each system.

Thus, the coefficient D I C defined in this work is considered to be useful as the parameter indicating the effects of solute-interaction on the

equilibrium distribution coefficient.

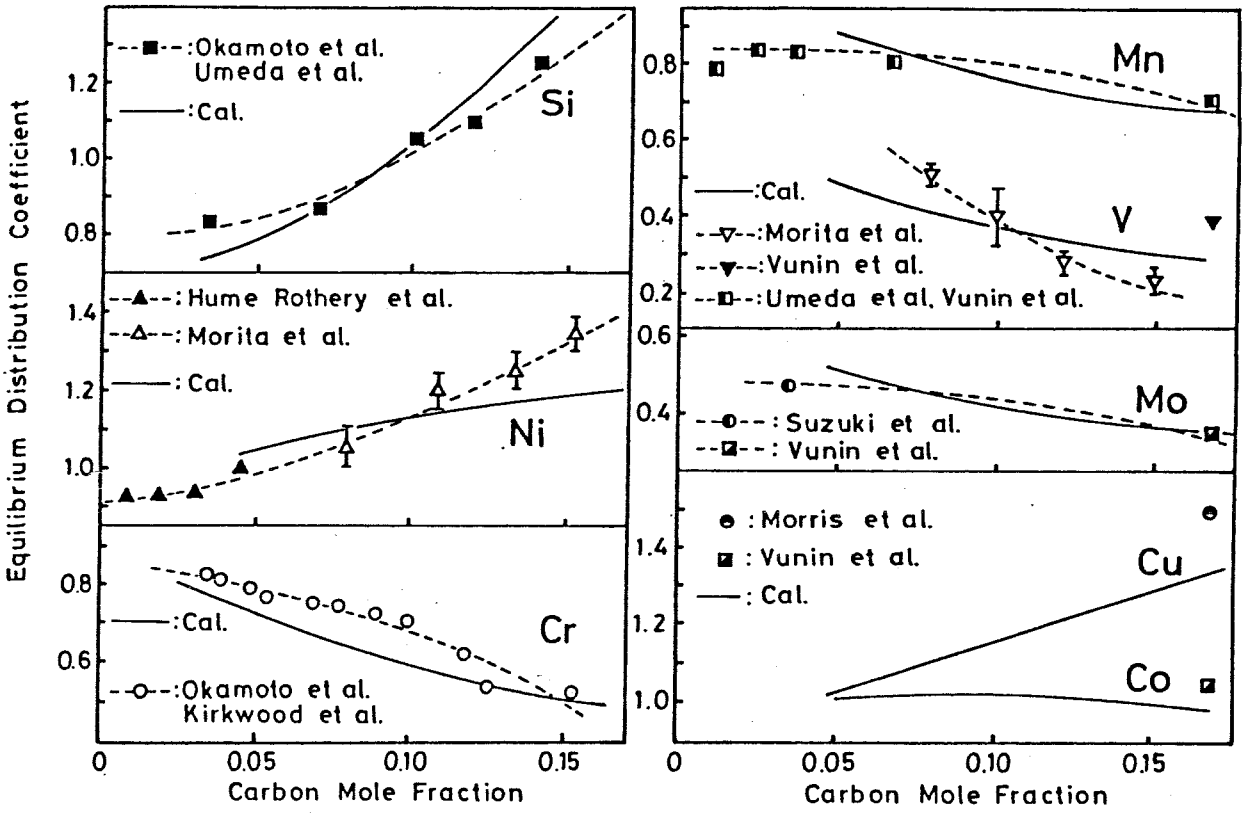

Fig.4-5 Change of the equilibrium distribution coefficient of some elements with carbon concentration in Fe−C base ternary system.

4.3.2 Effects of Various Alloying Elements on the Equilibrium Distribution of Nitrogen and Hydrogen between Solid and Liquid Phases in Fe−N, H Base Ternary Alloys.

It is important to know the equilibrium distribution behaviours of gaseous elements in relation to various phenomena during solidification of steels, but little information has been obtained so far concerning this problem. Then, the purpose of this section is to discuss the effects of various alloying elements on the equilibrium distributions of nitrogen and hydrogen between solid and liquid phases in iron base ternary system by using the foregoing DIC.

The variation of the DIC of nitrogen and hydrogen with the concentration of various alloying elements in Fe−i−X ternary system (i : N or H) is represented by Eq.(4-14).

$$\ln k_i^X = \ln k_0^{i,3} / k_0^{i,2} = (1 - k_0^{X,3})\ \varepsilon_i^{X,1} N_X^1 \qquad (4\text{-}14)$$

Since the solubilities of nitrogen and hydrogen in solid and liquid alloys are considerably small, the effects of these gaseous elements on the distribution of the alloying element X between solid and liquid phases can be neglected. Then, in this work, the value of $k_0^{X,2}$ in Fe−X binary system was used as $k_0^{X,3}$ in Fe−i−X ternary system in Eq.(4-14). Also the data of Sigworth et al., Ishii et al.[25,26] and Morita et al.[27] were used as $\varepsilon_i^{X,1}$. Figures 4-6 (A) and (B) show the variations of the coefficient DIC of nitrogen and hydrogen with the concentrations of various alloying elements in Fe−N and Fe−H base ternary system, respectively. In these figures, solid lines are the calculated results when α phase is assumed to crystallize out of liquid solution and the values of k_0^X for α phase are used in Eq.(4-14). Similarly, chain lines show the calculated results when the primary crystals are presumed to be γ phase. It is obvious from these figures that C, Si and so on indicating the repulsive effects against N and H increase the DIC of these gaseous elements, and on the other hand Cr, Ti and so on showing the attrac-

tive effects against N and H decrease the D I C of these gaseous elements.

A

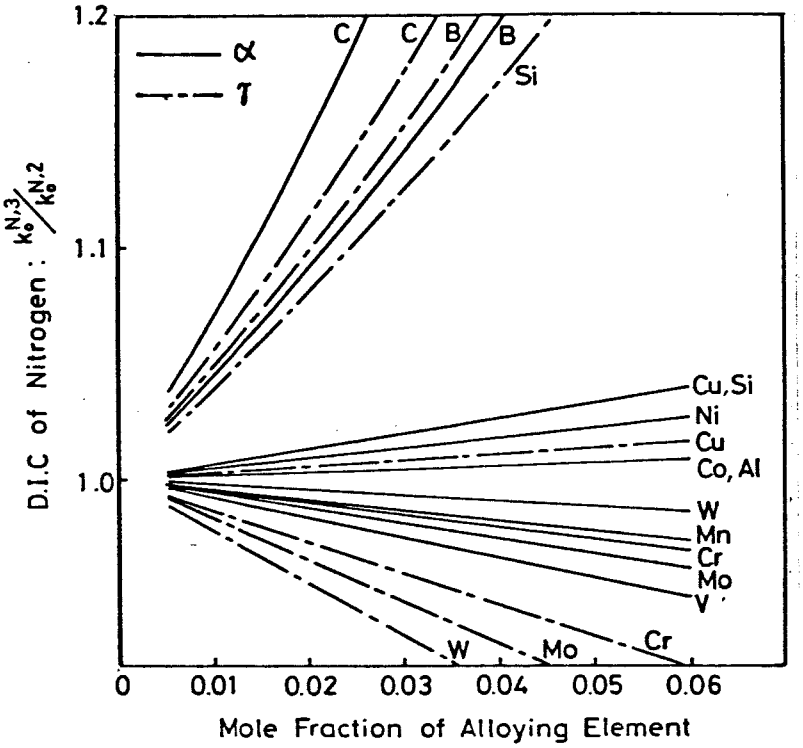

Fig.4-6(A) Change of D I C of nitrogen with the concentration of alloying elements.

B

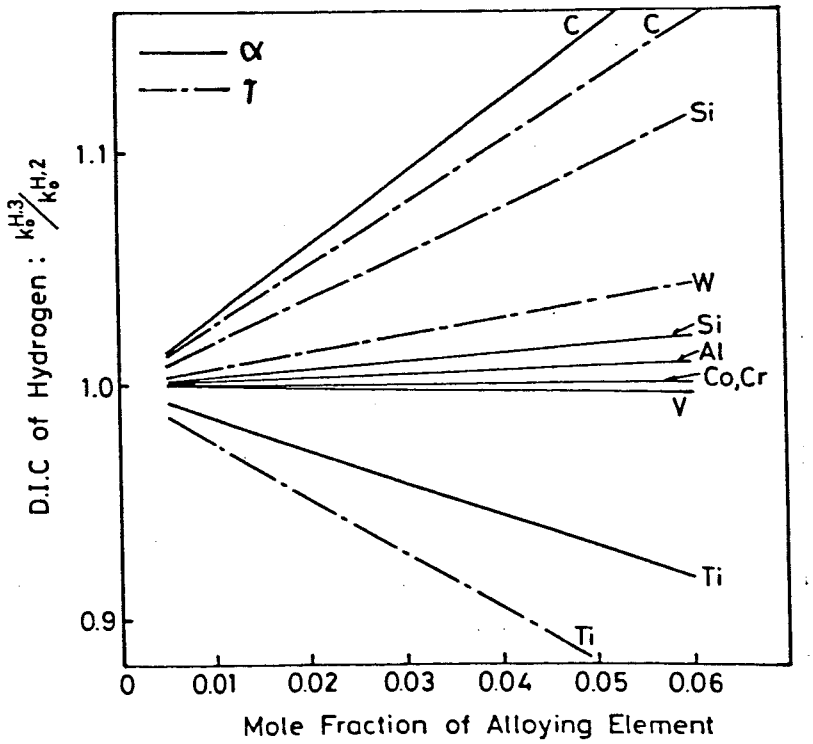

Fig.4-6(B) Change of D I C of hydrogen with the concentration of alloying elements

4.3.3 Application of Distribution Interaction Coefficient to the Equilibrium Distribution of P and S between Solid and Liquid Phases in Iron Base Ternary Alloys.

Although the concentrations of P and S are dilute in steels generally, these elements are known to play an important role in relation to the micro-segregation. So, many studies have been carried out in order to make clear the mechanisms of their segregations and also to improve them. However, the influences of various alloying elements on the equilibrium distributions of P and S have not yet been known quite well. In this section, these kinds of effects are discussed by using the foregoing coefficient D I C when the concentrations of P and S are dilute in Fe－i－X (i: P or S) ternary system. The change of D I C of P and S with the concentration of the alloying elements in Fe－i－X ternary system (i: P or S) is given by Eq.(4-15).

$$\ln k_i^X = \ln k_0^{i,3} / k_0^{i,2} = (1 - k_0^{X,3})\, \varepsilon_i^{X,1} N_X^1 \qquad (4\text{-}15)$$

As the concentrations of P and S are considered to be dilute in this work, the equilibrium distribution coefficient of the alloying element in iron base binary system can be used as $k_0^{X,3}$ in Eq.(4-15), as described in the last section. Also, the data of Sigworth et al.[1] and Ban-ya et al.[28] were adopted as $\varepsilon_i^{X,1}$. The changes of the coefficients D I C of P and S with various alloying elements are shown in Figs.4-7(A) and 4-7(B) in Fe－P and Fe－S base ternary systems respectively. In these figures, solid lines and chain ones indicate the calculated results for α phase and γ one, respectively. As can be seen from these figures, the elements denoting the repulsive effects against P and S, e.g. C, Si and so on, increase the D I C of P and S, while the elements indicating the attractive effects against P and S, e.g. Cr, V and so on, decrease those of P and S.

Thus, it is obvious that effects of solute-interaction on the equilibrium distributions of N, H, P and S, which are intimately concerned with the

micro-segregation of steels, can be discussed by using the coefficient D I C.

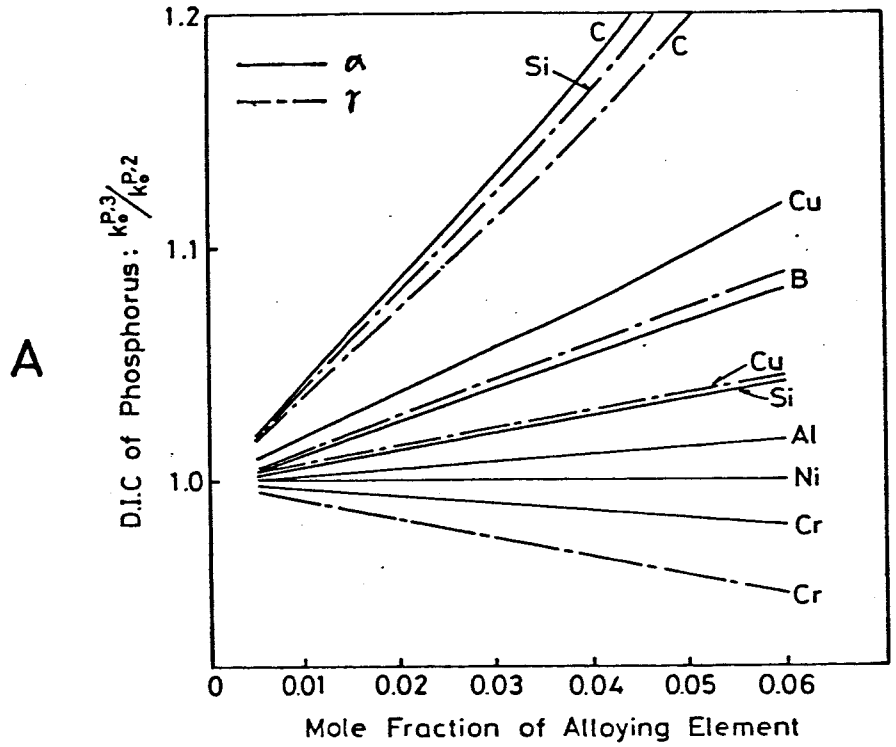

Fig.4-7(A) Change of D I C of phosphorus with the concentration of alloying elements.

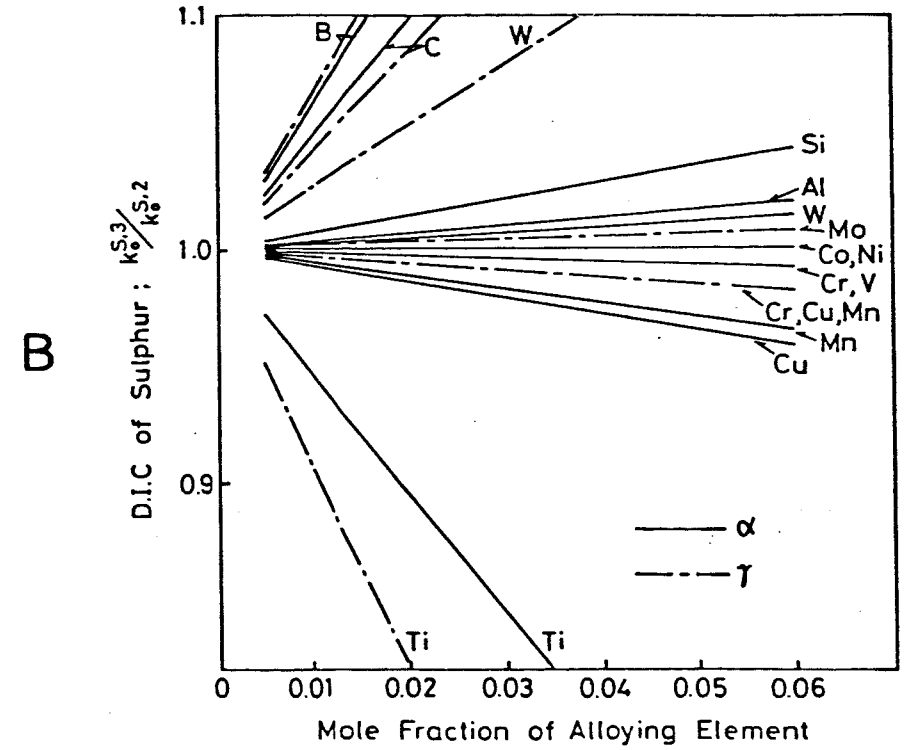

Fig.4-7(B) Change of D I C of sulphur with the concentration of alloying elements.

4.4 Conclusion.

The effects of solute interaction on the equilibrium distribution of solute elements between solid and liquid phases in iron base ternary system were studied thermodynamically.

The results obtained are summarized as follows.

① Distribution Interaction Coefficient (D I C), k_i^j, which is defined as the ratio of the equilibrium distribution coefficient of solute i in Fe−i−j ternary system to that in Fe−i binary one, was derived as shown in the following equation.

$$\ln k_i^j = \ln k_0^{i,3} / k_0^{i,2} = (1 - k_0^{j,3})\, \varepsilon_i^{j,1} N_j^1$$

D I C is considered to be the parameter indicating the change of the equilibrium distribution coefficient of solute i with the addition of j.

② Applying D I C for the equilibrium distribution of element i in Fe−C−i ternary system, the change of D I C of various elements with the temperature and carbon concentration corresponding to the liquidus in Fe−C binary system could be obtained. D I C of Si, Al, Ni and so on having the repulsive effects against carbon increase with increasing carbon concentration. On the other hand, D I C of Cr, V and so on having the attractive effect against carbon decrease with increasing carbon concentration.

The calculated values of k_0 of various alloying elements in Fe−C base ternary alloys from D I C are in good agreement with the experimental ones.

③ The effects of solute-interactions on k_0 of N, H, P and S in iron base ternary alloys could be estimated by the use of D I C. The elements denoting the repulsive effects against N, H, P and S in iron alloys, e.g., C, Si and so on, increase D I C of N, H, P and S, while the elements indicating the attractive effects against N, H, P and S in the alloys, e.g. Cr, V and so on, decrease those of N, H, P and S.

4.5 References.

(1) G. K. Sigworth and J. F. Elliott : Metal.Sci.,8 (1974),298

(2) E. J. Grinsey : J. Chem. Thermo., 9 (1979),415

(3) T. Wada, H. Wada, J. F. Elliott and J. Chipman : Met. Trans.,2 (1971),2199

(4) J. Chipman and J. F. Elliott : Trans. Met. Soc. AIME, 242 (1968),35

(5) T. Wada, H. Wada, J. F. Elliott and J. Chipman : Met. Trans.,3 (1972),2865

(6) T. Mori and E. Ichise : J. Japan Inst. Metals, 32 (1968),949

(7) A. Morooka and T. Mori : The reports of the Third Japan-USSR Joint Symposium of Physical Chemistry of Metallurgical Processes, (1971),141

(8) H. Wada and T. Saito : J. Japan Inst. Metals, 35 (1961),159

(9) H. Wada, K.Gunji and T. Wada : J. Japan Inst. Metals, 30 (1966),613

(10) F. Neumann und H. Schenck : Arch. Eisenhüttenw., 30 (1959),477

(11) K. Fujimura, T. Mori, T. Azuma and S. Urakawa : Tutsu-to-Hagane, 59 (1973), 222

(12) S. Ban-ya, J. F. Elliott and J. Chipman : Met. Trans.,1 (1970),1313

(13) T. Mori and A. Morooka : Tetsu-to-Hagane,52 (1966),947

(14) J. Chipman : Met. Trans., 1 (1970),2163

(15) S. Suzuki, T. Umeda and Y. Kimura : The 19th Comm. (Solidification), Japan Soc. Promotion Sci. (JSPS), No.19-10254, (May, 1980)

(16) A. Kagawa and T. Okamoto : Metal. Sci., 14 (1980),519

(17) A. J. W. Ogilvy, A. Ostowskii and D. H. Kirkwood : Metal. Sci.,15 (1981), 168

(18) K. Parameswaran, K. Metz and A. Morris : Met. Trans.,10A (1979),1929

(19) R. A. Buckley and W. Hume-Rothery : JISI,197 (1964),895

(20) B. A. Rickinson and D. H. Kirkwood : Met. Sci.,12 (1978),138

(21) K. P. Vunin and U. N. Taran : "On the Structure of Cast Iron", The new Japan Society for the Casting and Forging, (1979)

(22) A. Kagawa, S. Moriyama and T. Okamoto : J. Mat. Sci.,17 (1982),135

(23) K. Suzuki, A. Taniguchi and K. Hirota : Tetsu-to-Hagane, 64 (1978),S606

(24) T. Takahashi et al.: "Solidification of Iron and Steel" (A Data Book on the Solidification Phenomena of Iron and Steel), (1977) Solidification subcommittee, Basic Research Committee on Iron and Steel, ISIJ.

(25) F. Ishii, S. Ban-ya and T. Fuwa : Tetsu-to-Hagane, 68 (1982),1551

(26) F. Ishii and T. Fuwa : Tetsu-to-Hagane, 68 (1982),1560

(27) Z. Morita and K. Kunisada : Tetsu-to-Hagane, 63 (1977), 1663 : Trans. ISIJ, 18 (1978),648

(28) S. Banya, N. Maruyama and S. Fujino : Tetsu-to-Hagane, 69 (1983),921

Chapter 5

Effects of Solute Interactions on the Equilibrium Distribution of Solute Elements Between Solid and Liquid Phases in Iron Base Multi-component Alloys.

5.1 Introduction.

In the foregoing chapter 4, the effects of solute-interactions on the equilibrium distribution of solute elements in iron base ternary alloys could be explained by the use of Distribution Interaction Coefficient (D I C) defined in that chapter. In this chapter, D I C was applied to the equilibrium distribution of solutes in iron base multi-component systems and the new parameter was derived. Also, the influences of S i , V and C o on the variations of k_0 of S n and C u with carbon in F e − C base quarternary alloys were obtained experimentally and those results were discussed by means of the new parameter. In particular, S n is one of the impurities which are difficult to be removed from steels and it shows unique thermodynamical behaviour in F e − C base alloys.[1] Also, the equilibrium distribution coefficient of S n in F e − C base alloys have not been reported. So, it is considered very important to investigate k_0 and the effects of the solute interactions on k_0 in F e − C alloys.

5.2 Derivation of a Parameter describing the Effect of Solute Interaction on the Equilibrium Distribution Coefficient.

The equilibrium distribution coefficient of solute i in F e − i binary system, $k_0^{i,2}$, is given by Eq.(5-1).

$$\ln k_0^{i,2} = (\dot{\mu}_i^l - \dot{\mu}_i^s) / RT + \ln \dot{\gamma}_i^l / \dot{\gamma}_i^s + (\varepsilon_i^{i,l} - \varepsilon_i^{i,s} k_0^i) N_i^l \quad (5\text{-}1)$$

Assuming that the effects of solute interactions on the solute i in

Fe－i－p－q－r－－－ multi-component system are approximately described by a simple term of Wagner's formalism concerning the activity coefficient of the solute in multi-component system, the equilibrium distribution coefficient of solute i in multi-component system can be derived in the following equation (5-2).

$$\begin{aligned} \ln k_0^{i,n} = (\mu_i^l - \mu_i^s)/RT + \ln \gamma_i^l / \gamma_i^s + (\varepsilon_i^{i,l} - \varepsilon_i^{i,s} k_0^i) N_i^l \\ + (\varepsilon_i^{p,l} - \varepsilon_i^{p,s} k_0^p) N_p^l + (\varepsilon_i^{q,l} - \varepsilon_i^{q,s} k_0^q) N_q^l \\ + (\varepsilon_i^{r,l} - \varepsilon_i^{r,s} k_0) N_r^l + \cdots \end{aligned} \qquad (5\text{-}2)$$

Here, this multi-component system is supposed to be the n-components system and the equilibrium distribution coefficient of the solute i is indicated as k_0^{in}. When the concentration of the solute i is very dilute, the parts from the first term to the third one in the rigth-hand side of Eq.(5-2) are nearly equal to $k_0^{i,2}$ of Eq.(5-1). Then, the equation (5-3) can be obtained.

$$\begin{aligned} \ln k_0^{i,n} / k_0^{i,2} = (\varepsilon_i^{p,l} - \varepsilon_i^{p,s} k_0^p) N_p^l + (\varepsilon_i^{q,l} - \varepsilon_i^{q,s} k_0^q) N_q^l \\ + (\varepsilon_i^{r,l} - \varepsilon_i^{r,s} k_0^r) N_r^l + \cdots \end{aligned} \qquad (5\text{-}3)$$

As described in the previous chapter, when the temperature of liquid phase is equal to that of solid one, the interaction parameter of j on i, ε_i^j, in liquid phase may be assumed to be approximately equal to that in solid phase, i.e

$$\varepsilon_i^{j,l} \fallingdotseq \varepsilon_i^{j,s} \qquad (5\text{-}4)$$

From Eqs.(5-3) and (5-4), the ratio of the equilibrium distribution coefficient of the solute i in iron base n-components system to that in Fe－i binary system is represented by the simple equation (5-5).

$$\ln k_0^{i,n} / k_0^{i,2} = (1-k_0^p)\,\varepsilon_i^{p,1} N_p^1 + (1-k_0^q)\,\varepsilon_i^{q,1} N_q^1 + (1-k_0^r)\,\varepsilon_i^{r,1} N_r^1 + \cdots\cdots$$
$$= \delta_i^p N_p^1 + \delta_i^q N_q^1 + \delta_i^r N_r^1 + \cdots\cdots \qquad (5\text{-}5)$$

$$\delta_i^j \equiv (1-k_0^j)\,\varepsilon_i^{j,1} \qquad (5\text{-}6)$$

Here, the parts of $(1-k_0^j)\cdot\varepsilon_i^{j,1}$ in Eq.(5-5) for each solute element p, q, r and so on are defined as δ_i^j in Eq.(5-6) and called Distribution Interaction Parameter (D I P). The D I P, δ_i^j, is considered to be a parameter indicating the effect of the alloying element j on the equilibrium distribution of the solute i between solid and liquid phases in Fe − i − j ternary system. That is to say, if δ_i^j is positive, the element j has the tendency to increase the equilibrium distribution coefficient of the solute i. On the other hand, if δ_i^j is negative, the solute j decreases k_0^i.

The effects of the solute interactions on the equilibrium distribution coefficients of the solute elements in a few kinds of iron base multi-component systems were discussed in this work by using the parameter δ_i^j. First of all, the change of the equilibrium distribution coefficients of some elements with the carbon concentration in Fe − C base alloys were determined experimentally, and the results were examined by the use of δ_i^j.

5.3 Experimental.

In order to investigate the equilibrium distribution of some elements between austenite and liquid phases in Fe − C base alloys, austenite-liquid coexisted samples were quenched and the concentrations of solutes in each phase were determined by EPMA. The apparatus for preparing quenched specimens is shown in Fig.5-1. The experimental procedure was almost the same as described

in chapter 2 and 3. In this experiment, however, the specimens were quenched on the copper plate with argon gas blow in order to quench the specimens more rapidly than by KOH aqua or oil used at the experiments in chapter 2 and 3. The equilibration time was determined to be 2.5 or 3 hours. Moreover, area analysis by EPMA was performed to measure the concentration of the solute elements, so that the error in the concentration analysis caused by rough structures in liquid phase part could be as small as possible.

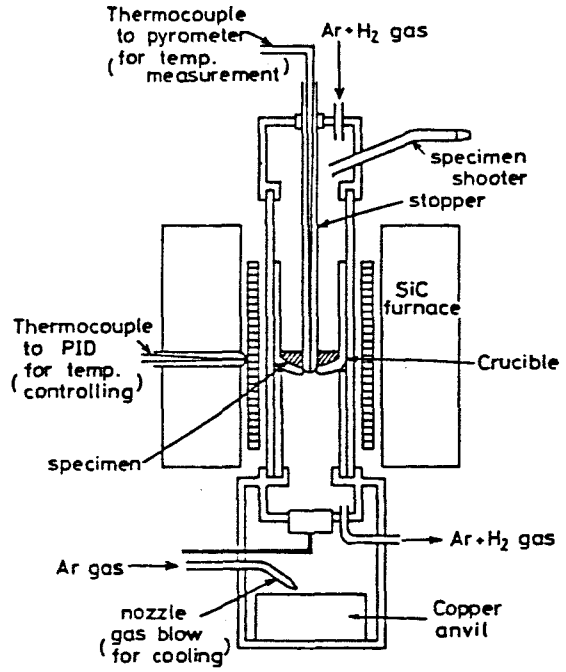

Fig.5-1 Apparatus for quenched specimens.

5.4 Results and Discussion.

5.4.1 Effects of Solute Interactions on the Equilibrium Distribution of Solute Elements between Solid and Liquid Phases in Fe-C Base Quarternary Alloys.

Compositions of the samples and the experimental results are listed in Table 5-1. Alloy systems investigated in this work are Fe-C-Sn, Fe-C-Cu and Fe-C-Co for Fe-C base ternary systems, and also Fe-C-Sn with Si, V or Co and Fe-C-Cu with V or Co for

Table 5-1 Compositions of the samples (wt%), holding temperature (K) and the results of k_0.

Fe−C−Sn

Temp.	C	Sn	k_0^{Sn}
1418	4.02	1.66	0.84
1485	3.58	1.10	0.63
1586	2.91	1.03	0.42
1613	2.42	1.64	0.37

Fe−C−Cu

Temp.	C	Cu	k_0^{Cu}
1443	4.03	1.23	1.64
1495	3.45	1.15	1.43
1563	3.09	1.08	1.25
1636	2.19	0.96	1.14

Fe−C−Co

Temp.	C	Co	k_0^{Co}
1465	3.68	1.69	1.24
1548	3.16	2.06	1.16
1644	2.46	2.15	1.05

Fe−C−Sn−Si

Temp.	C	Sn	Si	k_0^{Sn}	k_0^{Si}
1426	3.92	1.01	1.45	0.58	1.22
1484	3.54	1.53	1.49	0.46	1.20
1558	2.53	1.37	1.26	0.32	1.03
1623	2.07	1.50	1.41	0.28	1.03

Fe−C−Cu−V

Temp.	C	Cu	V	k_0^{Cu}	k_0^{V}
1473	3.42	1.37	1.45	1.63	0.24
1586	2.52	1.49	1.48	1.21	0.34
1643	1.94	1.60	1.51	1.06	0.40

Fe−C−Sn−V

Temp.	C	Sn	V	k_0^{Sn}	k_0^{V}
1493	3.58	1.46	1.28	0.60	0.27
1536	3.13	1.33	1.16	0.50	0.31
1613	2.06	1.60	1.41	0.37	0.40

Fe−C−Cu−Co

Temp.	C	Cu	Co	k_0^{Cu}	k_0^{Co}
1485	3.50	1.47	1.23	1.55	1.21
1580	2.68	1.23	1.30	1.18	1.12
1643	2.05	1.85	1.60	1.04	1.03

Fe−C−Sn−Co

Temp.	C	Sn	Co	k_0^{Sn}	k_0^{Co}
1483	3.55	1.43	1.41	0.57	1.18
1573	2.69	1.52	1.49	0.39	1.10
1613	2.43	1.46	1.30	0.36	0.96

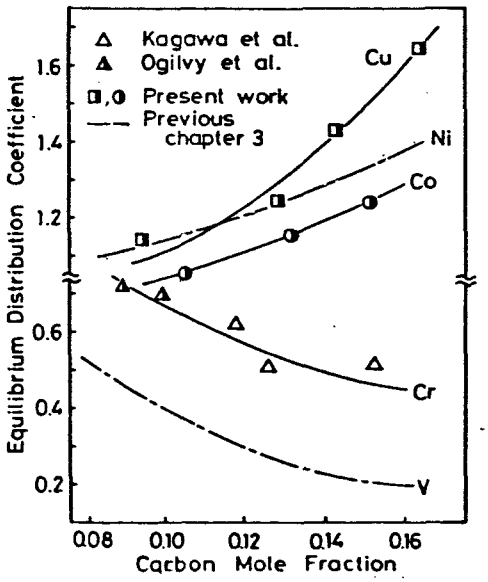

Fig.5-2 Change of the equilibrium distribution coefficients of various elements with the concentration of carbon in Fe−C base alloys.

Fe－C base quarternary systems. In each alloy, carbon concentration were changed from 2.0 to 3.8 wt% and the concentrations of all solute elements except carbon were about 1.5wt%.

Figure 5-2 indicates the variation with carbon concentration of the equilibrium distribution coefficient of the third element in each Fe－C base ternary system. In this figure, k_0^{Cr} is the results obtained by Kagawa et al.[2,3] and k_0^{Ni} and k_0^{V} are the results obtained in the previous chapter 3. As shown in Fig.5-2, the magnitude of effects of carbon on the equilibrium distribution coefficients of various elements becomes larger in orders of V, Cr, Co, Ni and Cu. These experimental results are discussed by using the parameter δ in Eq.(5-7), which shows the effects of carbon on the equilibrium distribution of these elements between solid and liquid phases in Fe－i－C ternary system.

$$\delta_i^C = (1 - k_0^C)\ \varepsilon_i^{C,l} \qquad (5\text{-}7)$$

Since the concentration of the solute i is assumed to be dilute in this work, the values of the equilibrium distribution coefficient of carbon in Fe－C binary system can be used as k_0^C in Eq.(5-7). Namely, δ_i^C is considered to be dependent only on $\varepsilon_i^{C,l}$. Neumann et al.[4] reported that $\varepsilon_i^{C,l}$ changes regularly against atomic number on each period of the periodic table, so that the variations of the equilibrium distribution coefficients of various elements with carbon concentration in Fig.5-2 are thought to correspond to the regular change of $\varepsilon_i^{C,l}$.

The effects of Si, V and Co on the change of the equilibrium distribution coefficient of Sn with carbon concentration are represented in Figs.5-3 (A),(B) and (C), respectively. In these figures, chain lines show the change of the equilibrium distribution coefficients of Sn in Fe－C－Sn ternary

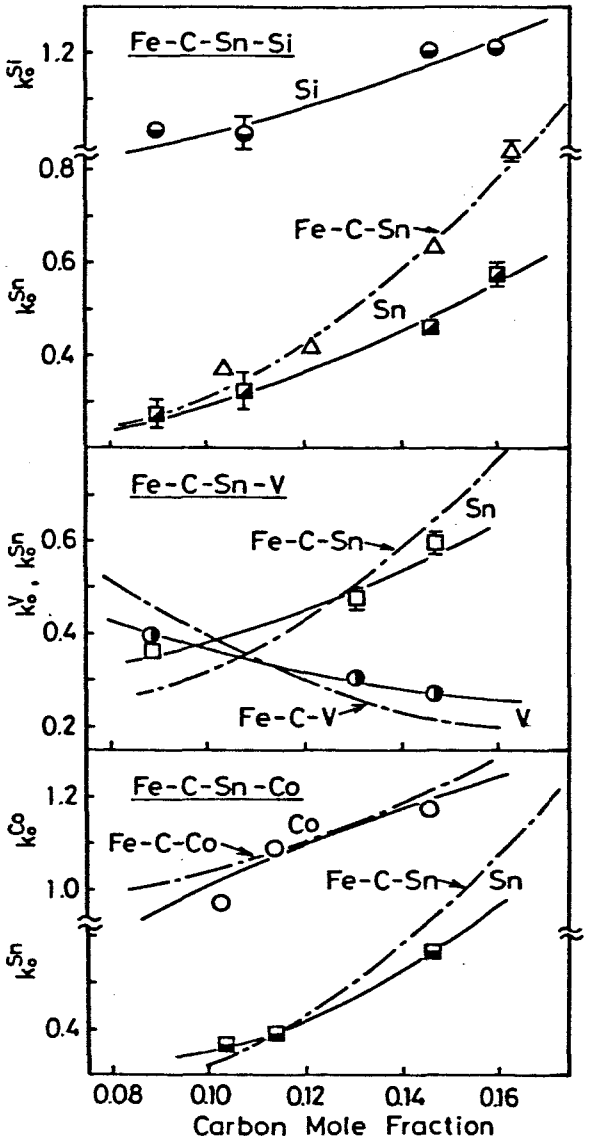

$\varepsilon_{Si}^{C} = 9.69, \quad \varepsilon_{Sn}^{C} = 19.1$

$\delta_{Si}^{C} = (1 - k_0^{C}) \cdot \varepsilon_{Si}^{C} > 0$

$\delta_{Sn}^{C} = (1 - k_0^{C}) \cdot \varepsilon_{Sn}^{C} > 0$
$= 10.5$

$\varepsilon_{Sn}^{Si} = 7.18$

$\delta_{Sn}^{Si} = (1 - k_0^{Si}) \cdot \varepsilon_{Sn}^{Si} < 0$
$= -1.72$

$\varepsilon_{Sn}^{V} = 5.35$
$\varepsilon_{Sn}^{V} < 0$ (From phase diagram)

$\delta_{Sn}^{V} = (1 - k_0^{V}) \cdot \varepsilon_{Sn}^{V} < 0$

$\varepsilon_{Sn}^{Co} = 2.09$

$\delta_{Sn}^{Co} = (1 - k_0^{Co}) \cdot \varepsilon_{Sn}^{Co}$
$= -0.387$

Fig.5-3 Change of the equilibrium distribution coefficients of Sn, Co, V and Si with the concentration of C in Fe−C−Sn base systems.

system and solid lines indicates the effects of the addition of Si, V and Co. The equilibrium distribution coefficient of Sn increases with carbon concentration in Fe−C base alloys and the additions of Si decrease k_0 as can be seen in Fig.5-3(A). Here, ε_{Sn}^{Si} is given as 7.18[5], positive and large value. If only ε_{Sn}^{Si} is taken into account, Si is thought to increase the equilibrium distribution coefficient of Sn as described in Fig.5-2. However,

as the equilibrium distribution coefficient of Si is larger than unity in the high carbon concentration range, the parameter δ_{Sn}^{Si} is negative. So the decrease of the equilibrium distribution coefficient of Sn with the addition of Si can be explained by δ_{Sn}^{Si}. Also, as is illustrated in Fig.5-3(B), the addition of V hardly changes the value of k_0^{Sn} and the effects of C on k_0^{Sn} is smaller than those in Fe−C−Sn alloys. In this alloy, ε_{Sn}^{V} is shown to be positive, but it is known that there exist a few kinds of stable intermetallic compounds in V−Sn binary alloys,[6] so that the interaction between V and Sn is considered to be attractive. In this case, δ_{Sn}^{V} becomes negative and then the experimental results can be understood by this negative δ_{Sn}^{V}. Moreover, Fig.5-3(C) indicates that the effect of the addition of Co on k_0^{Sn} of Sn is small, in which the value of δ_{Sn}^{Co} is very small because ε_{Sn}^{Co} is smaller than ε_{Sn}^{Si}

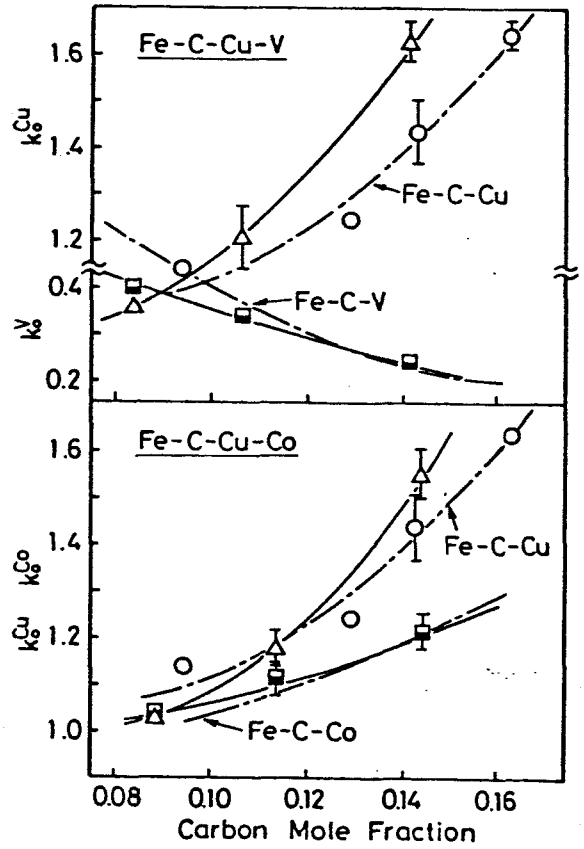

$$\varepsilon_{Cu}^{V} = 2.08$$

$$\delta_{Cu}^{V} = (1 - k_0^{V}) \cdot \varepsilon_{Cu}^{V} > 0$$
$$= 1.50$$

$$\varepsilon_{Cu}^{Co} = -0.23$$

$$\delta_{Cu}^{Co} = (1 - k_0^{Co}) \cdot \varepsilon_{Cu}^{Co}$$
$$= 0.044$$

Fig.5-4 Change of the equilibrium distribution coefficients of Cu, V and Co with the concentration of C in Fe−C−Cu base systems.

and ε_{Sn}^{V} , and the value of k_0^{Co} of Co is about unity. The experimental results are thought to correspond to this smaller value of δ_{Sn}^{Co}.

The experimental results of the equilibrium distribution coefficient of Cu in Fe−C−Cu−V and Fe−C−Cu−Co alloys are shown in Figs. 5-4(A) and (B), respectively. These figures indicate that V increases the equilibrium distribution coefficient of Cu and the effect of Co is very small. These results can be interpreted by the use of δ_{Cu}^{V} and δ_{Cu}^{Co} because δ_{Cu}^{V} is positive and the value of δ_{Cu}^{Co} is very small as shown in Figs.5-4(A) and (B).

In this discussion, the calculated values of ε_{Sn}^{V} , ε_{Sn}^{Co} , ε_{Cu}^{V} and ε_{Cu}^{Co} obtained by the following equation (5-8)[7] are used since the measured values of these parameters have not been obtained.

$$\varepsilon_i^j = (-W_{Fe-j}+W_{i-j}-W_{Fe-i}) / RT$$
$$W_{i-j} = Vm\ (\delta_i - \delta_j)^2 - 23060\ n\ (\chi_i - \chi_j)^2 \qquad (5\text{-}8)$$

where R is gas constant, Vm the atomic volume of the alloy, δ the solubility parameter, χ the electronegativity and n the number of A−B bonding. The numerical values[8] used for the calculation of Eq.(5-8) are represented in Table 5-2.

Thus, the δ defined in this work is considered to be very useful as the parameter indicating the effect of the solute interaction on the equilibrium distribution coefficient of the solute element. By the way, the interaction parameter in liquid was assumed to be equal to that in solid in Eq.(5-4). In the previous chapter, this relation was proposed to be useful for mainly the interstitial element (for example N, H, C), and DIC was used for the interstitial-interstitial and the interstitial-substitutional solute-interactions. However, it is obvious from the foregoing discussion in this work that

Eqs.(5-5) and (5-6), i.e. D I C are also useful for the substitutional-substitutional solute interactions.

Table 5-2 Values for calculating ε_i^j .

element	Co	Cu	Fe	Sn	V
solubility parameter	126	107	117	65	119
electronegativity	2.1	1.9	2.0	1.7	1.7
atomic volume	6.6	7.09	7.10	16.3	8.5
valence	5.78	5.44	5.78	2.44	5.0

5.4.2 Effects of Various Solute Elements on the Equilibrium Distribution of N, H, P and S between Solid and Liquid Phases in Iron Base Multi-component Alloys.

In this section, the influences of various alloying elements on the equilibrium distribution of N, H, S and P between solid and liquid phases in iron base multi-component systems, for example, stainless steels and chromium steels were discussed by the use of the parameter δ_i^j . The parameter δ_i^j of N, H, P and S calculated from the equilibrium distribution coefficients of various elements[9] and the interaction parameters[10~13] are shown in Table 5-3.

First of all, the change of the equilibrium distribution coefficient of N with the concentration of C r and N i in iron base alloys is represented in Fig.5-5. In this figure, the change of the equilibrium distribution coefficient of N is denoted as the ratio of the equilibrium distribution coefficient of N in multi-component system to that in binary one. It is obvious from Fig.5-5 that the equilibrium distribution coefficient of N increase with the increasing of nickel concentration and decrease with the increasing of chromium one. Also, the addition of M o does not change the dependence of N i or C r on the equilibrium distribution of N but it decrease the absolute value of k_0^N .

The changes of the equilibrium distribution coefficients of S and P

with the concentration of Cr and C in the chromium steel are shown in Fig.5-6 and Fig.5-7(A),(B), respectively. As shown in Fig.5-6, the equilibrium distribution coefficient of S decreases with the concentration of Cr while it increases with carbon concentration. Also, k_0^S increases with the addition of Si and it decreases with additing Mn. Figs.5-7(A) and (B) show that k_0^P increases with carbon concentration and decreases with chromium one, and also it increases with the addition of Si in the region of the high concentration of Cr.

Consequently, δ_i^j defined in this work is considered to be a very simple parameter indicating the effects of the solute-interactions on the equilibrium distribution coefficient of the solute elements in iron base multi-component systems, and it is very useful in some practical uses.

Table 5-3 Values of δ_i^j in iron alloys.

	k_0^j [8]	$\varepsilon_N^{j,l}$	$\varepsilon_H^{j,l}$ [5]	$\varepsilon_P^{j,l}$	$\varepsilon_S^{j,l}$ [5]	δ_N^j	δ_H^j	δ_P^j	δ_S^j
Al	δ 0.92	1.63[9]	1.96	3.57[14]	4.41	0.13	0.157	0.286	0.353
B	δ 0.11	4.99[5]	3.03	1.49[14]	6.59	4.44	2.70	1.33	5.87
	γ 0.05					4.74	2.88	1.42	6.26
C	δ 0.17	7.9[9]	3.75	5.43[14]	6.23	6.87	3.11	4.51	5.17
	γ 0.32					5.37	2.55	3.69	4.24
Co	δ 0.94	2.61[5]	0.38	·····	0.58	0.157	0.023	·····	0.035
	γ 0.95					0.131	0.019	·····	0.029
Cr	δ 0.95	-10.1[10]	-0.4	-6.36[5]	-2.29	-0.505	-0.02	-0.318	-0.115
	γ 0.87					-1.31	-0.052	-0.827	-0.298
Cu	δ 0.70	2.22[5]	-0.007	6.15[5]	-2.34	0.666	-0.002	1.85	-0.702
	γ 0.88					0.266	-0.001	0.738	-0.281
Mn	δ 0.90	-4.46[9]	-0.30	0.0[5]	-5.87	-0.446	-0.03	0.00	-0.587
	γ 0.95					-0.233	-0.015	0.00	-0.294
Mo	δ 0.86	-4.6[10]	0.15	·····	0.349	-0.644	0.021	·····	0.049
	γ 0.60					-1.84	0.06	·····	0.140
Ni	δ 0.83	2.7[9]	-0.05	0.0[3]	-0.05	0.459	-0.009	0.00	-0.009
	γ 0.95					0.135	-0.003	0.00	-0.003
Si	δ 0.91	7.8[9]	3.62	7.68[14]	7.78	0.702	0.326	0.691	0.700
	γ 0.50					3.90	1.81	3.84	3.89
Ti	δ 0.60	-118.2[13]	-3.61	·····	-14.1	-47.3	-1.44	·····	-5.64
	γ 0.30					-82.7	-2.53	·····	-9.87
V	δ 0.96	-21.2[10]	-1.47	·····	-3.27	-0.848	-0.059	·····	-0.131
W	δ 0.95	-4.6[10]	1.34	·····	5.05	-0.23	0.067	·····	0.253
	γ 0.50					-2.3	0.67	·····	2.53
Zr	δ 0.50	-237[5]	-3.94	·····	-20.2	-119	-1.97	·····	-10.1

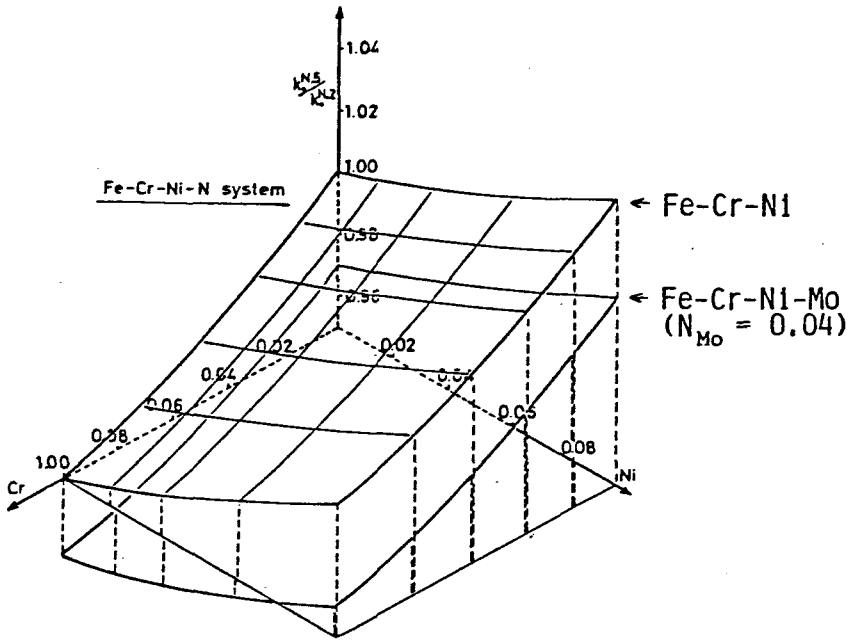

Fig.5-5 Change of D I C of N with the concentration of Cr, Ni and Mo in stainless steels.

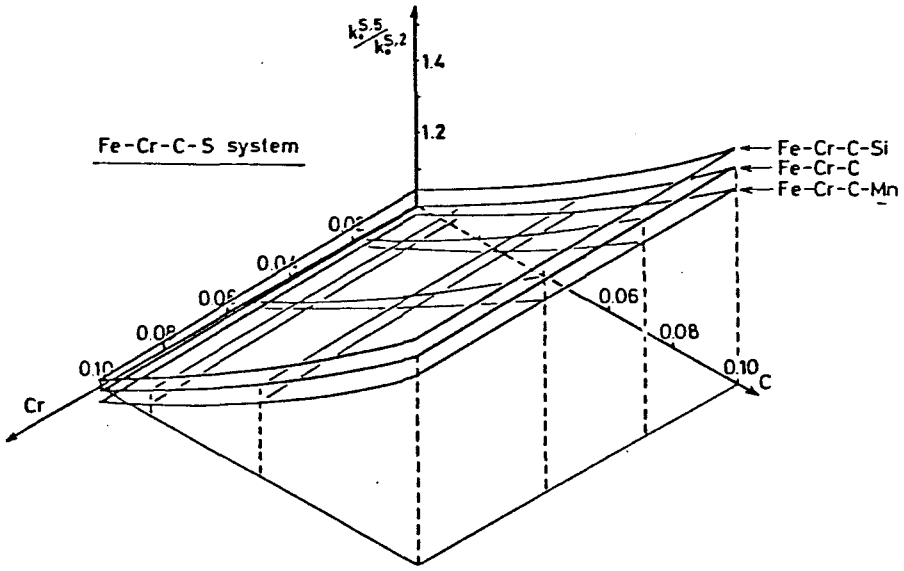

Fig.5-6 Change of D I C of S with the concentration of Cr, C, Si and Mn in chromium steels.

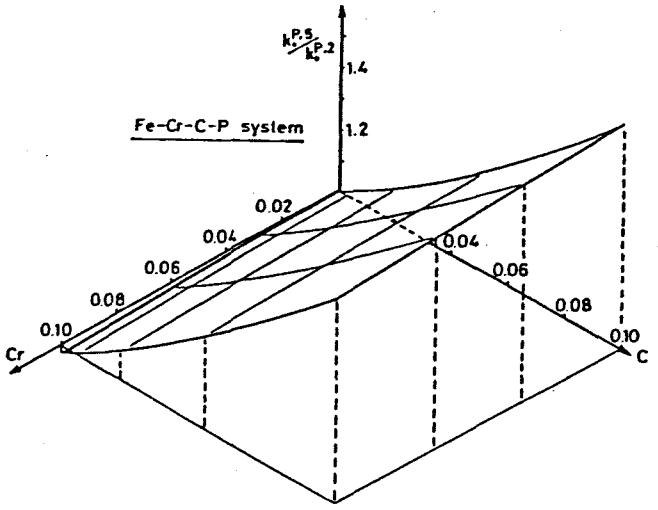

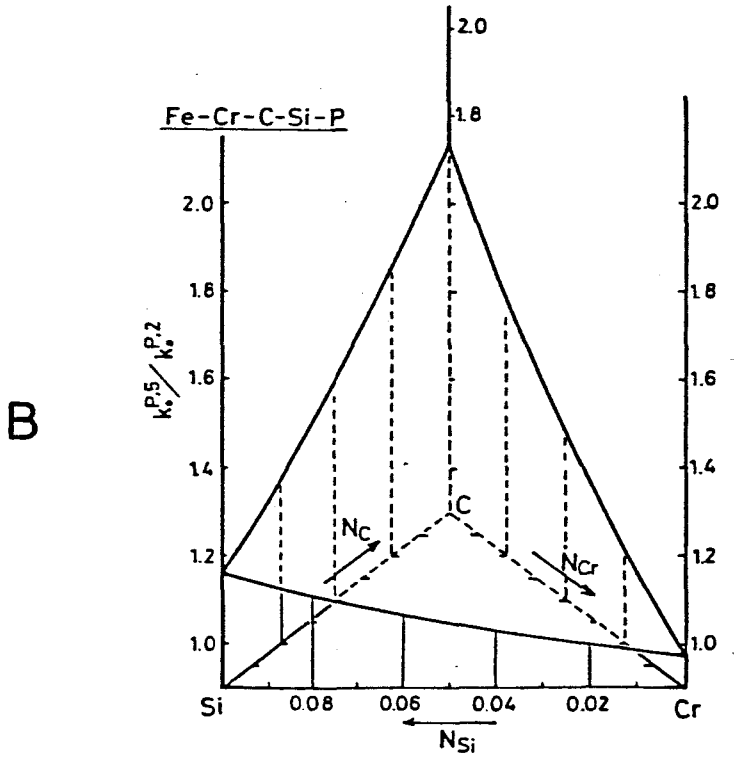

Fig.5-7 Change of D I C of P with the concentration of C r , C and S i in chromium steels.

5.5 Conclusion.

In this chapter, so as to describe the effects of the solute interactions on the equilibrium distribution of solute elements between solid and liquid phases in iron base multi-component systems, Distribution Interaction Coefficient defined in chapter 4 was extended to iron base multi-component systems. Also, the influences of Si, V and Co on the variation of k_0 of Sn and Cu with carbon concentration were obtained experimentally.

The results obtained are summarized as follows.

① Distribution Interaction Parameter (DIP), δ_i^j was defined as

$$\delta_i^j = (1 - k_0^j) \cdot \varepsilon_i^j$$

This parameter shows the effect of the element j on k_0^i of the element i in Fe−i−j ternary system.

② k_0 of Sn increases with the increasing of carbon concentration and the addition of Si decreases k_0^{Sn} of Sn at high carbon concentration in Fe−C base alloys. The addition of V decreases k_0^{Sn} of Sn and the influence of Co on k_0^{Sn} is very small. These experimental results could be explained by use of DIP.

③ k_0's of Cu and Co increase with the increasing of carbon in Fe−C−Cu and Fe−C−Co alloys, respectively. The addition of V increases k_0^{Cu} of Cu and that of Co doesn't change k_0^{Cu} of Cu sufficiently in Fe−C base alloys. These results could be also interpreted by means of DIP.

④ Values of DIP of various alloying elements for P, S, N and H were determined. Using those parameters, the variation of k_0^N of N with the concentration of Cr and Ni in stainless steels and the variation of k_0 of P and S with the concentration of Cr and C in chromium steels were calculated.

5.6 References.

1) T.Mori, M.Fujimura, H.Okajima and A.Yamauchi: Tetsu-to-Hagane, 54 (1968), 321

2) A.Kagawa and T.Okamoto: Metal. Sci., 14 (1980),519

3) B.A.Rickinson and D.H.Kirkwood: Met.Sci., 12 (1978), 138

4) F.Neumann and H.Schenck: Arch. Eisenhüttenw., 30 (1959), 321

5) G.K.Sigworth and J.F.Elliott: Met. Sci., 8 (1974), 298

6) M.Hansen: Constitution of Binary Alloys, McGraw-Hill Book Company, New York, (1958)

7) H.Wada and T.Saito: J. Japan Inst. Metals, 25 (1961), 159

8) T.Sugiyama and S.Inagaki: Denki Seiko, 34 (1963), 469

9) T.Takahashi, M.Kudo and K.Ichikawa: Solidification of Iron and Steel, A Data Book on the Solidification Phenomena of Iron and Steel, ed. by Solidification Comm., Joint Soc. Iron Steel Basic Research of ISIJ, ISIJ, Tokyo, (1977)

10) F.Ishii, S.Ban-ya and H.Fuwa: Tetsu-to-Hagane, 68 (1982), 1551

11) F.Ishii and H.Fuwa: Tetsu-to-Hagane, 68 (1982), 1560

12) Z.Morita and K. Kunisada : Tetsu-to-Hagane, 63 (1977), 1663 : Trans. ISIJ, 18 (1978), 648

13) S.Ban-ya, N.Maruyama and S.Fujino: Tetsu-to-Hagane, 69 (1983), 921

Chapter 6

Equilibrium Distribution Coefficient of Phosphorus in Iron Alloys.

6.1 Introduction.

The effects of solute-interactions on k_0^P of P were discussed thermodynamically in the previous chapters 4 and 5. Furthermore, the absolute value of k_0^P is necessary to examine the micro-segregation of P in steels.

In this chapter, the equilibrium distribution coefficients of P in Fe−P binary and Fe−P−C ternary alloys were determined experimentally to give value of k_0^P for α and γ phases. Also, the effect of carbon on the equilibrium distribution of P between solid and liquid phases and the segregation of P in Fe−C base steels were discussed. The relation between k_0 of various elements for α phase and that for γ phase was also studied thermodynamically.

6.2 Experimental.

Also in this chapter, so as to investigate the equilibrium distribution of P between solid and liquid phases in Fe−P base alloys, solid-liquid phases equilibrated were quenched and the phosphorus concentration in each phase was determined by EPMA . The apparatus for preparing quenched specimens is the same as shown in Fig.5-1. After melting down the sample, it was cooled to a fixed temperature, at which α phase and liquid phase coexisted, and held at that temperature for 30 or 45 minutes. When the equilibrium was achieved, by withdrawing the stopper, the sample fell through the hole at the bottom of the crucible and was quenched on the copper plate with Argon gas blow as described in 5.4.

Area analysis by EPMA were performed in this experiment so that the error in the measurement of the concentration of P in the liquid phase could be as small as possible.

6.3 Results and Discussion.

6.3.1 Equilibrium Distribution Coefficient of P between α and Liquid Phases in Fe−P Binary Alloys.

The compositions of P and the equilibration temperature of the sample used in this experiment to obtain k_0^P in Fe−P binary alloys are listed in Table 6-1. In this work, five samples were used as shown in this table. The temperature range was from 1733 to 1405 K and the equilibration temperatures were determined to make the ratio of solid in the samples, which included both solid and liquid phases in the elevated temperature, about 10 %.

Figure 6-1 indicates the experimental results of the concentration of P in both solid and liquid phases at various temperatures in Fe−P binary alloys with the liquidus and solidus published by other investigators.[1~6] As obvious from this figure, the present results are in good agreement with the results by Schürmann.[6] In this experiment, the solid phase equilibrated with

Table 6-1 Chemical composition and equilibration temperature for Fe−P binary alloys.

No.	Mole Fraction of Phosphorus	Weight Percent of Phosphorus	Holding Temperature/K
1	0.041	2.31	1733
2	0.053	3.02	1695
3	0.089	5.12	1603
4	0.134	7.88	1478
5	0.151	8.99	1405

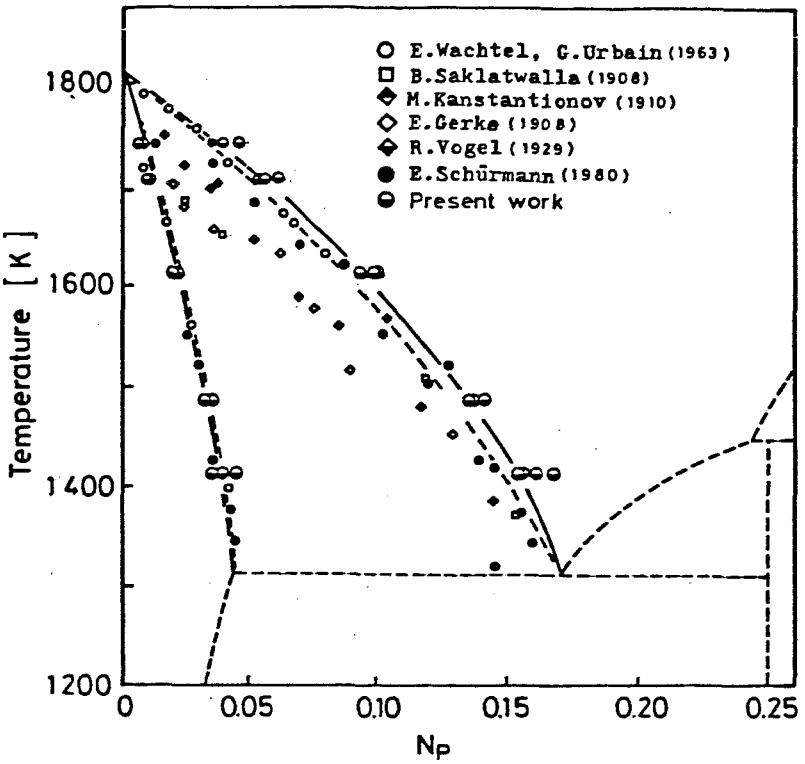

Fig.6-1 Experimental results of phosphorus concentrations in solid and liquid phases in Fe−P binary alloys.

liquid one is α phase. Then, using the concentrations of P in both α and liquid phase, the equilibrium distribution coefficient of P for α phase, $k_0^{P,\alpha}$ were obtained. The temperature dependence of the equilibrium distribution coefficient of P is shown in Fig.6-2. As obvious from this figure, the value of $k_0^{P,\alpha}$ changes from 0.16 to 0.26 in the range of temperature and concentration of P measured in this work. Also, $k_0^{P,\alpha}$ increases as the temperature decreases, in other words, the concentration of P increases. Furthermore, the linear relation holds between the equilibrium distribution coefficientt of P, $k_0^{P,\alpha}$, and temperature, T within the experimental error as shown in Fig.6-2. If the temperature dependence of $k_0^{P,\alpha}$ is regressed approximately by an order of temperature T, the following equation can be derived.

$$k_0^{P,\alpha} = 0.72 - 3.2\times10^{-4}\,T \qquad (6\text{-}1)$$

When the equilibrium distribution coefficint of P at the melting point of pure iron, that is to say, 1809K, is calculated using the above equation, $k_0^{P,\alpha}$

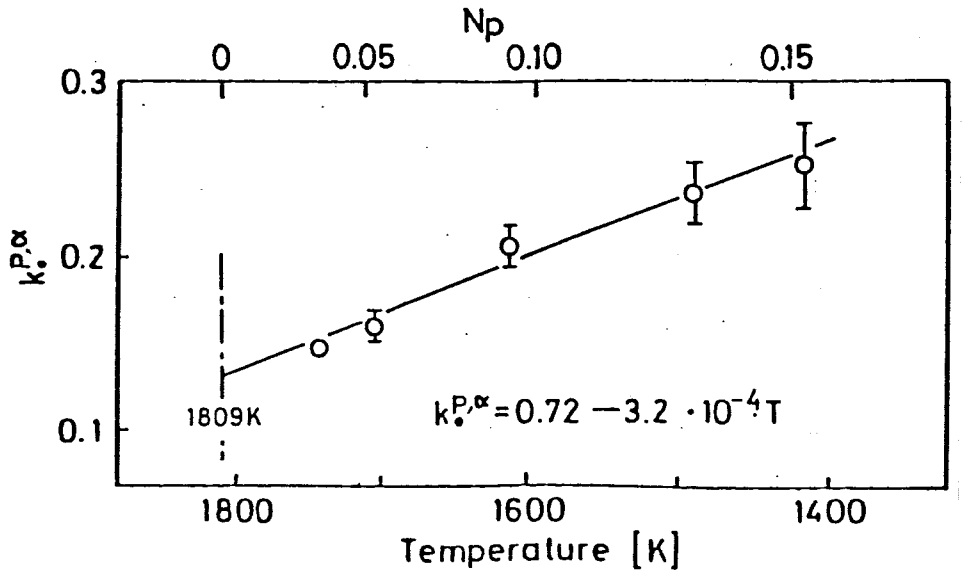

Fig.6-2 Temperature dependence of k_0 of P in Fe−P binary alloys.

can be obtained as 0.14. $k_0^{P,\alpha}$ at that temperature corresponds practically to $k_0^{P,\alpha}$ at infinite dilution of P in engineering steels which contain quite small amount of phosphorus.

Table 6-2 gives the equilibrium distribution coefficeint of P for both α and γ phases equilibrated with liquid one published by other workers[7-17] together with the present results. In this table, the present experimental result of $k_0^{P,\alpha}$ shows 0.14 at infinite dilution for α phase and it coincides with the results by Chipman[7] and Wada et al.[8]

6.3.2 Equilibrium Distribution Coefficient of P for γ Phase and the Effect of Carbon on k_0^P.

As can be seen in Table 6-2, the equilibrium distribution coefficient of P for γ phase was reported as 0.06 by Chipman,[15] 0.08 by Wada et al.[8] and 0.13 by Nakamura et al.[16] Generally these values are smaller than those for α phase.

In order to obtain the equilibrium distribution coefficient of P for

Table 6-2 Equilibrium distribution coefficient of P for both α and γ phases in Iron Alloys.

Phase	Composition	k_0^P	
α		0.13	Hays & Chipman (1938)
		0.14	Wada et al. (1967)
		0.15 - 0.18	Oeter , Ruttiger, Diener & Zahns (1969)
	0.015 - 0.092 (wt%)	0.16 + 0.04	Fischer & Frye (1970)
	0.204 - 0.211 (wt%)	0.17	Fischer, Spilzer & Hishimuma (1960)
		0.2	Tiller (1959)
		0.2 - 0.5	Smith & Rutherford (1957)
	0.07 - 0.28 (wt%)	0.23	Takahashi et al.(1977)
		0.27	Smith & Rutherford (1957)
		0.28	Fischer & Frye (1970)
		0.23	Nakamura et al.(1981)
		0.29	Suzuki et al. (1981)
	0.04 - 0.15 (mole frac.)	0.14 0.16 - 0.26	Present work (1984)
γ		0.06	Chipman (1951)
		0.08	Wada et al. (1967)
		0.13	Nakamura et al.(1981)

γ phase, the equilibrium distribution coefficients of P between liquid and γ phases in Fe−C−P ternary alloys, which contain about 0.5 wt% of P, are measured at the mole fraction of carbon between 0.09 and 0.16.

The experimental method is the same as described in previous section. The results are represented in Fig.6-3. It is obvious from this figure that the equilibrium distribution coefficient of P indicates about 0.09 and the effect of carbon on $k_0^{P,\gamma}$ can not be seen remarkably in the concentration of carbon measured in the experiment. However,if the equilibrium distribution coefficient of P for γ phase in Fe−P binary system is assumed to be 0.06 and the effect of carbon on $k_0^{P,\gamma}$ is taken into account using the Distribution Interaction Coefficient of C on P, the calculated result given by the chain line in Fig.6-3 is in good agreement with the experimental one. Consequently, it is supposed that the equilibrium distribution coefficient of P for γ phase is about 0.06 and it increases to about 0.09 at the high carbon concentration.

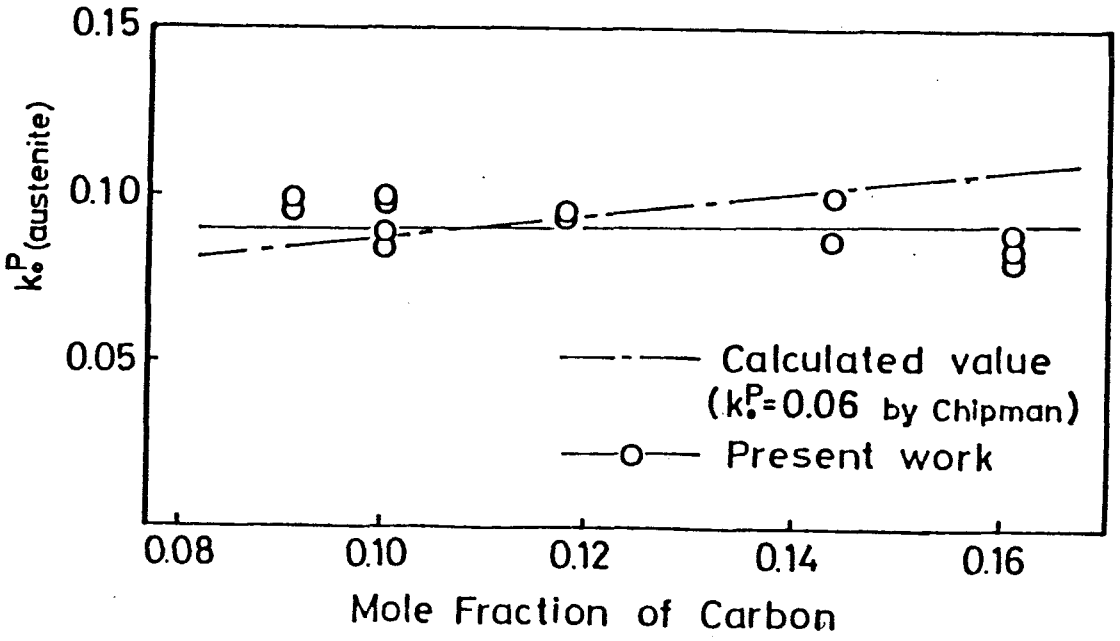

Fig.6-3 Change of $k_0^{P,1}$ of P with the concentration of C in Fe−C base ternary alloys.

By the way, the value 0.06 assumed as the equilibrium distribution coefficient of P for γ phase is consistent with the result by Chipman.[15)]

6.3.3 Change of the Equilibrium Distribution Coefficient and the Segregation Coefficient of P with the Concentration of Carbon.

In this section, the effect of carbon on the segregation of P in steels is discussed using the results obtained above. Figure 6-4 shows the change of the equilibrium distribution coefficient of P, k_0^P, (Fig.6-4(B)) and the segregation cofficient of P, $1-k_0^P$, (Fig.6-4(C)) for both α and γ phases with the concentration of carbon in the range which includes the peritectic reaction of Fe−C binary system. In these figures, the equilibrium distribution coefficient of P can be estimated to be 0.14 for α phase at the melting point of pure iron and 0.06 for γ phase at the infinite dilution respectively. The effect of carbon on the phosphorus distribution can be also evaluated using the Distribution Interaction Coefficient. Since the equilibrium distribution coefficient of P in the peritectic reaction region may possibly change between

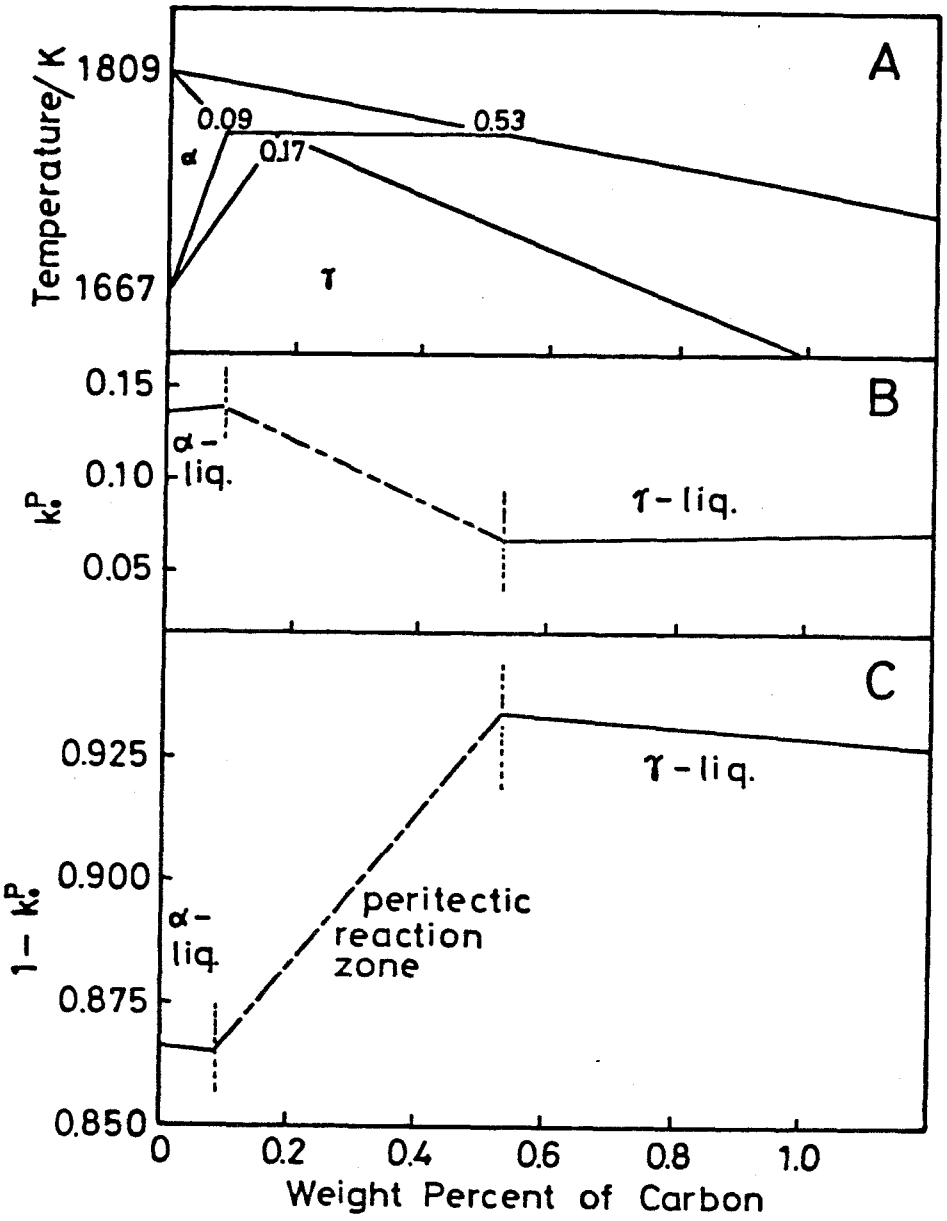

Fig.6-4 Change of the equilibrium distribution coefficient and the segregation coefficient of P with the concentration of C in Fe−C base alloys.

k_0^P for α phase and that for γ phase, then the variation of k_0^P for that region is hypothetically indicated as straight line in Fig.6-4. As exhibited in Fig.6-4(B), the equilibrium distribution coefficient of P gives about 0.14 for α phase and about 0.06 for γ phase and it increases slightly with the increasing of the concentration of carbon for both α and γ phases. Fig.6-4(C) shows that the segregation coefficient of P increases as the solid phase equilibrated with liquid one changes from α phase to γ one, and it decreases with the increasing of the concentration of carbon in each phase.

The change of the segregation coefficient of P with carbon content is compared with the experimental results of the segregation of P in steels previously published by other investigators. Figure 6-5(A) represents the variation of the segregation coefficient of P shown in Fig.6-4(C) with the concentration of carbon up to 0.2 wt%. Fig.6-5(B) denotes the change of the concentration of P in liquid phase with that of carbon when the solidification ratio of uni-directional solidified steels is regarded as 0.9983, reported by Matsumiya et al.[18] Misumi et al.[19] reported the effect of carbon content on the area where the segregation ratio of P at the center of the continuously cast slab is larger than 10 % as illustrated in Fig.6-5(C). Fig.6-5(d) gives the experimental results by Ichikawa et al.[20] about the influence of carbon on the maximum segregation ratio of P in the continuously cast slab. All of these figures indicate that the carbon content dependence of the segregation of P and the segregation ratio of P increases with the concentration of carbon. Compared with the results of this work in Fig.6-5(A), it is suggested that the effect of carbon on the segregation of P in steels depends strongly on the variation of the segregation coefficient of P accompanied with the change of the solid phase equilibrated with liquid one from α phase to γ one due to the peritectic reaction.

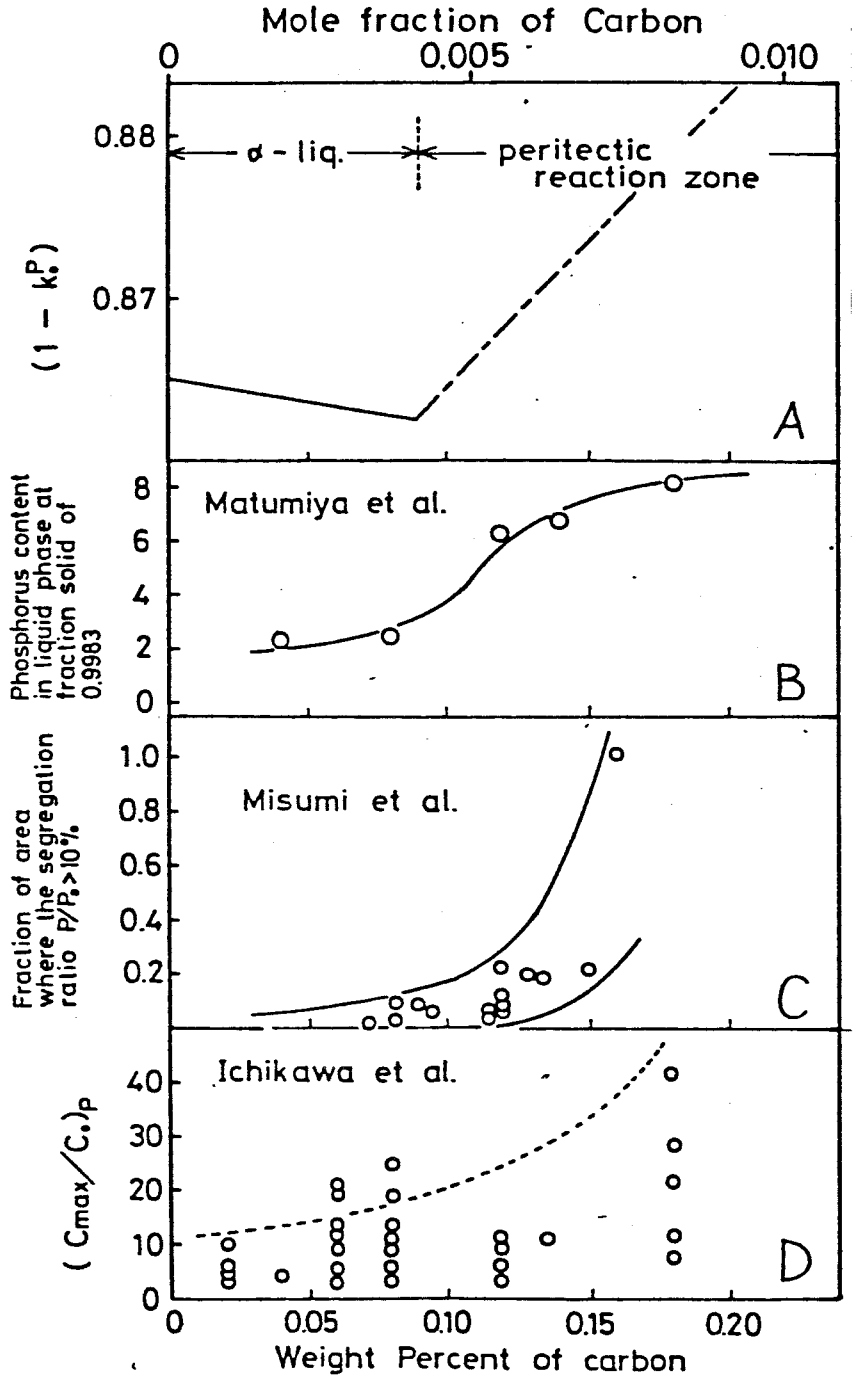

Fig.6-5 Change of the segregation coefficient of P with the concentration of C in Fe−C base alloys.

6.3.4 Thermodynamical Relation between Equilibrium Distribution Coefficients of Various Solute Elements for α Phase and those for γ Phase.

As is seen in the previous section, in order to discuss the segregation of solute elements in Fe−C base steels, it is very important to know the equilibrium distribution coefficients of these elements for both α phase and γ one.

The purpose of this section is to derive the relation between the equilibrium distribution coefficients of various elements for α phase and those for γ one thermodynamically and to discuss the validity of this relation compared with the experimental results. Also, the changes of the equilibrium distribution coefficients and the segregation coefficients of various elements with the concentration of carbon are studied in Fe−C base steels.

At the infinite dilution of solute element X in iron alloy, the equilibrium distribution coefficients of the solute element for the equilibrium of liquid - α phases and liquid - γ phases, $k_0^{X,\alpha}$ and $k_0^{X,\gamma}$, are given in the following equations (6-2) and (6-3), respectively.

$$RT\ln k_0^{X,\alpha} = (\dot{\mu}_X^{l} - \dot{\mu}_X^{\alpha}) + RT\ln \dot{\gamma}_X / \dot{\gamma}_X^{\alpha} \qquad (6\text{-}2)$$

$$RT\ln k_0^{X,\gamma} = (\dot{\mu}_X^{l} - \dot{\mu}_X^{\gamma}) + RT\ln \dot{\gamma}_X / \dot{\gamma}_X^{\gamma} \qquad (6\text{-}3)$$

The following equation (6-4) is obtained from Eqs.(6-2) and (6-3).

$$RT\ln k_0^{X,\alpha} / k_0^{X,\gamma} = (\dot{\mu}_X^{\gamma} - \dot{\mu}_X^{\alpha}) + RT\ln \dot{\gamma}_X^{\gamma} / \dot{\gamma}_X^{\alpha} \qquad (6\text{-}4)$$

In Eq.(6-4), the right hand side is equal to Ferrite / Austenite Stabilizing Parameter $\Delta G_X^{\alpha\text{-}\gamma}$ defined as the the free energy change accompanied by transfer of one mole of each alloying element from ferrite to austenite.[21] That is to say,

$$\ln k_0^{X,\alpha} / k_0^{X,\gamma} = \Delta G_X^{\alpha\text{-}\gamma} / RT \qquad (6\text{-}5)$$

It is clear from Eq.(6-5) that $\Delta G_X^{\alpha\text{-}\tau}$ gives the thermodynamical relation between $k_0^{X,\alpha}$ for the equilibrium of liquid - α phase and $k_0^{X,\tau}$ for that of liquid - τ phase. Values of $\Delta G_X^{\alpha\text{-}\tau}$ of various elements have been reported by many investigators. Particularly, Ishida et al.[21] reported the temperature dependence of $\Delta G_X^{\alpha\text{-}\tau}$ of various elements as shown in Fig.6-6. The ratio of $k_0^{X,\alpha} / k_0^{X,\tau}$ can be calculated in Eq.(6-5) by using $\Delta G_X^{\alpha\text{-}\tau}$ obtained from the results of Ishida et al. at 1768K, the temperature of the peritectic reaction in Fe−C binary alloy. The results are shown in Table 6-3. As is obvious from this table, for ferrite stabilizing elements:

$$k_0^{X,\alpha} > k_0^{X,\tau} \qquad (6\text{-}6)$$

for anstenite stabilizing elements:

$$k_0^{X,\alpha} < k_0^{X,\tau} \qquad (6\text{-}7)$$

The relations in Eqs.(6-5), (6-6) and (6-7) are compared to the experimen-

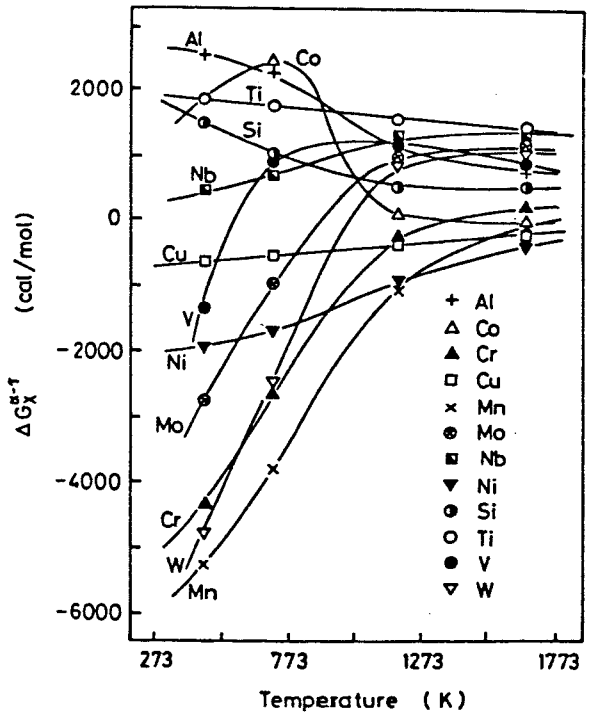

Fig.6-6 Temperature dependence of Ferrite/Austenite Stabilizing Parameter $\Delta G_X^{\alpha\text{-}\tau}$ of various elements in iron alloys.

Table 6-3 Ratio of $k_0^{X,\alpha}/k_0^{X,\gamma}$ of various elements in iron alloys.

	Element	$\Delta G_X^{\alpha-\gamma}$ (cal)	$k_0^{X,\alpha}/k_0^{X,\gamma}$
Ferrite Stabilizing Elements	Ti	1450	1.51
	Nb	1350	1.47
	Mo	1170	1.40
	W	1070	1.36
	V	900	1.29
	Al	760	1.24
	Si	550	1.17
	Cr	220	1.06
	P	2200	1.87
Austenite Stabilizing Elements	Co	−50	0.99
	Mn	−70	0.98
	Cu	−170	0.95
	Ni	−360	0.90

tal results of some elements[14] in Figs.6-7~6-14 . In these figures, the relations for Mo, Ni, Cr, Cu obtained from Eq.(6-5) are in good agreement with the experimental ones. For Mn, the relation in Eq.(6-5) is almost satisfied except the result by Fischer et al.[10] for α phase.

For P , some reported that the equilibrium distribution coefficient $k_0^{P,\alpha}$ is 0.13 ~ 0.15 for α phase and about 0.06 for γ one, others showed $k_0^{P,\gamma}$ as 0.2 ~0.23 for α phase and about 0.13 for γ one. However, the values reported by each group are satisfied with the relation in Eq.(6-5) as shown in Fig.6-14. So, it seems questionable, for instance, to use the equilibrium distribution coefficient of P as about 0.2 for α phase and about 0.6 for γ phase.

The equilibrium distribution coefficients of V and Al for γ phase have not been reported, but they can be estimated from those for α phase by using Eq.(6-5). The results are indicated in Fig.6-15. It is obvious from this figure that $k_0^{V,\gamma}$ = 0.7 ~ 0.75 for V and $k_0^{Al,\gamma}$ = 0.48~ 0.75 for Al. By the way, it has been already descrived in chapter 4 that the calculated result of the equilibrium distribution of V for γ phase in Fe−C−V system agreed

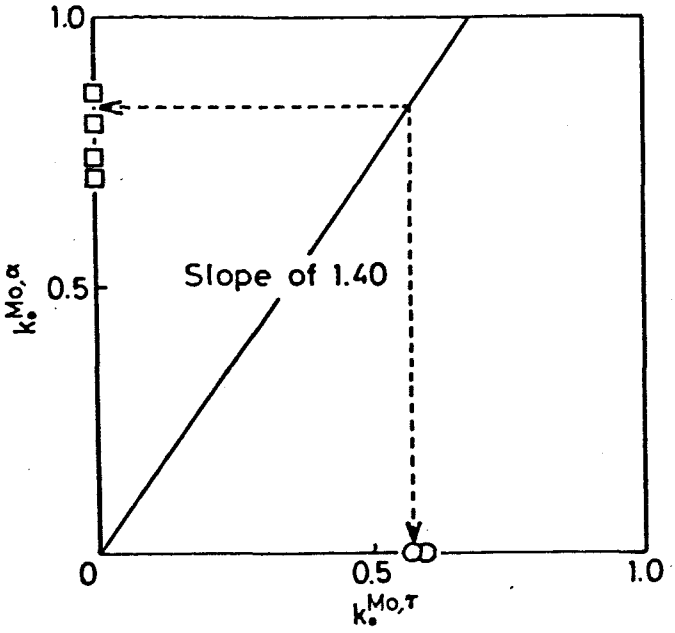

Fig.6-7 Comparison of calculated $k_0^{Mo,\alpha}/k_0^{Mo,\tau}$ of Mo with the experimental results.

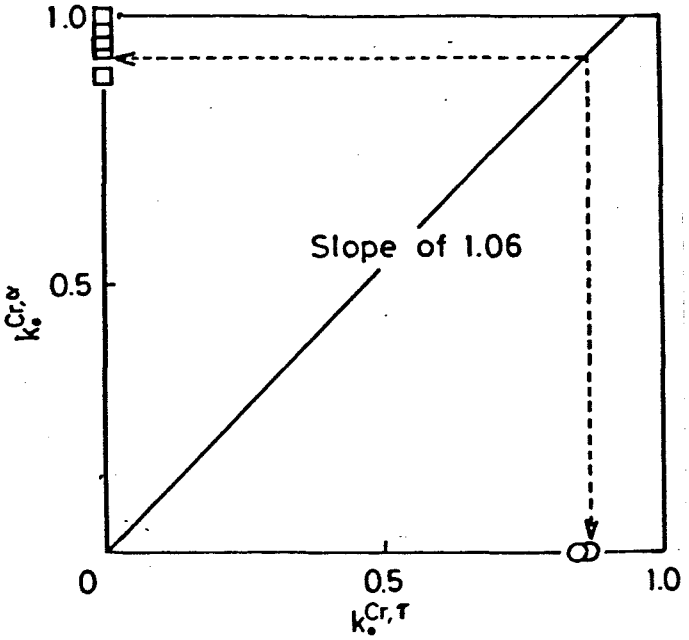

Fig.6-8 Comparison of calculated $k_0^{Cr,\alpha}/k_0^{Cr,\tau}$ of Cr with the experimental results.

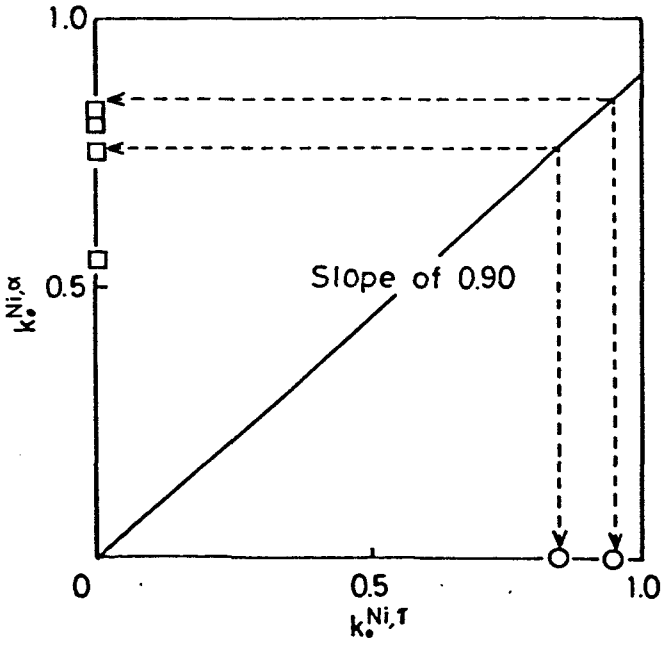

Fig.6-9 Comparison of calculated $k_0^{Ni,\alpha}/k_0^{Ni,\tau}$ of Ni with the experimental results.

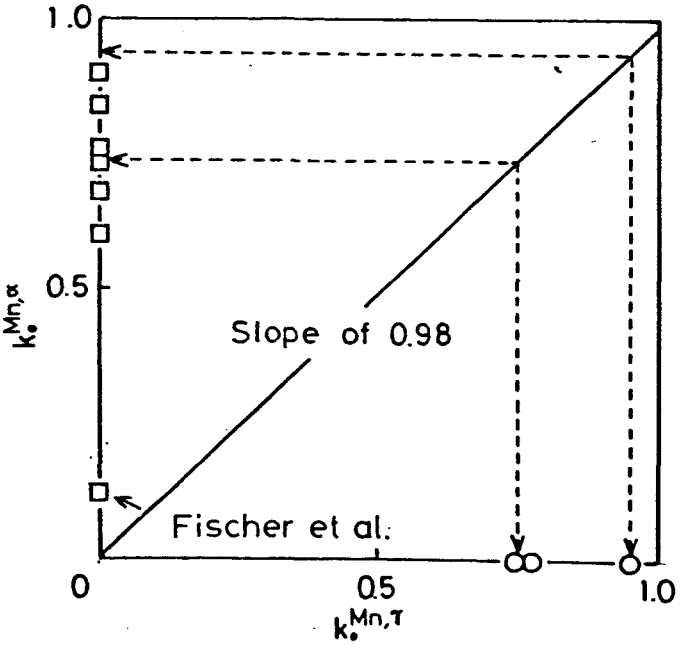

Fig.6-10 Comparison of calculated $k_0^{Mn,\alpha}/k_0^{Mn,\tau}$ of Mn with the experimental results.

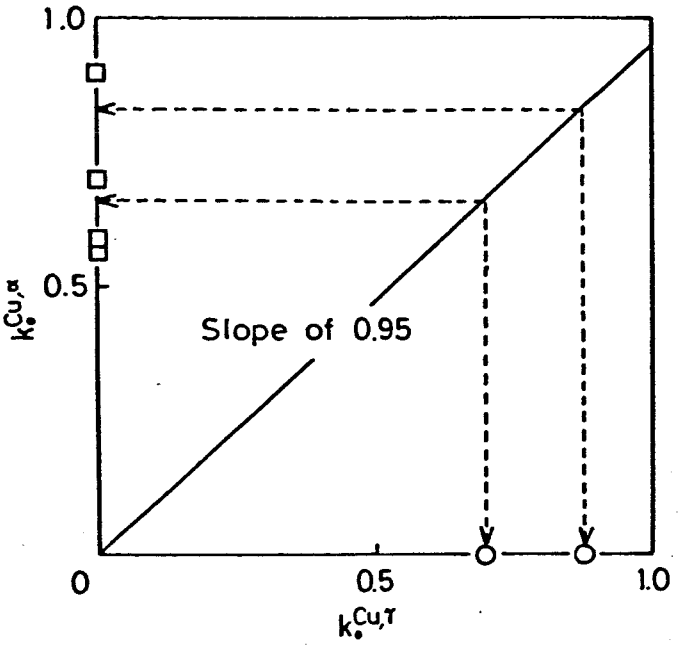

Fig.6-11 Comparison of calculated $k_0^{Cu,\alpha}/k_0^{Cu,\tau}$ of Cu with the experimental results.

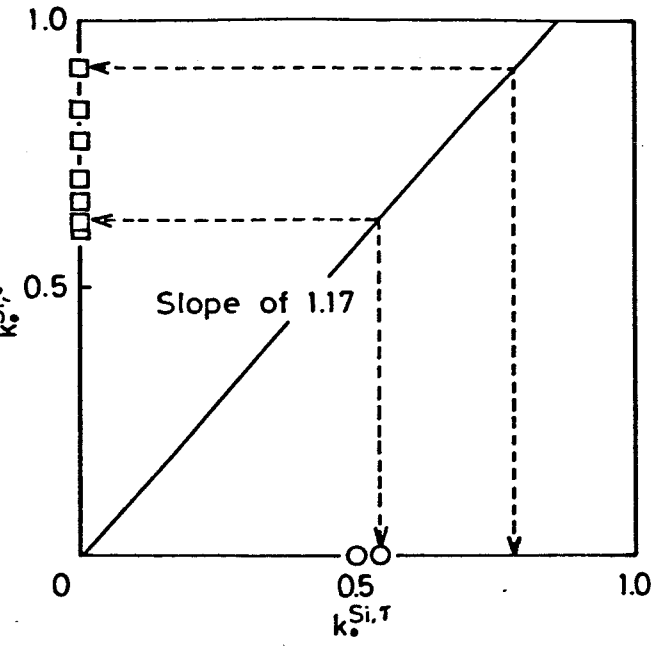

Fig.6-12 Comparison of calculated $k_0^{Si,\alpha}/k_0^{Si,\tau}$ of Si with the experimental results.

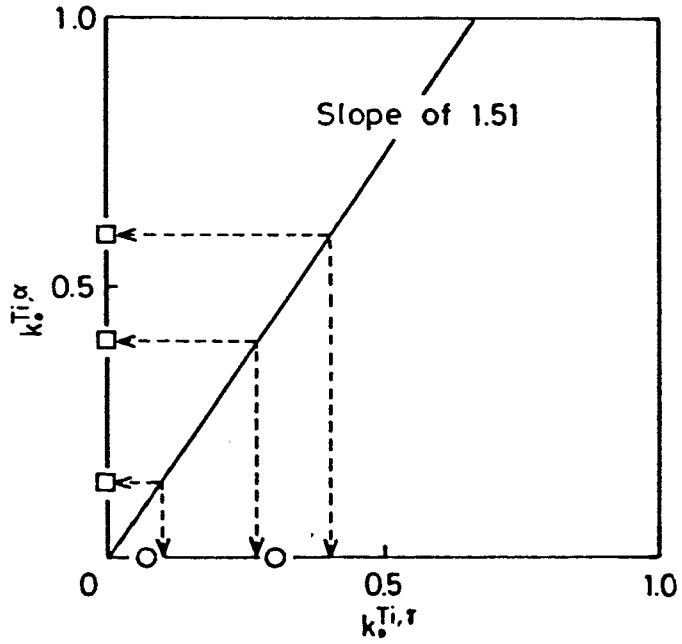

Fig.6-13 Comparison of calculated $k_0^{Ti,\alpha}/k_0^{Ti,\tau}$ of Ti with the experimental results.

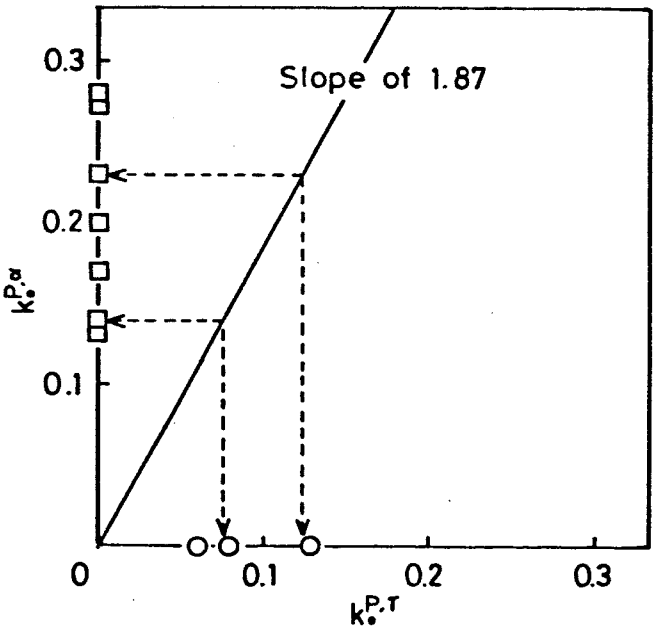

Fig.6-14 Comparison of calculated $k_0^{P,\alpha}/k_0^{P,\tau}$ of P with the experimental results.

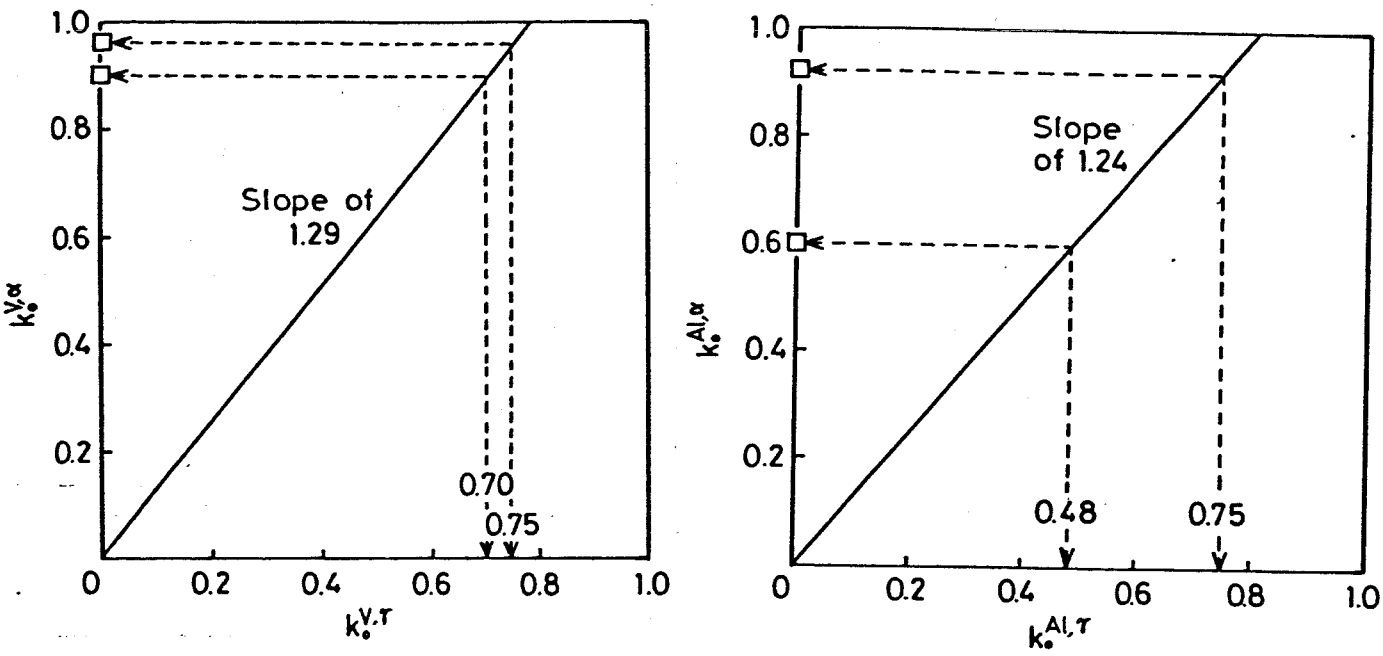

Fig.6-15 Estimation of $k_0^{V,\gamma}$ and $k_0^{Al,\gamma}$ from $k_0^{X,\alpha}/k_0^{X,\gamma}$.

with the experimental one well when the value 0.76 was used as $k_0^{V,\gamma}$.

Figure 6-16 shows the variation of the segregation coefficients of various alloying elements with the change of solid phase equilibrated with liquid one from α phase to γ one due to the peritectic reaction in Fe−C base steels. In this figure, the abscissas indicates the concentration of carbon up to 0.8 wt% where the peritectic reaction is included. As is seen from Fig.6-16, the segregation coefficients of the ferrite stabilizing elements increase with the increasing of the concentration of carbon, on the other hand, those of the austenite stabilizing elements decrease.

Figure 6-17 represents the experimental results of the variations of the segregation ratios for Cr and Ni with carbon contents.[22] In Figs.6-5 and 6-17, P and Cr are ferrite stabilizing element and their segregation ratios increase with carbon content, while Ni is austenite stabilizing element and the segregation ratio of Ni decreases. Consequently, the calculated results from Eqs.(6-5),(6-6) and (6-7) are in good agreement with the experimental ones.

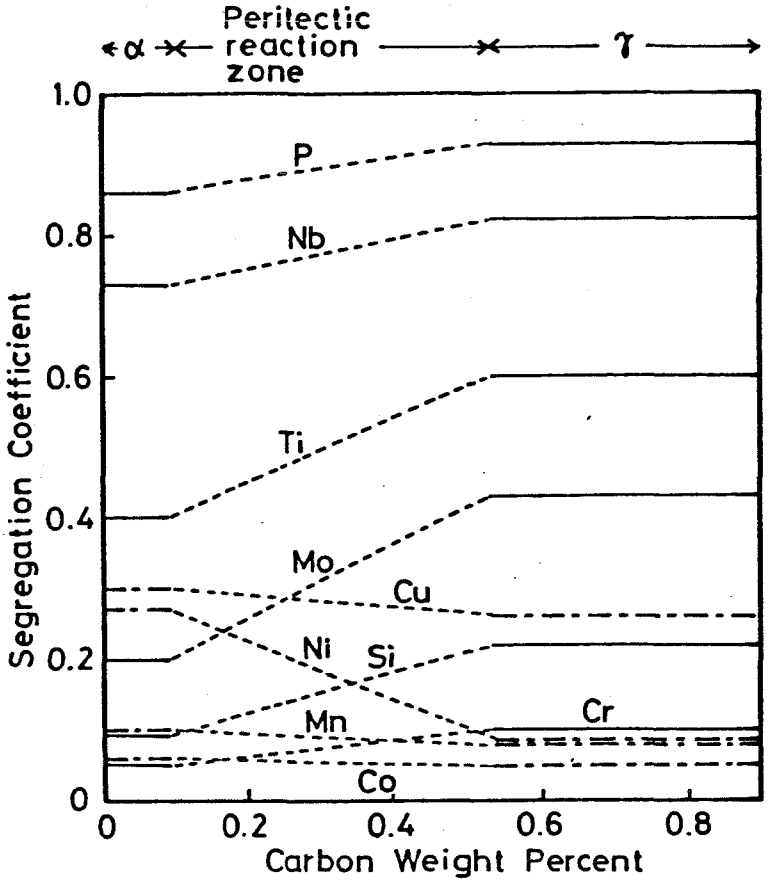

Fig.6-16 Variation of the segregation coefficients of various elements with carbon content in Fe−C base alloys.

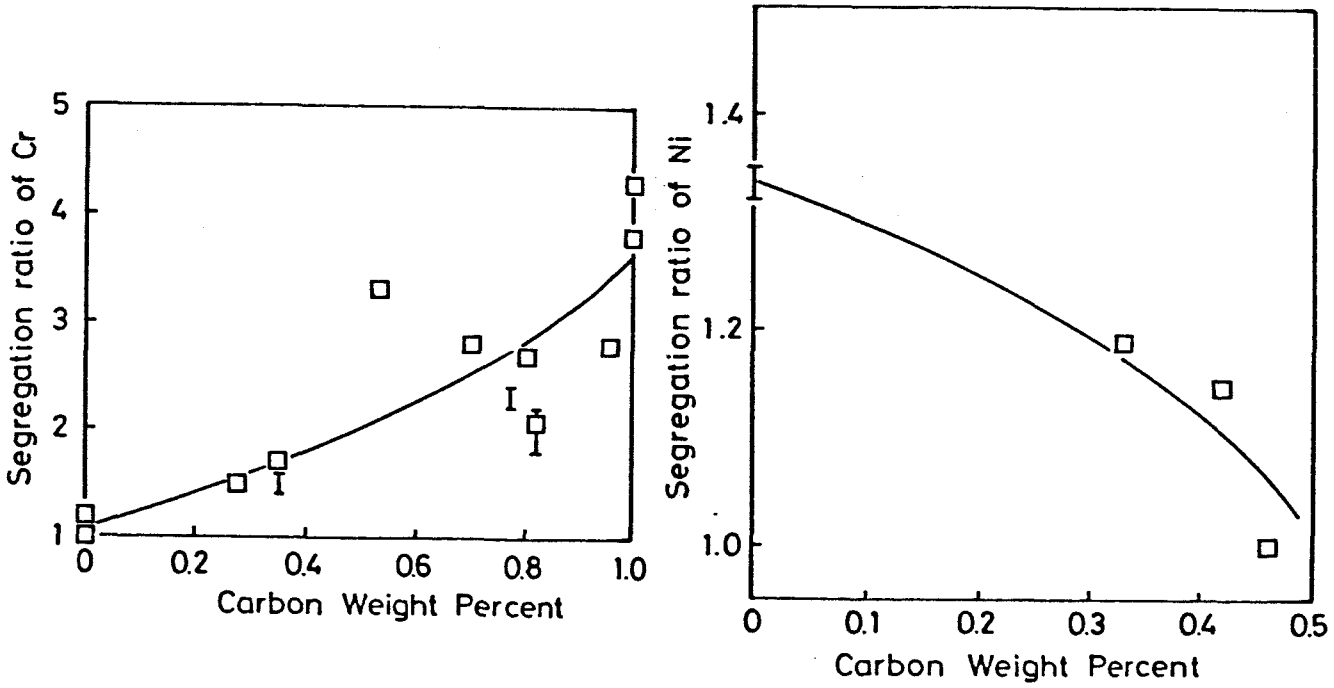

Fig.6-17 Variation of the segregation ratios of Cr and Ni with carbon content in steels.

6.4 Conclusion.

In this chapter, the equilibrium distribution coefficients of P in Fe−P binary and Fe−P−C ternary systems were obtained experimentally and the carbon content dependence of the equilibrium distribution coefficient of P was discussed using Distribution Interaction Coefficient. Also, the relation between $k_0^{P,\alpha}$ for α phase and that for γ one was derived thermodynamically.

The results obtained are summarized as follows.

① Temperature dependence of $k_0^{P,\alpha}$ for α phase in Fe−P binary alloy is given by

$$k_0^{P,\alpha} = 0.72 - 3.2\times10^{-4}\,T$$

For the above equation, $k_0^{P,\alpha}$ at infinite dilution of P is 0.14.

② $k_0^{P,\gamma}$ for γ phase at high concentration of carbon from 0.09~0.16 is about 0.09. $k_0^{P,\gamma}$ increases with the concentration of carbon and $k_0^{P,\gamma}$ at infinite dilution is 0.06.

③ The increase of the segregation ratio of P with carbon content in steels is dependent on the change of the equilibrium distribution coefficient of P accompanied with the transformation of the solid phase equilibrated with liquid one due to the peritectic reaction.

④ The equilibrium distribution coefficients of solute element X, $k_0^{X,\alpha}$, for α phase and $k_0^{X,\gamma}$ for γ phase are related to Ferrite / Austenite Stabilizing Parameter $\Delta G_X^{\alpha\text{-}\gamma}$ as shown in the following equation.

$$\ln k_0^{X,\alpha} / k_0^{X,\gamma} = \Delta G_X^{\alpha\text{-}\gamma} / RT$$

The ratio of $k_0^{X,\alpha} / k_0^{X,\gamma}$ can be calculated from $\Delta G_X^{\alpha\text{-}\gamma}$.

⑤ For ferrite stabilizing elements: $k_0^{X,\alpha} > k_0^{X,\gamma}$

and for austenite stabilizing elements: $k_0^{X,\alpha} < k_0^{X,\gamma}$.

⑥ In Fe−C base steels, as the solid phase equilibrated with liquid one changes from α phase to γ phase with the increaseing of the concentration of carbon due to the peritectic reaction, the segregation coefficients of ferrite stabilizing elements increase while those of austenite stabilizing elements decrease.

6.5 References.

1) E.Wachtel, G.Urbain und E.Ubelacker: C.R.hebd. Seances, Acad. Sci. 257 (1963) S.2470

2) B.Saklatwalla: Metallurg., 5 (1908), S.331 u.S.711

3) W.Konstantinov: Stahl u. Eisen, 30 (1910), S.1120

4) E.Gerke: Metallurg., 5 (1908), S.604

5) R.Vogel: Arch. Eisenhuttenwes., 3 (1929/30), S.369

6) E.Schurmann und H.P.Keizer: Arch. Eisenhüttenwes., 51 (1980), 325

7) A.Hays and J.Chipman: Trans. AIME, 135 (1939), 85

8) T.Wada and H.Wada: The Abstract for the 61st Lecture Meeting of Japan Institute of Metals, JIM, Sendai, (1967), 174

9) F.Oeters, K.Ruttiger, A.Diener and G.Zahs: Arch. Eisenhüttenwes., 40 (1961), 611

10) W.A.Fischer and H.Frye: Arch. Eisenhüttenwes., 41 (1970), 293

11) W.A.Fischer, H.Spilzer and M.Hishimura: Arch. Eisenhüttenwes.,31 (1960), 365

12) W.A.Tiller: JISI, 192 (1959), 338

13) R.L.Smith and J.L.Rutherford: J.Metals, 9 (1957),478

14) T.Takahashi, M.Kudo and K.Ichikawa: Solidification of Iron and Steel, A Data Book on the Solidification Phenomena of Iron and Steel, ed. by Solidification Comm., Joint Soc. Iron SteeL Basic Research of ISIJ, ISIJ, Tokyo, (1977)

15) J.Chipman: Physical Chemistry of Steelmaking Committee, Iron and Steel Division, AIME, Basic Open Hearth Steelmaking, The American Institute of Mining and Metallurgical Engineering, (1951), 632

16) T.Nakamura and H.Esaka: Tetsu-to-Hagane, 67 (1981), S140

17) S.Suzuki, T.Umeda and Y.Kimura: Tetsu-to-Hagane, 67 (1981), S142

18) T.Matsumiya, H.Kajioka, S.Mizoguchi, Y.Ueshima and H.Esaka: Tetsu-to-Hagane, 69 (1983), A217

19) H.Misumi and K.Kitamura: Tetsu-to-Hagane, 69 (1983), S964

20) H.Ichikawa, M.Kawasaki, T.Watanabe, M.Toyota and Y.Sugitani: Tetsu-to-Hagane, 69 (1983), A213

21) K.Ishida and T.Nishizawa: J. Japan Inst. Metals, 36 (1972), 270

22) T.Okamoto: Solidification of Iron and Steel, ed. by Solidification Comm., Joint Soc. Iron Steel Basic Research of ISIJ, ISIJ, Tokyo,(1977).

Chapter 7

Equilibrium Distribution of Gaseous Elements between Solid and Liquid Phases in Fe, Co, Ni and Cu Base Alloys.

7.1 Introduction.

Informations on solubilities of gaseous elements in iron base alloys are necessarily important for understanding of their physico-chemical behaviour in steels and also for developing high quality of steels. In general the solubilities of N and H in liquid iron alloys seem to have fairly been established. Besides that, the detail information about the behaviour of gaseous elements in alloys during solidification is necessary to discuss the generation of bubbles during solidification, the influences of gaseous elements on physical and mechanical properties of alloys and so on.

In this chapter a simple equation of the equilibrium distribution coefficients of N and H between solid and liquid phases in iron alloys was derived thermodynamically. Also, Distribution Interaction Coefficient (D I C) and Distribution Interaction Parameter (D I P) were applied to the evaluation of k_0 of N and H in Co, Ni and Cu base ternary alloys and the effects of various alloying elements on the equilibrium distribution of these gaseous elements between solid and liquid phases in these alloys were presumed.

7.2 Equations for Equilibrium Distribution Coefficient of N and H in Iron Base Alloys.

As stated in the previous chapter, the equilibrium distribution coefficient of element i(i=N or H) in Fe−i−X ternary system can be shown by

$$\ln k_0^i = (\dot{\mu}_i^l - \dot{\mu}_i^s)/RT + \ln \dot{\gamma}_i^l / \dot{\gamma}_i^s + (\varepsilon_i^{i,l} - \varepsilon_i^{i,s} k_0^i) N_i^l + (\varepsilon_i^{X,l} - \varepsilon_i^{X,s} k_0^X) N_X^l \qquad (7\text{-}1)$$

Since it is well known that the dissolution of nitrogen or hydrogen in pure

iron, either in the liquid state or in the solid one, obeys Sievert's law, the self-interaction parameters of nitrogen or hydrogen in iron are shown as

$$\varepsilon_i^i \fallingdotseq 0 \tag{7-2}$$

As already mentioned, Mori and Ichise[1] proposed that a linear relation holds approximately between ε of some elements X in liquid phase and ε in austenite and the gradient of this straight line becomes unity as the temperature of the liquid phase approaches that of solid one. So, the following equation can be assumed at the temperatures at which the liquid and the solid coexist.

$$\varepsilon_i^{X,l} \fallingdotseq \varepsilon_i^{X,s} \tag{7-3}$$

Substituting Eqs.(7-2) and (7-3) into Eq.(7-1) yields

$$\begin{aligned} \ln k_0^i = {} & (\dot{\mu}_i^l - \dot{\mu}_i^s) / RT + \ln \dot{\gamma}_i^l / \dot{\gamma}_i^s \\ & + (1 - k_0^X)\, \varepsilon_i^{X,l} N_X^l \end{aligned} \tag{7-4}$$

The above equation describes that the equilibrium distribution coefficient consists of the terms $(\dot{\mu}_i^l - \dot{\mu}_i^s) / RT + \ln \dot{\gamma}_i^l / \dot{\gamma}_i^s$ being dependent on the property of nitrogen or hydrogen and the term $(1 - k_0^X)\, \varepsilon_i^{X,l} N_X^l$ showing the the effect of the alloying element X on k_0.

On the other hand, as the same way described in Eq.(7-1), the equilibrium distribution coefficient of the alloying element X, k_0 is given by

$$\begin{aligned} \ln k_0^X = {} & (\dot{\mu}_X^l - \dot{\mu}_X^s) / RT + \ln \dot{\gamma}_X^l / \dot{\gamma}_X^s \\ & + (\varepsilon_X^{X,l} - \varepsilon_X^{X,s} k_0^X)\, N_X^l + (\varepsilon_X^{i,l} - \varepsilon_X^{i,s} k_0^i)\, N_i^l \end{aligned} \tag{7-5}$$

As the fourth term of the right-hand side of the above equation shows the effect of element i on k_0 but the i is gaseous element and its solubility

is quite small, this term can be neglected. The third term of the right-hand side of Eq.(7-5) indicates the dependence of k_0 on the concentration of X. The contribution of this term to k_0 is known to be much smaller than that of the first and second terms of the right-hand side of Eq.(7-5). So this term can be ignored, too. Thus, k_0 depends on only the first and the second terms

$$(\dot{\mu}_X^l - \dot{\mu}_X^s)/RT + \ln \dot{\gamma}_X^l / \dot{\gamma}_X^s$$

and it can be considered to be constant at a given temperature.

Consequently, k_0 can be calculated by substituting the thermodynamic data into Eq.(7-4). Also, the effects of various alloying elements X on k_0 can be discussed.

It is obvious from Eq.(7-4) that the fundamental factor controlling k_0 of nitrogen and hydrogen,

$$(\dot{\mu}_i^l - \dot{\mu}_i^s)/RT + \ln \dot{\gamma}_i^l / \dot{\gamma}_i^s$$

is equal to k_0 of these gaseous elements in Fe−N and Fe−H binary systems. Namely:

$$(\dot{\mu}_i^l - \dot{\mu}_i^s)/RT + \ln \dot{\gamma}_i^l / \dot{\gamma}_i^s = \ln k_0^i \quad (\text{Fe}-i \text{ binary system})$$

In order to obtain the fundamental factor controlling k_0 in Fe−i−X ternary system, k_0's of nitrogen and hydrogen in Fe−N and Fe−H binary systems are estimated as follows. Figure 7-1 shows the temperature dependence of the solubilities of nitrogen and hydrogen in Fe−N and Fe−H binary systems.[2] In this figure, extrapolating the solubility curves, we can obtain the solubilities of nitrogen and hydrogen in both the solid and the liquid phases at a given temperature and subsequently k_0. Thus, the factor

$$(\dot{\mu}_i^l - \dot{\mu}_i^s)/RT + \ln \dot{\gamma}_i^l / \dot{\gamma}_i^s$$

can be estimated as shown in Table 7-1.

Also, the second term of the right-hand side of Eq.(7-4) indicates the effects of various alloying elements on k_0 of these gaseous elements, but this term is equal to DIC and it was already stated in detail in chapter 4.

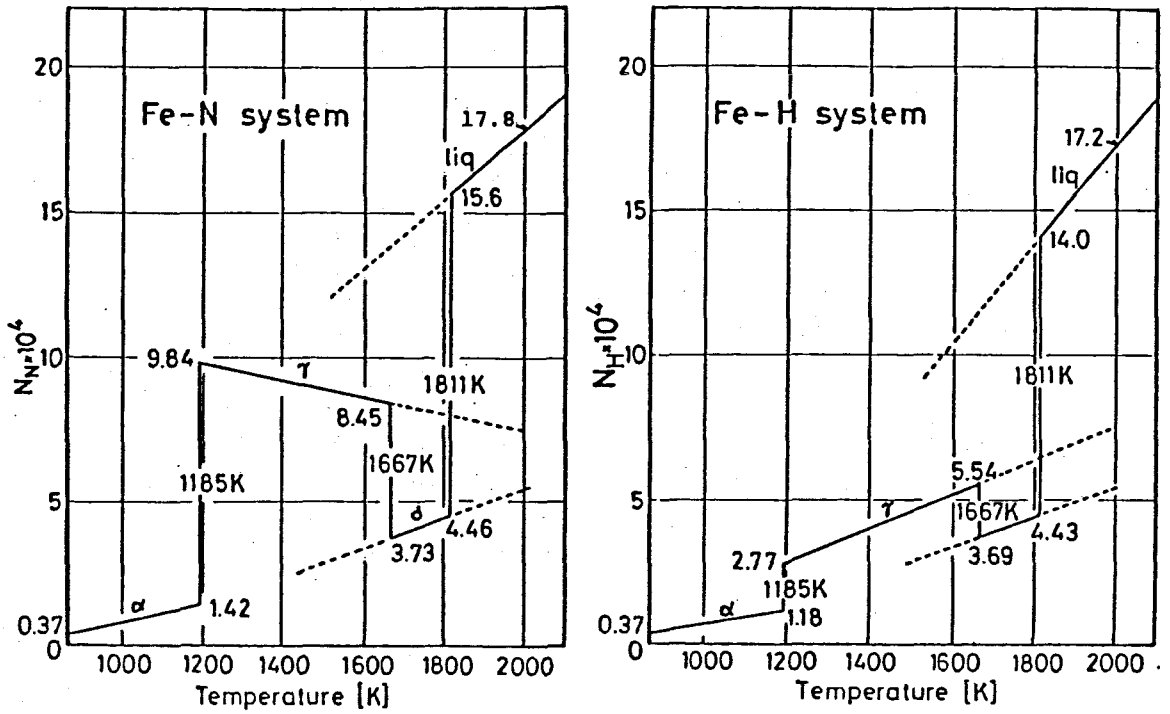

Fig.7-1 Solubilities of nitrogen and hydrogen in iron.

Table 7-1 Equilibrium distribution coefficients of nitrogen and hydrogen.

Temp. [K]	Temp. [°C]	$N_N \cdot 10^4$ sol.	$N_N \cdot 10^4$ liq.	k_o^N	$N_H \cdot 10^4$ sol.	$N_H \cdot 10^4$ liq.	k_o^H
1500	1227	γ8.90	11.8	0.75	γ4.60	8.70	0.53
		δ2.90		0.24	δ2.80		0.32
1600	1327	γ8.60	13.1	0.65	γ5.20	10.4	0.50
		δ3.40		0.26	δ3.35		0.32
1700	1427	γ8.30	14.2	0.58	γ5.75	12.1	0.47
		δ3.90		0.27	δ3.80		0.31
1800	1527	γ8.00	15.4	0.52	γ6.30	13.8	0.46
		δ4.40		0.28	δ4.30		0.31

7.3 Effects of Various Solute Elements on the Equilibrium Distribution of N and H between Solid and Liquid Phases in Co, Ni and Cu Base Alloys.

Mukai[3] showed that there exist the distinct correlations between the interaction parameters of alloying elements on nitrogen or hydrogen and the number of effective free electron in liquid iron alloys. He also represented the same correlations for liquid cobalt, nickel and copper alloys. So, the interactions of nitrogen or hydrogen and various alloying elements in these nonferrous alloys are considered to be caused by the same mechanism of the interaction in iron alloys. Kato et al.[4,5] also represented that the correlation holds between the interactions of alloying elements on hydrogen in iron base alloys and those in copper base ones. Then, the relations between the interaction parameters of alloying elements on N and H in iron base alloys and those in cobalt, nickel and copper base alloys are given in Figs.7-2~ 7-6.[4~18] It is obvious from these figures that the distinct correlations exist particularly in Figs.7-2 ~ 7-4.

Consequently, it is thought that as the interactions of alloying elements on gaseous elements in cobalt, nickel and copper base alloys are seemingly based on the same mechanism in iron base alloys, D I C and D I P can be applied to these nonferrous alloy systems.

In the definition of D I C and D I P, the equilibrium distribution coefficient of the alloying elements, k_0^X , is strictly that in ternary alloys. Since, however, the solubility of gaseous elements in alloys is very small, the effects of these gaseous elements on the equilibrium distribution coefficient of the alloying elements is negligibly small. Thus, it is assumed that the equilibrium distribution coefficient of the alloying element in binary alloys can be used as k_0^X in D I C and D I P.

The data of the equilibrium distribution coefficient of the alloying element obtained from the phase diagrams by Hultgren et al.[19] and Hansen[20] are applied to the equilibrium distribution coefficient of the alloying element in the definition of D I P. The calculated results of Distribution Interaction

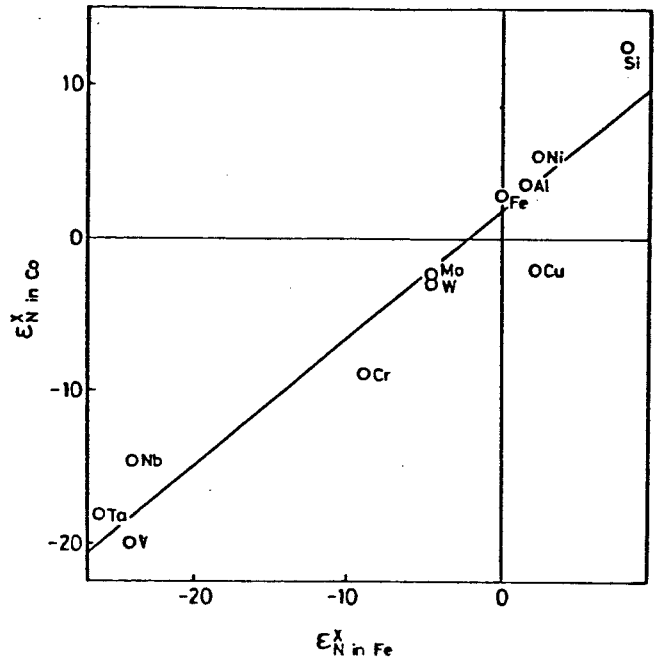

Fig.7-2 Relation between ε_N^X in liquid Co alloys and ε_N^X in liquid Fe alloys.

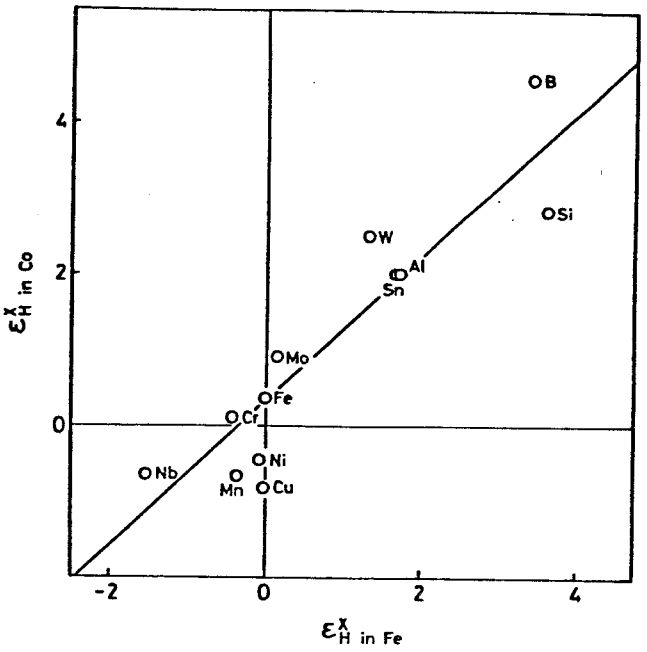

Fig.7-3 Relation between ε_H^X in liquid Co alloys and ε_H^X in liquid Fe alloys.

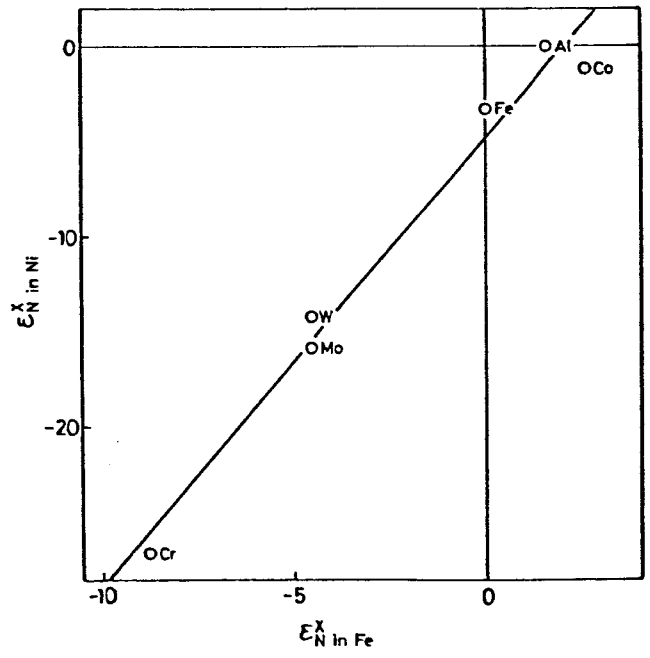

Fig.7-4 Relation between ε_N^X in liquid Ni alloys and ε_N^X in liquid Fe alloys.

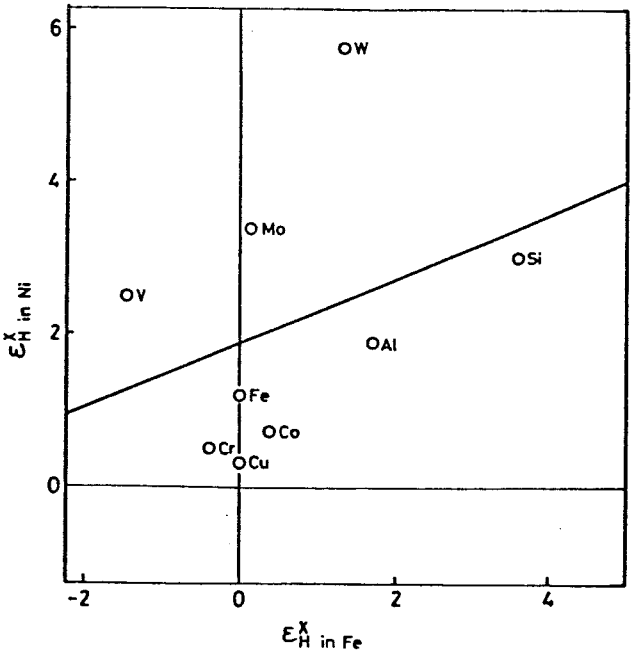

Fig.7-5 Relation between ε_H^X in liquid Ni alloys and ε_H^X in liquid Fe alloys.

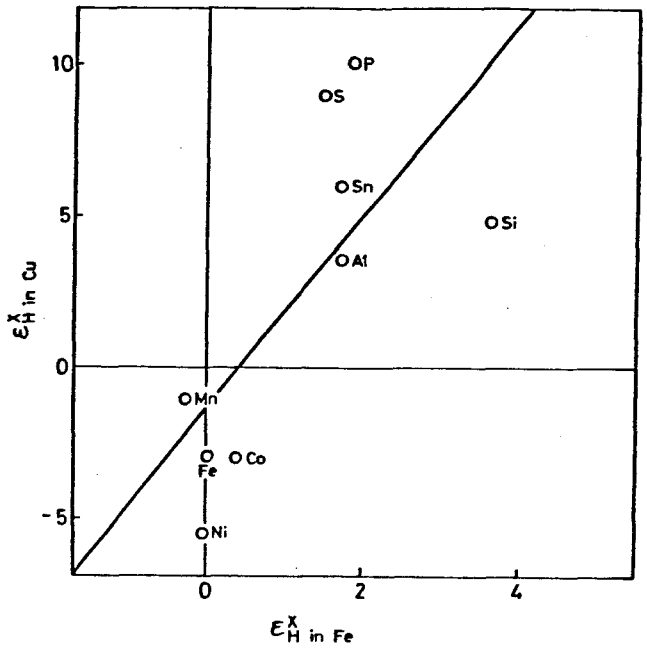

Fig.7-6 Relation between ε_H^X in liquid Cu alloys and ε_H^X in liquid Fe alloys.

Parameter of various elements on gaseous elements, $\delta_i^X = (1 - k_0^X)\ \varepsilon_i^{X,l}$, are indicated in Table 7-2 with the data[4~17,19,20] used in the calculation. Figs.7-7 ~ 7-11 represent the variation of D I C 's of N and H with the concentration of the alloying elements in various alloys. It is obvious from these figures that the alloying elements denoting the repulsive effects against nitrogen and hydrogen have the tendency to increase D I C 's of N and H, while the element indicating the attractive effects against these gaseous elements decrease those coefficients of N and H. Also, it can be seen that D I C 's of various alloying elements on N or H in cobalt, nickel and copper alloys change in almost similar tendency for each element and in each alloy.

Table 7-2 Data of $\varepsilon_i^{X,I}$, k_0^X and calculated results of $\delta_i^X = (1 - k_0^X) \cdot \varepsilon_i^{X,I}$ in Co, Ni and Cu alloys.

	Cobalt alloy					Nickel alloy					Copper alloy		
	Nitrogen			Hydrogen		Nitrogen			Hydrogen		Hydrogen		
	k_0^X [19,20]	$\varepsilon_N^{X,I}$ [1,6]	δ_N^X	$\varepsilon_H^{X,I}$ [7]	δ_H^X	k_0^X [19,20]	$\varepsilon_N^{X,I}$	δ_N^X	$\varepsilon_H^{X,I}$	δ_H^X	k_0^X [19,20]	$\varepsilon_H^{X,I}$	δ_H^X
Al	0.55	3.7	1.7	2.0	0.9	0.84	0.0 [10]	0.0	1.9 [11]	0.30	0.60	3.6 [16]	1.4
Ag											0.24	-0.47 [17]	-0.36
Au						0.25			3.5 [11]	2.6	0.58	-1.9 [17]	-0.80
Co						0.95	-1.24 [9]	-0.06	0.73 [14]	0.04			
Cr	0.80	-8.8	-1.8	0.0	0.0	0.80	-26.6 [8]	-5.3	0.5 [13]	0.10			
Cu	0.49	-2.2	-1.1	-0.85	-0.43	0.54			0.33 [14]	0.15			
Fe	0.95	2.8	0.14	0.31	0.02	0.80	-3.3 [8]	-0.66	1.2 [14]	0.24			
Mn				-0.68	-0.36						0.60	-1.1 [5]	-0.44
Mo	0.64	-2.4	-0.86	0.90	0.32	0.80	-15.8 [10]	-3.2	3.4 [12]	0.68			
Nb	0.47	-14.7	-7.8	0.0	0.0								
Ni	0.95	5.5	0.28	-0.46	-0.02								
Sb											0.15	13.0 [5]	11.1
Si	0.45	12.6	6.9	2.8	1.54	0.51			3.0 [13]	1.5	0.49	4.8 [4]	2.4
Sn	0.13			2.0	1.74						0.18	6.0 [4]	4.9
Ta	0.25	-18.4	-13.8										
Ti	0.47	-84.3	-44.7			0.71	-41.1 [10]	-12.0					
V	0.36	-20.0	-12.8			0.90			2.5 [15]	0.25			
Zn											0.82	6.8 [5]	1.2

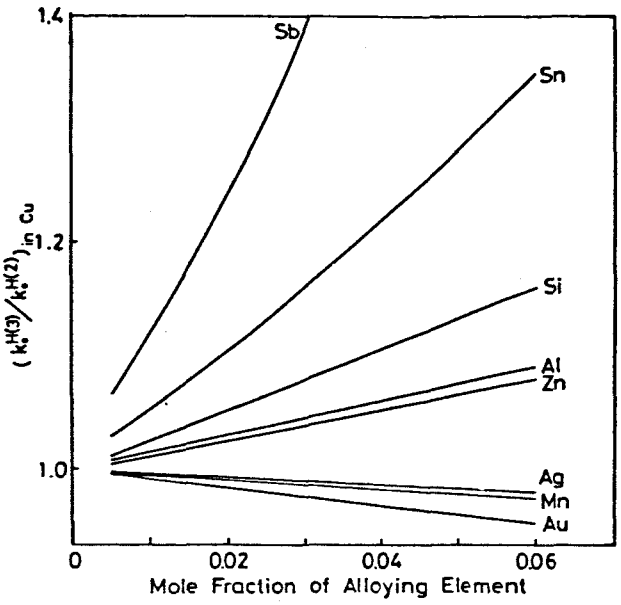

Fig.7-7 Change of D I C of H in Cu alloys with various alloying elements.

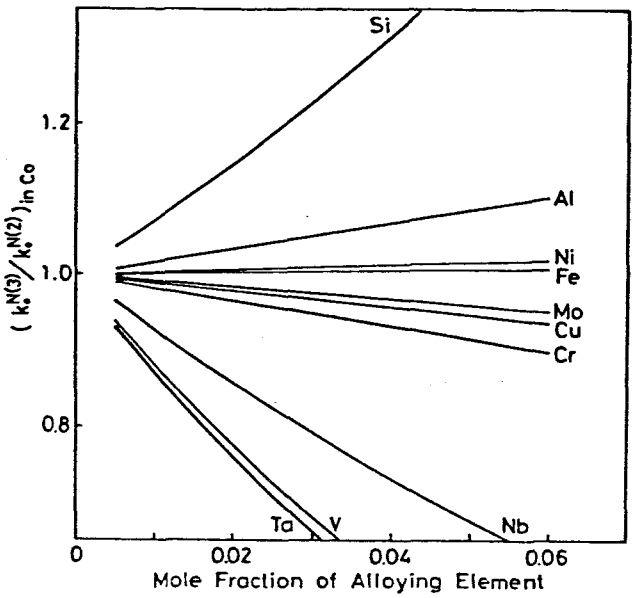

Fig.7-8 Change of D I C of N in Co alloys with various alloying elements.

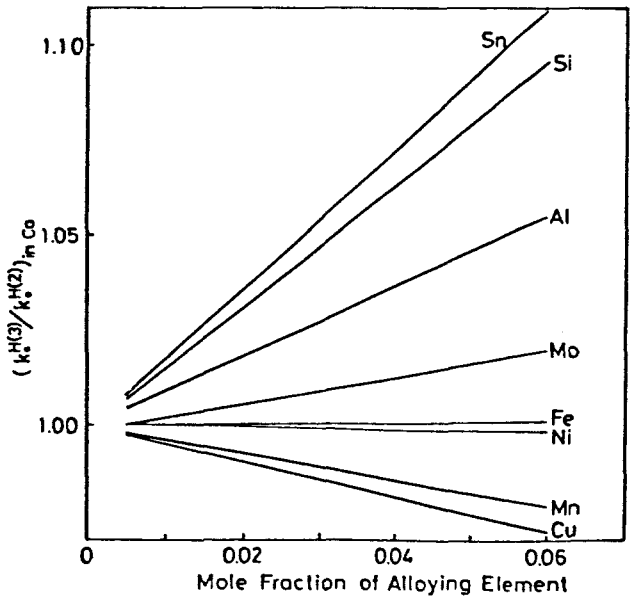

Fig.7-9 Change of D I C of H in Co alloys with various alloying elements.

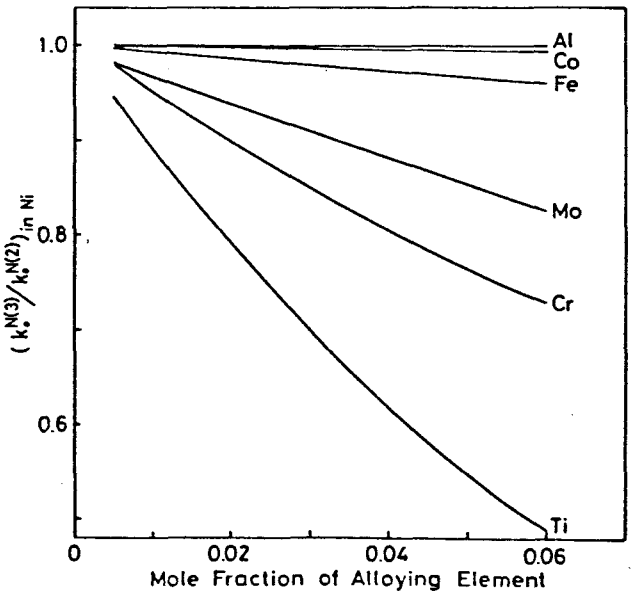

Fig.7-10 Change of D I C of N in Ni alloys with various alloying elements.

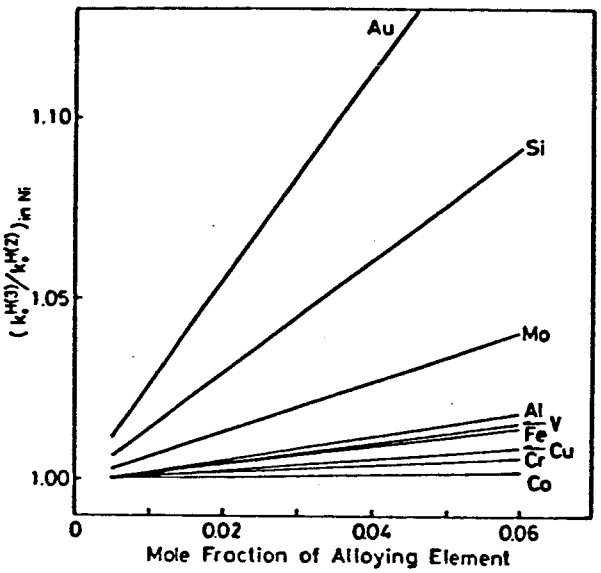

Fig.7-11 Change of D I C of H in N i alloys with various alloying elements.

7.4 Conclusion.

In this chapter, the equilibrium distribution of N and H between solid and liquid phases in iron, cobalt, nickel and copper base alloys were discussed thermodynamically. The results obtained are summarized as follows.

① The simple equation describing the equilibrium distribution coefficients of nitrogen and hydrogen, k_0^N and k_0^H, in iron alloys were derived thermodynamically in the following equation.

$$\ln k_0^i = (\dot{\mu}_i^l - \dot{\mu}_i^s) / RT + \ln (\dot{\gamma}_i^l / \dot{\gamma}_i^s) + (1 - k_0^X) \cdot \varepsilon_i^{X,l} \cdot N_X^l$$

② The effects of various alloying elements on the equilibrium distribution of nitrogen and hydrogen between solid and liquid phases in nickel, cobalt and copper base alloys were calculated by means of D I C and D I P.

7.5 References.

1) T.Mori and H.Ichise: J.Japan Inst. Metals, 2 (1968), 949

2) Basic Open Hearth Steelmaking, ed. by Physical Chemistry of Steelmaing Comm., The Metallurgical Soc. of AIME, New York, (1964), 646

3) K.Mukai: J.Japan Inst. Metals, 38 (1974), 271

4) E.Kato and T.Orimo : J.Japan Inst. Metals, 33 (1969), 1165

5) E.Kato and H.Ueno: J.Japan Inst. Metals, 33 (1969), 1161

6) R.G.Blossey and R.D.Pehlke: Trans. Met. Soc. AIME, 236 (1966), 28

7) F.E.Woolley and R.D.Pehlke: Trans. Met. Soc. AIME, 233 (1965), 1454

8) J.C.Humbert and J.F.Elliott: Trans. Met. Soc. AIME, 218 (1960), 1076

9) R.G.Blossey and R.D.Pehlke: Trans. Met. Soc. AIME, 236 (1965), 566

10) V.V.Averin, A.V.Reviakin, V.I.Fedorchenko and L.N.M.Kozina: Nitrogen in Metals, The New Japan Soc. Casting and Forging, Osaka,(1979), 69 and 80

11) K.W.Lange und H.Schenck: Z. Metallk., 60 (1969), 639

12) K.W.Lange und H.Schenck: Z. Metallk., 60 (1969), 63

13) H.Schenck und K.W.Lange: Arch. Eisenchüttenw., 39 (1968), 673

14) H.Schenck und K.W.Lange: Arch. Eisenchüttenw., 37 (1966), 739

15) T.Bagshaw and A.Mitchell: J.Iron Steel Inst. (London), 204 (1966), 87

16) P.Rontgen und W.Moller: Metal Wirtschaft, 13 (1934), 97

17) A.Sieverts und W.Krumbhaar: Ber. Deutsch. Chem. Ges., 43 (1910),893

18) G.K.Sigworth and J.F.Elliott: Met. Trans., 8 (1974),288

19) R.Hultgren, P.D.Desai, D.T.Hawkings, M.Gleiser and K.K.Kelley: Selected Values of the Thermodynamic Properties of Binary Alloys, ASM, Ohio, (1973)

20) M.Hansen: Constitution of Binary Alloys, McGraw-Hill Book Company, New York, (1958)

Chapter 8

Summary

In this work, in order to explain the mechanisms of the equilibrium distributions of the solute elements between solid and liquid phases in iron alloys, which are closely related not only to the micro-segregation of the solute but also to various phenomena during solidification, the physico-chemical characteristics of the equilibrium distribution coefficients and the influences of the solute interactions on the equilibrium distributions of the solute element between solid and liquid phases in iron alloys were discussed experimentally and theoretically.

In chapter 1, the metallurgical significance of the studies on the equilibrium distribution of the solute elements between solid and liquid phases in iron alloys was described. Also, the surveys and problems of the studies published by the other investigators were pointed out.

The experimental procedures to obtain k_0^X were discussed in chapter 2. In this method, the solid-liquid coexisted phases were quenched and the concentrations of the solute elements in both solid and liquid phases were measured by EPMA to determine k_0. The diffusion of the solute at the interface between solid and liquid phases during quenching, which is one of the serious problems in this experiment, was discussed. Consequently, the results showed that this method was valid for even the Fe−C alloys including carbon whose diffusivity is very large.

The influences of carbon on k_0^X of the solute elements in Fe−C base ternary alloys were studied experimentally and theoretically in chapter 3. Also, the factors governing k_0^X of the solute element were discussed. The fundamental factors to determine k_0^X are thought to be both the free energy of fusion of the solute element X and the difference of the interchange energies of iron with X between solid and liquid phases which is mainly based on the size mismatch energy in solid solution. Furthermore, the equilibrium distribution coef-

ficient of the solute element seems to change periodically against the atomic number of the element in iron base binary alloys. Particularly, in Fe－C base ternary alloys, it is considered that the most important factor controlling k_0 of the third element X is the interaction energy between C and X, and with the increase of carbon content, the equilibrium distribution coefficient of the third element X, k_0^X, increases for the repulsive interaction between C and X while k_0^X decreases for the attractive one.

In chapter 4, the effects of the solute-interactions on k_0^X of the solute element X in iron base ternary alloys were discussed thermodynamically and Distribution Interaction Coefficient (DIC), which is the ratio of k_0^X in ternary system to that in binary one, was defined. This coefficient is the simple parameter giving the variation of k_0^X with the addition of other alloying element. Also, the changes of k_0^X of some third elements with carbon concentration in Fe－C base ternary systems calculated by means of DIC were in good agreement with the experimental results. Furthermore, the variation of k_0 of N, H, P and S with the additions of various alloying elements were predicted by using the above DIC.

The Distribution Interaction Coefficient in iron base ternary systems defined in the foregoing chapter was extended to iron base multi-component systems and Distribution Interaction Parameter (DIP), δ_i^j, was defined in chapter 5. This parameter δ_i^j shows the effect of the element j on k_0^i of the element i. Also, in this chapter, the influences of Si, V and Co on the variation of k_0 of Sn with carbon and the influences of V and Co on the variation of k_0 of Cu with carbon were obtained experimentally, and those results could be explained by using DIP. Furthermore, the DIP's of various alloying elements for P, S, N and H were determined. Using those parameters the variation of k_0 of N with the concentration of Cr and Ni in stainless steels and the variation of k_0 of P and S with the concentration of Cr and C in chromium steels were calculated.

In order to reveal the mechanisms of the micro-segregation of P in engi-

neering steels, the temperature and concentration dependence of k_0^P of P and the effects of carbon on k_0^P were obtained experimentally in chapter 6. The result showed that k_0^P for α phase at infinite dilution of P was 0.14 and that for γ phase was 0.06. Also, the effect of carbon on the segregation of in Fe－C base steels was discussed. Thus, it has become clear that the increase of segregation ratio of P with carbon content in Fe－C base steels is dependent on the change of the equilibrium distribution coefficient of P accompanied with the variation of the solid phase equilibrated with liquid one due to the peritectic reaction. Hence, in order to discuss the segregation of the solute elements in Fe－C base steels, it is very important to know k_0^X for both α and γ phases. Then, the relation between k_0^X for α phase and that for γ one was derived thermodynamically. It was found from the relation derived above that $k_0^{X,\alpha}$ was larger than $k_0^{X,\gamma}$ for the ferrite stabilizing elements while $k_0^{X,\alpha}$ was smaller than $k_0^{X,\gamma}$ for the austenite stabilizing elements, and also the segregation coefficient for the former elements increases and that for the latter elements decreases accompanied with the change of the solid phase from α to γ phases due to the peritectic reaction in Fe－C base steels.

In chapter 7, the equilibrium distributions of N and H between solid and liquid phases were discussed thermodynamically and the simple equation to determine k_0's of N and H in iron alloys was derived. Also, the influences of various alloying elements on k_0 of N and H in Co, Ni and Cu base alloys could be estimated by the use of DIC and DIP.

The micro-segregation of the solute elements is one of the most important problems in the metallurgical processes. So, it is considered that the systematical results obtained in this work about the equilibrium distribution of the solute elements between solid and liquid phases in iron alloys would give the useful information to solve those problems fundamentally and also they would contribute to more comprehensive understanding of various phenomena during solidification of alloys in metallurgical processes.

ACKNOWLEDGEMENTS

The auther is greatly indebted to Professor Z. Morita of the Department of Metallurgical Engineering, Osaka University for his constant help and constructive discussion throughout the present studies.

The auther would like to express his appreciation to Professor T. Okamoto of the Institute of Scientific and Industrial Research, Osaka University and Professor T. Fukusako of the Department of Metallurgical Engineering, Osaka University for their useful advice and the preliminary examination of this thesis.

The auther wishes to thank Dr. T. Iida, Mr. Y. Kita, Mr. M. Ueda and Mr. A. Kagawa of Osaka University for their constant help and useful advice to the present studies.

Publications Relevant to the Thesis.

The major part of the present thesis is based on the following publications and some parts have been revised.

(1) Partition of Carbon between Solid and Liquid in Fe－C Binary System.

T. Okamoto, Z. Morita, A. Kagawa and T. Tanaka

: Trans. ISIJ, 23 (1983),266

: Tetsu-to-Hagane, 68 (1982),244

: The 19th Comm.(Solidification), Japan Soc. Promotion Sci.(JSPS), Rep. No.19-10319 (Feb.,1981)

(2) Thermodynamics of Solute Distribution between Solid and Liquid Phases in Iron- base Ternary Alloys.

Z. Morita and T. Tanaka

: Trans. ISIJ, 23 (1983), 824

: Tetsu-to-Hagane, 70 (1984), 1575

: Proceedings of the Second Japan-U.S. Seminar on Advances in Science of Iron-and Steelmaking, May (1983), P.37, in Kyoto.

: The 19th Comm.(Solidification), Japan Soc. Promotion Sci.(JSPS), Rep. No.19-10429 (Oct.,1982)

(3) Effects of Solute-interaction on the Equilibrium Distribution of Solute between Solid and Liquid Phases in Iron Base Ternary System.

Z. Morita and T. Tanaka

: Trans. ISIJ, 24 (1984),206

: Tetsu-to-Hagane, 70 (1984), 1583

: The 19th Comm.(Solidification), Japan Soc. Promotion Sci.(JSPS), Rep. No.19-10521 (Oct.,1983)

(4) Effects of Solute Interaction on the Equilibrium Distribution of Solute between Solid and Liquid Phases in Iron Base Multi-component System.

Z. Morita and T. Tanaka

: The 19th Comm.(Solidification), Japan Soc. Promotion Sci.(JSPS), Rep. No.19-10535 (Feb.,1984)

(5) Equilibrium Distribution Coefficient of Phosphorus in Iron Alloys.

Z. Morita and T. Tanaka

: The 19th Comm.(Solidification), Japan Soc. Promotion Sci.(JSPS), Rep. No.19-10556 (May, 1984)

(6) Effects of Various Alloying Elements on the Equilibrium Distribution of Gaseous Elements between Solid and Liquid Phases in Fe, Co, Ni and Cu Base Alloys containing Gaseous Elements (Oxygen, Nitrogen and Hydrogen).

Z. Morita and T. Tanaka

: The 19th Comm.(Solidification), Japan Soc. Promotion Sci.(JSPS), Rep. No.19-10563 (May, 1984)